

**This PDF was created from the British Library's microfilm copy of the original thesis. As such the images are greyscale and no colour was captured.**

**Due to the scanning process, an area greater than the page area is recorded and extraneous details can be captured.**

**This is the best available copy**



**DX**



**170578**





THE BRITISH LIBRARY DOCUMENT SUPPLY CENTRE

AN INVESTIGATION OF RADIOLYTIC DAMAGE  
TO BIOMOLECULES IN FOODSTUFFS

TITLE

.....  
.....

AUTHOR

REETU JAIN

.....

INSTITUTION  
and DATE

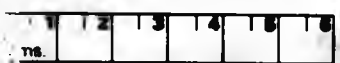
(Polytechnic of North London) CNA  
1991.

.....

Attention is drawn to the fact that the copyright of this thesis rests with its author.

This copy of the thesis has been supplied on condition that anyone who consults it is understood to recognise that its copyright rests with its author and that no information derived from it may be published without the author's prior written consent.

THE BRITISH LIBRARY  
DOCUMENT SUPPLY CENTRE  
Boston Spa, Wetherby  
West Yorkshire  
United Kingdom



20

REDUCTION X .....

CAMERA 5

**AN INVESTIGATION OF RADIOLYTIC DAMAGE  
TO BIOMOLECULES IN FOODSTUFFS**

**REETU JAIN**

**A thesis submitted in partial fulfilment of the  
requirements of the Council for National Academic Awards  
for the degree of Doctor of Philosophy**

**September 1991**

**The Polytechnic of North London in collaboration  
with the Royal London Hospital**

**THE BRITISH LIBRARY DOCUMENT SUPPLY CENTRE**

## **BRITISH THESES NOTICE**

The quality of this reproduction is heavily dependent upon the quality of the original thesis submitted for microfilming. Every effort has been made to ensure the highest quality of reproduction possible.

If pages are missing, contact the university which granted the degree.

Some pages may have indistinct print, especially if the original pages were poorly produced or if the university sent us an inferior copy.

Previously copyrighted materials (journal articles, published texts, etc.) are not filmed.

Reproduction of this thesis, other than as permitted under the United Kingdom Copyright Designs and Patents Act 1988, or under specific agreement with the copyright holder, is prohibited.

**THIS THESIS HAS BEEN MICROFILMED EXACTLY AS RECEIVED**

**THE BRITISH LIBRARY  
DOCUMENT SUPPLY CENTRE  
Boston Spa, Wetherby  
West Yorkshire, LS23 7BQ  
United Kingdom**

Dedicated to my Family

'Where shall I begin,  
please your majesty?' he asked.  
'Begin at the beginning',  
the King said, gravely, 'and go  
on till you come to the end: then stop'.

Lewis Carroll

#### Acknowledgements

I would like to express my sincere gratitude to my supervisors Dr. M. Grootveld, Dr. D.E.M. Spillane and Professor L.I.B. Haines for their guidance and encouragement throughout the course of this work.

I would like to thank Wimal Dissanayake for his invaluable help and advice.

I would also like to extend a special thanks to my sister and also to Alex, Ismail and Arif for their wholehearted support and patience.

Finally, I am very grateful to Ken Bell, MBE, of Ken Bell International, Newcastle for financial support, the Royal London Hospital Medical College (Department of Immunology) for the irradiation of food samples and the University of London Intercollegiate Research Services for the provision of NMR facilities.

#### **ABSTRACT**

The development of an effective test system for detecting the irradiation status of foodstuffs is essential for the establishment of legislative control and consumer choice. For foodstuffs consisting mainly of water, treatment with ionising radiation initially generates highly reactive free radical species (hydroxyl radical (OH), hydrated electrons ( $e_{aq}^-$ ) or hydrogen atoms (H)). These react extremely rapidly with a wide variety of "target" molecules in foodstuffs resulting in small, but detectable chemical changes. Hence, assays for the assessment of OH radical activity involve the identification and/or quantification of chemical species produced by the attack of OH radical on a range of biomolecules occurring in foodstuffs.

This study involves an investigation of radiolytically-induced chemical modifications arising from the interaction of OH radical with naturally occurring aromatic compounds in fruits and vegetables. High performance liquid chromatography coupled with electrochemical detection has been applied to the analysis.

In addition, the chemical nature of intermediates in, and end-products arising from the interaction of OH radical with polyunsaturated fatty acids and carbohydrates is reviewed by application of second-derivative (2D) electronic absorption spectrophotometry. The 2D spectrophotometric technique has not been previously applied to food studies and may serve as a potential "probe" for the measurement of radiolytic products generated as a consequence of irradiation treatment.

Additionally, high-field, high-resolution proton nuclear magnetic resonance spectroscopy has been employed to assess radiolytically-induced damage to biomolecules present in shellfish.



<u>CONTENTS</u>	<u>PAGE</u>
<b><u>CHAPTER 1 : INTRODUCTION</u></b>	1
1.1 Radiation Chemistry of Water	4
1.2 Methods for the Identification of Irradiated Foods	9
1.2.1 Electron Spin Resonance (ESR) Spectroscopy	9
1.2.2 Chemiluminescence and Thermoluminescence	10
1.2.4 Analysis of Volatiles from Lipids	12
1.2.5 Analysis of Radiolytic Products Derived from DNA	13
1.2.6 Alternative Tests for Irradiated Foodstuffs	14
1.3 Aims of this Project	15
<b><u>CHAPTER 2 : ANALYTICAL TECHNIQUES AND EXPERIMENTAL PROCEDURES</u></b>	17
2.1 Reversed Phase High Performance Liquid Chromatography	
2.1.1 Theory of Liquid Chromatography	18
2.2 HPLC/Electrochemical Detection (LC/ECD)	22
2.2.1 Brief Theory	23
2.3 Ultra-Violet/Visible Spectrophotometry	
2.3.1 Theory	26
2.4 <sup>1</sup> H NMR Spectroscopy	
2.4.1 Brief Theory	30
2.5 Instrumentation	35
2.6 Materials	36
2.7 Experimental Procedures	37
2.7.1 Phenolic Acid Analysis in Celery and Strawberry: Extraction	37
2.7.2 Calibration of Standards	37
2.7.3 Hydroxylation of Phenolic Acids	38
2.7.4 Ascorbate Analysis in Irradiated Strawberry	38
2.7.5 Determination of Conjugated Diene Species	39
2.7.6 Thiobarbituric Acid (TBA) Test	40
2.7.7 Analysis of Prawn Supernatants by <sup>1</sup> H NMR Spectroscopy	41

<b><u>CHAPTER 3 : RADIOLYTIC DAMAGE TO AROMATIC COMPOUNDS AND VITAMIN C</u></b>	43
3.1 Aromatic Hydroxylation	43
3.2 Mechanism of Aromatic Hydroxylation	44
3.3 Electrochemical Oxidation of Phenols	46
3.4 Detection of <sup>•</sup> OH Radical in Biological Systems	49
3.4.1 <sup>•</sup> OH Radical Attack on DNA	53
3.5 <sup>•</sup> OH Radical Attack on Vitamin C	56
3.6 Results	58
3.6.1 Hydroxylation of Standard Phenolic Acids	58
3.6.2 HPLC/EC Detection of Phenolic Constituents in Celery Homogenates Subjected to $\gamma$ -radiation Treatment	75
3.6.3 Comparison of Celery Homogenates Prior and Subsequent to Irradiation Treatment	84
3.6.4 Quantification of Phenolic Constituents Present in Celery	92
3.6.5 HPLC/EC Detection of Phenolic Constituents in Strawberry Homogenates Subjected to $\gamma$ -radiation Treatment	96
3.6.6 Comparison of Strawberry Homogenates Prior and Subsequent to Irradiation Treatment	101
3.6.7 Quantification of Phenolic Constituents Present in Strawberry	105
3.6.8 Vitamin C Analysis of Control and $\gamma$ -irradiated Strawberry Homogenates	109
3.7 Summary and Conclusion	113
<b><u>CHAPTER 4 : LIPID PEROXIDATION</u></b>	115
4.1 Introduction	115
4.2 Methods for Measurement of Lipid Peroxidation	120
4.2.1 Identification of Conjugated Diene Species by UV Spectroscopy	121
4.2.2 The Thiobarbituric Acid (TBA) Test	122
4.3 Results	125
4.3.1 2D Spectrophotometric Analysis of TBA-Reactive Material in Peroxidised Samples of Corn Oil	125
4.3.2 Application of 2D Spectrophotometry to TBA Reactivity in Peroxidised Commercially- Available PUFAs	129

4.3.3	Determination of Conjugated Diene Species in Peroxidised Commercially-Available PUFAs	132
4.3.4	2D Spectrophotometric Analysis of Conjugated Diene Species in Corn Oil Subjected to Peroxidation	138
4.4	Summary and Conclusion	144
4.4.1	Conjugated Diene Method	144
4.4.2	Thiobarbituric Acid Method	145
<b><u>CHAPTER 5 : RADIOLYTICALLY-MEDIATED OXIDATIVE DAMAGE TO CARBOHYDRATES</u></b>		147
5.1	Introduction	147
5.1.1	Hydroxyl (OH) Radical Attack on Glucose	147
5.1.2	Formation of Malondialdehyde (MDA) in Carbohydrates Subjected to OH Radical Attack	150
5.2	Results	153
5.2.1	2D Spectrophotometric Analysis of TBA-Reactive Material in a Range of Carbohydrates Subjected to an OH Radical Flux Generated by the Fenton System	153
5.2.2	2D Spectrophotometric Identification of the TBA-Reactive Materials	162
5.3	Discussion and Conclusion	168
<b><u>CHAPTER 6 : NMR SPECTROSCOPY OF PRAWN SUPERNATANTS</u></b>		171
6.1	Introduction	171
6.1.1	Application of High-Field <sup>1</sup> H NMR Spectroscopy to the Analysis of Irradiated Foodstuffs	172
6.2	Results	174
6.2.1	Analysis of Radiolytically-Mediated Modifications in the Chemical Composition of Prawn Samples by <sup>1</sup> H NMR Spectroscopy	174
6.2.2	Radiolytic Damage to the Amino Acid Methionine	176
6.3	Summary and Conclusion	179
<b><u>CHAPTER 7 : DISCUSSION AND CONCLUSIONS</u></b>		181
<b>REFERENCES</b>		187
<b>APPENDIX : PUBLISHED PAPERS</b>		

**CHAPTER 1**

**INTRODUCTION**

## 1. INTRODUCTION

Food irradiation is one of the more recent preservation techniques, supplementing traditional methods such as canning, freezing, smoking, curing, drying and pickling. Radiation processing of food results in the eradication of food spoilage organisms including bacteria, moulds and yeasts, thereby effectively prolonging the shelf-life of perishable commodities.

Nearly all national governments have imposed regulatory control on the sale of irradiated commodities. At present, approximately seventy countries have active research and development programmes in food irradiation and about thirty-seven of these countries apply it commercially for processing of one or more food items. Regulations concerning irradiated foods differ from country to country. In order to enforce such legislation and allow consumer choice, there is an increasing interest in developing methods which allow the identification of irradiated foods and quantification of the radiation dose employed.

Food irradiation is a physical process (in which energy is imparted to matter) and employs high energy ionising electromagnetic radiation. Usually, X-rays or gamma rays produced by a cobalt-60 or caesium-136 source are used. The radiation dose used in food processing ranges from 50 Gy to 10 kGy and is largely dependent on the nature of the foodstuff being irradiated.

Ionising radiation penetrates the foodstuff resulting in the formation of a large number of reactive chemical species

(i.e. ions, positively and negatively charged atoms/molecules) which in turn can initiate the production of free radicals capable of chain reactions. However, the amount of energy transferred to the material is usually very small in comparison to heat treatments (since irradiation results in minor temperature increases<sup>1</sup>). The reactions of the ions and free radicals in foods are responsible for the chemical changes occurring during and after irradiation. However, the changes induced in the chemical composition of most foodstuffs are usually very small and, in addition, many of the changes observed may arise from other processing methods which may also have been employed. Consequently, it is very difficult to detect chemical modifications occurring in irradiated foodstuffs.

Many investigations have been carried out with the prime objective of developing reliable methods to discriminate between irradiated and non-irradiated foodstuffs (cf. section 1.2). Physical, chemical and biological methods have been applied, the results indicating that there exists no single general method that is applicable for all types of foodstuff.

Much of the research in this field has been carried out in dilute aqueous solutions since the majority of foods are hydrated. Therefore, many of the chemical reactions taking place in foodstuffs are initiated by the indirect action of radicals derived from the radiolysis of water, giving rise to the formation of so-called radiolytic products<sup>2</sup>. Radiolytic

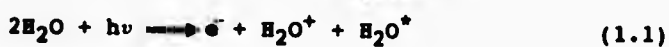
products are, however, not confined solely to water and are also formed in non-aqueous components of foods, for example as a consequence of the autoxidation of fats and fatty acids.

### 1.1 RADIATION CHEMISTRY OF WATER

When high energy photons (i.e. X-rays or gamma-rays) interact with matter, energy is transferred from the photon to water molecules of the aqueous system. This process results in the production of ions. In addition, excited water molecules are also produced. These primary species may decompose or react with components of the system, thereby bringing about chemical changes. Free radicals formed from the excited and ionised molecules are largely responsible for these changes.

The primary radiolytic products of water are hydrated electrons ( $e_{aq}^-$ ), hydroxyl radicals (OH) and the hydrogen atom (H). The secondary chemical species include hydrogen peroxide ( $H_2O_2$ ), hydrogen gas ( $H_2$ ) and the hydrated hydrogen ion ( $H_3O^+$ ). The highly reactive hydroxyl radicals and hydrated electrons account for the principle chemical changes which occur in irradiated foods containing water as a major constituent. However, hydrogen peroxide may also participate in many radiation-induced chemical reactions<sup>3</sup>.

The interaction of ionising radiation with water (Reaction 1.1), initially consists of energy transfer to the system (the physical stage of the process)<sup>4,5</sup>



where  $e^-$  represents an electron and  $H_2O^+$  a water molecule with excited electrons.

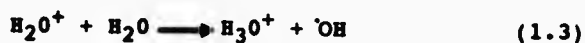
Ionisation and excitation of water takes place within  $10^{-16}s$  of exposure to radiation. The electrons released in the



ionisation event become hydrated. This process entails the orientation of H<sub>2</sub>O molecules about the charged species. Hydration occurs within 10<sup>-12</sup> s.



H<sub>2</sub>O<sup>+</sup> ion reacts with water (by a proton transfer reaction) to produce the hydrogen ion and the hydroxyl radical



Moreover, the excited water molecule can dissociate to give the hydrogen atom and the hydroxyl radical



Reactions (1.3) and (1.4) occur within 10<sup>-14</sup>-10<sup>-13</sup> s.

The primary species (e<sub>aq</sub><sup>-</sup>, ·OH, H) react with a wide range of chemical constituents of foodstuffs at diffusion controlled rates and have half-lives (t<sub>1/2</sub>) of less than 10<sup>-9</sup> s. Approximately 5x10<sup>-3</sup> mole of these radicals are produced per kg of food when exposed to the maximum permitted food irradiation dose of 10 kGy.

Table 1.1 illustrates the yields of the primary radicals and secondary chemical species from water when exposed to gamma-irradiation<sup>6</sup>, and Table 1.2 shows their rates of reactions with a range of biomolecules<sup>6,7</sup> (pp. 7-8).

The hydrated electrons are powerful reducing agents capable of addition to a large number of organic constituents in foodstuffs such as aromatic and carbonyl compounds which are located at or close to their site of formation. The hydroxyl (·OH) radical is a powerfully oxidising short-lived species and its reaction with a range of biological molecules present in foodstuffs (e.g. proteins, lipids, carbohydrates,

vitamins) usually produces secondary radicals of lower reactivity. These species are also capable of attacking other molecules thereby resulting in the production of further compounds which may be classed as radiation-induced species. The  $\cdot\text{OH}$  radical reacts with organic compounds containing aromatic rings or carbon-carbon multiple bonds by addition, whilst its reaction with saturated organic compounds containing the carbonyl group is predominantly by abstraction.

Generally, chemical identification of irradiated foodstuffs is therefore based on some chemical change occurring in a particular compound i.e. the formation or depletion of a compound which may act as a radiolytic marker or a radiation-induced chemical species. Such radiolytic markers can also consist of "trapped" free radicals, the life-time of which depends on a number of variables including the moisture content of the food<sup>7</sup>.

A number of techniques are under investigation with the aim of discriminating between irradiated and non-irradiated foods. Some of these techniques are discussed in section 1.2.

**TABLE 1.1**

**Yields of the Primary Radicals and Molecular Products of Gamma-Irradiated Water<sup>6,7</sup>**

Species	$e_{aq}^-$	H $\cdot$	$\cdot$ OH	H <sub>2</sub>	H <sub>2</sub> O <sub>2</sub>	H <sub>3</sub> O <sup>+</sup>
G value	2.60	0.60	2.70	0.45	0.70	2.6

Where, G = Radical Chemical Yield

$$= \frac{\text{No. of molecules formed}}{100 \text{ eV}}$$

The values given in the table refer to the numbers of primary oxygen radicals and molecular products produced per 100 eV of energy absorbed by water (after  $10^{-17}$  s) at neutral pH.

The radical chemical yield, G (as above) in  $\text{nmol J}^{-1} = 103.6 \times G$  (or  $0.1036 \text{ } \mu\text{mol J}^{-1}$ ).

**TABLE 1.2**

**Rate Constants for the Reactions of Primary Radiolytic Products With Various Compounds in Aqueous Solution ( $\times 10^{10}$  mol<sup>-1</sup> dm<sup>3</sup> s<sup>-1</sup>)**

Compounds	H <sup>•</sup>	•OH	e <sub>aq</sub> <sup>-</sup>
Arabinose	0.0052 (1.0)	0.18 (7.0)	0.0004 (7.0)
Glucose	0.0076 (7.0)	0.23 (6.5)	0.0004 (7.0)
Deoxyribose	0.0029 (7.0)	0.25 (8.0)	0.001 (7.0)
Sucrose	0.0015 (1.0)	0.23 (7.0)	0.0005 (7.0)
Ascorbic acid	0.03 (7.0)	1.1 (1.5)	0.03 (1.0)
Citric acid	0.00004 (1.0)	0.007 (1.0)	0.00001 (1.0)
Succinic acid	0.0003 (1.0)	0.031 (5.0)	0.037 (6.0)
Salicylic acid	0.24 (2.0)	1.2 (2.0)	1.0 (7.0)
Glutathione	1.0 (1.5)	1.4 (1.0)	0.45 (7.2)
Phenylalanine	0.071 (6.4)	0.66 (6.0)	0.012 (6.5)
Tryptophan	0.20 (6.0)	1.3 (6.0)	0.025 (6.0)
Tyrosine	0.04 (6.0)	1.3 (7.0)	0.028 (6.5)
Alanine	0.00002 (1.0)	0.007 (6.5)	0.0012 (6.5)
Uracil	0.047 (2.5)	0.57 (7.0)	1.5 (7.0)
Phenol	0.21 (7.0)	0.66 (7.0)	0.002 (6.5)

Numbers in brackets indicate pH value for each compound studied

## 1.2 METHODS FOR THE IDENTIFICATION OF IRRADIATED FOODS

### 1.2.1 Electron Spin Resonance (ESR) Spectroscopy

ESR has been successfully used to detect irradiated foodstuffs and is based on the spin properties of the unpaired electron in free radical species.

Since one of the major effects of ionising radiation is the production of free radicals, the major application of ESR spectroscopy is in the detection and identification of these species, since the technique has the ability to detect the presence of unpaired electrons. An unpaired electron has a spin of either a  $+1/2$  or  $-1/2$  and therefore behaves as a small bar magnet. In the presence of an external magnetic field, the unpaired electron can align itself either parallel or anti-parallel to the field and consequently has two possible energy levels<sup>8</sup>. If electromagnetic radiation of the correct frequency is applied (energy from the microwave region) absorption of energy occurs resulting in the movement of an electron from the lower energy level to the upper one. An absorption spectrum is therefore obtained.

Free radicals produced by the irradiation of food are very reactive and tend to be short-lived in an aqueous medium. It is possible, however, for the radicals to become entrapped within hard or dry materials (bones, spices or seeds) from which stable ESR signals may be obtained<sup>9-11</sup>.

Previous work has suggested that free radicals may also be produced by heating and grinding. Results do however show that certain ESR signals in the material become more intense with increasing doses of ionising radiation, and in addition

the signal is distinguishable from that obtained by free radicals produced artefactually<sup>12</sup>.

ESR spectroscopy has been applied to a wide range of foods and ESR signals have been detected in irradiated chicken bone, the exoskeleton of shellfish, spices and fruit seeds<sup>13-15</sup>. In addition, the signals were found to remain after storage of the food for up to two weeks. The technique has also been used successfully to assess the irradiation status of strawberries where the achenes from irradiated strawberry exhibited ESR signals characteristic of free radical production<sup>18</sup>.

#### 1.2.2 Chemiluminescence and Thermoluminescence

Other methods under development for the identification of irradiated foods include Chemiluminescence (CL) and Thermoluminescence<sup>17</sup> (TL). When heterogenous organic solids (composed of various substances) are exposed to gamma-radiation, light emission occurs either

(a) at the time they come into contact with an aqueous medium, i.e. chemiluminescence

(b) when they are heated to temperatures between 50-400° C i.e. thermoluminescence.

Both techniques have been reported as reliable identification measures for gamma-radiation-processed spices<sup>19</sup>.

1.2.2(a) Chemiluminescence (CL)

When solid organic samples are irradiated and subsequently dissolved in water, light is emitted by them and oxidising agents such as hydrogen peroxide, organic peroxides and carbon-centred radicals are produced. The light is emitted in short pulses and generally the light yield depends on the administered radiation dose. The light can, however, be amplified by addition of a photosensitizer during the dissolution process e.g. luminol, a cyclic hydrazide of 3-aminophthalic acid. Luminol reacts with oxidising agents in the sample and in so doing decomposes with light of blue emission centred at a wavelength of 424 nm<sup>20</sup> (Figure 1.1).

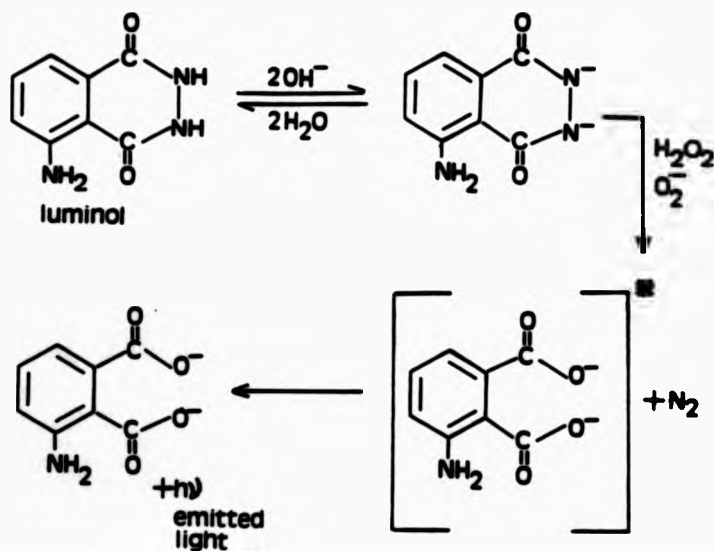


Figure 1.1

#### 1.2.2(b) Thermoluminescence (TL)

The TL phenomenon is initiated when solid substances are subjected to ionising radiation, and electrons transferred to an excited state return to the ground state with emission of light. Gamma-irradiation treatment results in changes or defects within the lattice<sup>21</sup>.

The valence state of solid substances is changed and electrons become "trapped" within the lattice (i.e. excitation and ionisation occurs). Subsequent to irradiation, the discrete energy levels that "trap" electrons during irradiation cause TL on heating with the emission of light. This results in a glow curve which is characteristic of the substance under analysis<sup>22</sup>. Many dried foods have been tested by these methods including dried vegetables (asparagus and celery), cocoa, milk powder and, most extensively, spices<sup>23</sup>. It appears that the origin of TL signals in irradiated foods arises primarily from inorganic materials including detrital mineral debris, dust, dirt or salt present as foodstuff impurities. In previous studies, the most sensitive samples to TL emission were those mixes containing salt and silicate minerals<sup>24</sup>.

CL and TL techniques seem reliable for the identification of irradiated foods but are limited to dry food materials.

#### 1.2.3 Analysis of volatiles from lipids

The volatile compounds produced by irradiation have been studied extensively by gas chromatography (amongst other techniques) and originate from the lipid fraction of



foods<sup>25,26</sup>. Volatile hydrocarbon gases such as pentane and ethane, aldehydes, methyl and ethyl esters, and free fatty acids are well known end-products of lipid peroxidation and their measurement in foodstuffs may be indicative of irradiation. The hydrocarbons produced from irradiated lipid fractions of meat have been studied in some detail<sup>27</sup>.

The major radiolytic hydrocarbons expected from the radiolysis of fatty acids include the  $C_{n-1}$  alkanes (i.e. the alkane with one carbon atom less than the parent fatty acid), the  $C_{n-2}$  alkenes (the alkene with two carbon atoms less) and  $C_n$  aldehydes (the aldehyde containing the same number of carbon atoms as the parent fatty acid). These hydrocarbons result from selective cleavage of the free fatty acid and are considered to be specific radiolytic products<sup>28</sup>.

#### 1.2.4 Analysis of radiolytic products derived from DNA

Other prospective tests include the analysis of radiolytically-modified nucleosides in DNA after irradiation. Ionising radiation causes a variety of effects in DNA including chemical modification of the purine and pyrimidine base moieties. For example, hydroxylation of guanine and cytosine by radiolytically-generated 'OH radical results in the formation of 8-hydroxyguanosine and 5-hydroxycytosine which have been detected by HPLC coupled with ECD from enzymatically digested DNA<sup>29,30</sup>. Other base products of 'OH radical attack on DNA include 5,6-dihydroxyuracil, 5-hydroxyuracil, and *cis*-thymine glycol. These have been identified/characterised by gas chromatography-mass spectrometry (GC-MS)<sup>31,32</sup>. Recently, thymidine glycol, a DNA

irradiation product, has been studied in irradiated wheat and in irradiated calf thymus DNA solution<sup>33</sup>.

In addition, radiolytic damage to DNA also gives rise to single- and double-strand breakages and this phenomenon may be of some toxicological significance<sup>34,35,36</sup>.

#### 1.2.5 Alternative tests for irradiated foodstuffs

Reviewed here are just a few of the many tests which are already under investigation. Others include the chemical analysis of proteins with particular reference to the hydroxylation of phenylalanine by 'OH radical<sup>37</sup>. Carbohydrates, fats and vitamins have also been studied extensively<sup>38-40</sup>.

Due to the wide diversity of foods and food components currently available, there is at present no single test for all foodstuffs. Consequently, it is necessary to develop as many tests as possible using a variety of systems, in order to allow the application of more than one test if required.

### 1.3 AIMS OF THIS PROJECT

In order to prevent illegal imports of irradiated foods and to allow consumer choice, a method of identification is required which can be used to distinguish between irradiated and non-irradiated foodstuffs. For individual foodstuffs, several different methods are possible depending on the chemical composition of the food, but no method has yet been internationally accepted. The aims of this project encompass the development of a diagnostic test for irradiated foods.

To demonstrate whether a foodstuff has been treated with ionising radiation, it is necessary that a change specific to radiation takes place within the food. For foodstuffs consisting mainly of water, treatment with ionising radiation results in the production of free radicals which react extremely rapidly with a variety of "target" molecules in foods resulting in a number of chemical modifications. Hence methodologies which involve the detection of free radical intermediates or their stable products may be employed as radiation markers.

The aim of this project is the detection of radiolytically-mediated chemical changes to various components in foodstuffs, primarily those attributable to the reactions of the hydroxyl radical (OH) generated by gamma-irradiation or by the radiolytically-mimetic Fenton reaction system. In addition, any chemical changes occurring within foodstuffs have been supported by studies of chemical model systems. Suitable candidates for specific radiation induced markers are aromatic compounds, polyunsaturated fatty acids

and carbohydrates. These classes of compounds are ubiquitous to most foods.

A variety of analytical techniques and procedures have been employed, and their potential application in the detection of irradiated foodstuffs is discussed.

All plant and animal samples investigated were obtained from commercial sources and no taxonomic data is given for these species.

**CHAPTER 2**

**ANALYTICAL TECHNIQUES**  
**AND**  
**EXPERIMENTAL PROCEDURES**

## 2. ANALYTICAL TECHNIQUES EMPLOYED

Chemical identification of multi-component food systems requires the presence of a selective analytical technique. The components of interest (e.g. aromatic compounds, either naturally occurring or derived from the reactions of radiolytically-generated  $\cdot\text{OH}$  radical) are normally present in extremely small quantities of parts per billion or less. Direct analysis of the food components, whilst desirable is generally not feasible. A variety of sample treatments have been employed comprising digestion, separation and extraction prior to analysis.

One possible instrumental method of analysis for phenols and phenolic acids is reversed phase HPLC. This technique has several advantages over other methods. It achieves highly resolvable separations and is fairly rapid. Its sensitivity is dependent upon the detection system employed. A variety of detectors may be employed, but the one specifically utilised in this study is the electrochemical detector (ECD) since it is particularly sensitive to phenolic compounds. Most phenols are electroactive (their oxidation potentials range from ca. +0.60V to +1.10V) and are oxidised at solid electrodes, for example, the glassy carbon electrode.

Ultra-violet/visible spectrophotometry has been applied to the detection of conjugated diene lipid hydroperoxides (e.g. products of the peroxidation process of corn oil) as these readily show strong absorbance in the UV region. The zero-order absorption spectrum of these species results in a large overlapping band which can be resolved by second-derivative

(2D) spectroscopy.

High field proton NMR spectroscopy has been applied to the analysis of radiolytically-induced modifications occurring in the chemical composition of prawns. The application of Hahn spin-echo pulse methods to the analysis results in spectral simplification by suppressing a large number of broad overlapping resonances frequently encountered in the NMR spectra of biological samples containing large macromolecules.

## 2.1 REVERSED-PHASE HIGH PERFORMANCE LIQUID CHROMATOGRAPHY (HPLC)

### 2.1.1 Theory of Liquid Chromatography

Chromatography has been employed as a separative analytical technique. The technique involves the partitioning of the sample mixture between two mutually immiscible phases (which may be liquid or solid). The stationary (solid) phase is contained within a column and the mobile (liquid) phase is forced under pressure through the column. The sample mixture is introduced at the head of the column into the mobile phase, and subsequently achieves an equilibrium distribution between the two phases and undergoes a series of interactions as it migrates through the column.

In liquid chromatography the separated components emerge in order of increasing interaction with the stationary phase. In reversed-phase chromatography the components preferentially distributed in the mobile phase (those with high polarity) elute first, and those retained strongly by

the stationary phase elute last. The time of elution of a component (to give a maximum peak) is termed the retention time ( $t_r$ )<sup>41</sup>.

#### Interactive Forces in Chromatography

A number of interactive forces occur between the solute molecules and molecules of each phase (solvent molecules) resulting in the distribution of the solute between the two phases. These forces can be polar, dispersive or ionic.

(a) Polar Interactions: These forces arise from the presence of permanent or induced dipoles within the molecule. When two adjacent molecules possess a permanent dipole, dipole orientation occurs (i.e. the positive end of the dipole is close to the negative end of the other dipole). For maximum energy, orientation of the dipoles should be linear.

(b) Dispersive Interactions: London dispersion forces/van der Waals' forces are relatively weak forces which exist between any adjacent pair of atoms or molecules. Interaction occurs due to formation of a transient dipole between adjacent molecules. Alignment of molecules occurs due to unequal distribution of electrons within atoms or molecules.

(c) Ionic Interactions: These occur when separating by ion-exchange or ion-pair chromatography. Ionic components possessing a net negative charge or net positive charge are able to take part in electrostatic interactions<sup>41,42</sup>.

#### Chromatographic Separation

Chromatographic separation generally involves two characteristic features: differential migration of various



compounds in the sample and a spreading of molecules of a given compound along the column<sup>42</sup>. Both processes contribute to band broadening, and this is stated in the form of the van Deemter equation:

$$H = A + B/\bar{u} + C\bar{u} \quad (2.1)$$

where

H = plate height

A = Eddy diffusion which results from the inhomogeneity of flow velocities and path lengths around the packing particles. It is defined as:

$$A = 2\lambda dp$$

where dp is the particle diameter of the packing and  $\lambda$  is an unspecified constant of packing uniformity and column geometry and usually has a numerical value in the range 1-6. The A term is therefore a measure of how well a column is packed. It is minimised by decreasing the particle diameter<sup>43</sup>.

The B term in the van Deemter equation accounts for longitudinal or axial diffusion, i.e. random molecular motion of the solute within the mobile phase. It is defined as:

$$B = 2\gamma D_m$$

where  $\gamma$  is the tortuosity constant which accounts for restriction to diffusion by particles and ranges between 0.01 and 1.0.  $D_m$  is the solute diffusion coefficient in the mobile phase.

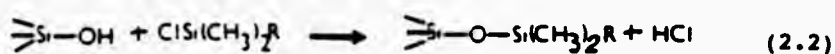
The C term describes dispersion due to slow mass transfer which occurs because of slow equilibration of the solute between the mobile and stationary phases.

$\bar{u}$  = average linear velocity of the mobile phase.

#### Bonded-Phase Chromatography

Chemically bonded stationary phases are the most widely used column packings in liquid chromatography. The term "bonded-phase" describes the attachment of a covalently bound organic hydrocarbon moiety to a silica support surface. Bonded phase packings are stable under high pressure liquid chromatographic conditions.

The siloxane (Si-O-Si-C) type of bond is the standard for commercial bonded phases and is formed by the reaction of di- or tri-alkyl-silane with the surface silanol groups of the hydroxylated silica gel. Equation 2.2. depicts a chlorosilane bonding reaction with the silanol groups



The bonded phase can be categorised as either normal (NP-BPC) or reversed (RP-BPC). The normal phase utilises the attachment of polar moieties to the silica gel surface. The term reversed-phase describes a hydrophobic, non-polar stationary phase consisting mainly of C<sub>8</sub> - C<sub>18</sub> (octyl - octadecyl) hydrocarbon chains attached to the silica support. The hydrophobicity increases with an increase in length of the hydrocarbon chain. RP-BPC relies mainly on strong hydrophobic interactions between the stationary phase and the solute molecule<sup>44</sup>.

The reversed-phase technique is the most widely used mode in HPLC and provides optimum retention and selectivity. Hydroxylated aromatic species are readily separated by this technique and detected by electrochemical oxidation.

#### 2.2 HPLC / ELECTROCHEMICAL DETECTION (LC / ECD)

The combination of these two techniques in analytical chemistry is becoming fairly widespread for the identification and quantification of oxidisable and reducible organic compounds<sup>45,46</sup>. The electrochemical detector is highly selective. The sensitivity and range of application depends on the electroactivity of the compounds of interest.

The ECD detector consists of an electrochemical cell equipped with a glassy carbon working electrode (which has an operating range from -1.30V in cathodic to +1.50V in the anodic range). The counter electrode is made from steel and the reference electrode is comprised of a silver/silver chloride ceramic gel and used to monitor the potential of the working electrode (Figure 2.1).

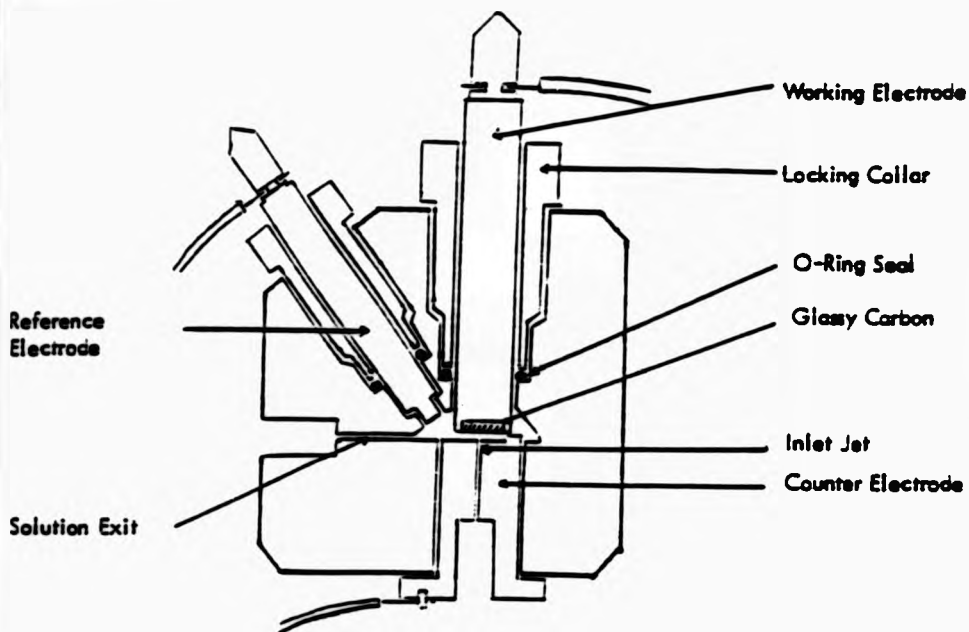
The electrochemical flow cell is based on the "wall-jet" principle where a solution from the chromatographic column flows through a small jet (size 0.1mm) in the counter electrode and impinges onto the surface of the glassy carbon working electrode (which acts as a wall)<sup>47</sup>.

This type of cell design provides rapid mass transfer and consequently results in a high degree of efficiency and selectivity, and minimises peak broadening. In addition, a cleaning effect is produced on the surface of the glassy carbon electrode reducing contamination. The use of glassy

carbon electrodes has become increasingly popular, particularly in the study of electrochemical oxidations, where the ECD can yield sub nanogram detection limits<sup>48</sup>.

Figure 2.1

Diagram of the Electrochemical Cell



Wall-Jet Cell

2.2.1 Brief Theory

In electrochemical detection, a potential difference is applied between the reference and working electrodes. This applied potential is the driving force for the electrochemical reaction. An electrochemically active substance passes to the electrode which is held at a

potential sufficient for electron transfer (either oxidation or reduction). In this manner a current is produced which is proportional to the concentration of the reactant passing through the cell<sup>49-51</sup>.

All Faradaic electrochemistry depends on Faraday's law

$$Q = nFN \quad (2.3)$$

where

Q = number of coulombs and is directly proportional to the number of moles (N) converted to product

n = number of electrons involved in the reaction

F = Faraday constant = 96,486.332 Coulombs/mole

Hydrodynamic voltammetry is used to select the optimal operating potential for a particular compound.

For organic substances the initial step in electro-oxidation involves the formation of a radical cation<sup>52</sup>. The greater the stability of this radical cation, the greater the ease with which the components are oxidised.

In general, for aromatic compounds, initial electron transfer for aromatic compounds is written as



where

Ar( $\delta+$ ) = aromatic electron deficient species

n = number of electrons involved in the transfer

Aromatic amines and phenolic species are the most important classes of components to which electrochemical detection has been applied<sup>45,53</sup>.

For foodstuff homogenates the methodology involves isolation and extraction of acidic, neutral and basic classes of phenolic components into an organic solvent (e.g. diethylether or ethylacetate) under appropriate pH conditions. The organic solvent is then evaporated to dryness, and the residue reconstituted into water or a mobile phase of controlled pH and then separated by reversed-phase HPLC and detected by ECD.

## 2.3 ULTRA-VIOLET/VISIBLE SPECTROPHOTOMETRY

### 2.3.1 Theory

Identification of organic compounds by their absorption spectra has been used as a routine analytical procedure for many years. Molecular absorption in the UV and visible regions of the electromagnetic spectrum is dependent on the electronic structure of the molecule.

Absorption of energy is quantised and the total energy of a molecule is given by

$$E_{\text{total}} = E_{\text{el}} + E_{\text{rot}} + E_{\text{vib}} \quad (2.5)$$

where

$E_{\text{total}}$  = Total energy of the molecule

$E_{\text{el}}$  = Electronic energy of the molecule

$E_{\text{rot}}$  = Energy associated with rotation of the molecule

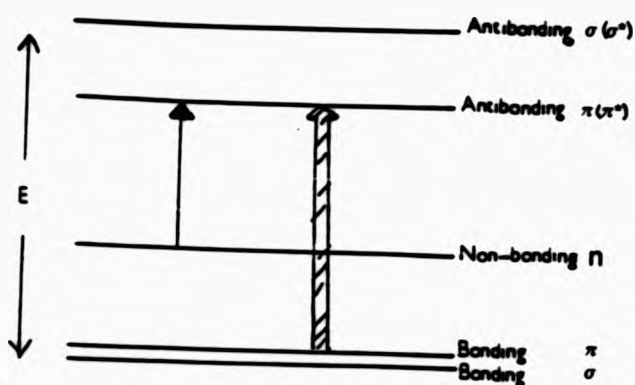
$E_{\text{vib}}$  = Energy associated with interatomic vibration

Electronic transitions are the most energetic and involve energies corresponding to UV-visible radiation. Energy absorbed produces an increase in the energy of the molecule and results in transitions of valence electrons in the molecule<sup>41,54</sup>.

Consequently, when UV/visible radiation passes through an absorbing substance, an interaction between the radiation and electrons of the absorbing species may take place. This absorption results in an increase in the energy of the electrons of the atom, ion or molecule. For molecules, the valence electrons occupy molecular orbitals of which sigma ( $\sigma$ ) and pi ( $\pi$ ) molecular orbitals are the most common.

Absorption of radiation by a molecule results in the promotion of electrons from the ground state bonding or non-bonding molecular orbitals to excited state, antibonding, molecular orbitals.

Electronic Energy Levels Representing  $n \rightarrow \pi^*$  and  $\pi \rightarrow \pi^*$  Electronic Transitions



When radiation of a specific frequency interacts with a molecule, the energy difference between the ground state and the excited state is equal to the energy given by

$$E = h\nu = hc/\lambda \quad (2.6)$$

where

$\nu$  = frequency in Hz

$h$  = Planck's constant ( $6.62 \times 10^{-27} \text{ J s}^{-1}$ )

$\lambda$  = wavelength in m

$c$  = speed of light in a vacuum ( $2.998 \times 10^8 \text{ ms}^{-1}$ )

Generally, the first step involved in predicting the absorption spectrum of a molecule is to consider its bonding (outer) electrons. The outer electrons of most organic



compounds are usually of three types:  $\sigma$ -electrons which participate in covalent bond formation,  $\pi$ -electrons, components of double and triple bonds and n-electrons which are the non-bonding electrons associated with heteroatoms such as N and O.

Excitation of  $\sigma$ -electrons requires the highest amount of energy and  $\sigma \rightarrow \sigma^*$  electronic transitions (for molecules containing single bonds) is usually restricted to the vacuum UV region below 185 nm. Saturated compounds containing atoms with unshared electrons (or non-bonding electrons) are capable of  $n \rightarrow \sigma^*$  electronic transitions. Less energy is required relative to that required for  $\sigma \rightarrow \sigma^*$  transitions and absorption of radiation in the UV region is found at longer wavelengths, i.e. between 150-250 nm.  $\pi \rightarrow \pi^*$  and  $n \rightarrow \pi^*$  transitions are the least energetic and are characteristic of conjugated systems<sup>55</sup>. Conjugation results in an increase in the number of  $\pi$  orbitals and consequently lowers the  $\pi \rightarrow \pi^*$  electronic transition. Conjugated diene species are readily detected by UV spectrophotometry.

Derivative spectrophotometry has also been employed to facilitate the resolution of overlapping absorption maxima. In derivative spectroscopy the first or higher derivative of absorbance or transmittance with respect to wavelength is recorded versus the wavelength. This may be represented as

$$A = f(\lambda) \quad (2.7)$$

then,

$$dA/d\lambda = f'(\lambda) = \text{1st derivative} \quad (2.8)$$

and

$$d^2A/d\lambda^2 = f''(\lambda) = \text{2nd derivative} \quad (2.9)$$

The derivative method results in the ability to detect and measure minor spectral features which are poorly resolved in the zero-order (absorbance) spectrum. It is particularly useful in determining the position of a peak of interest where interferences from other component peaks occur<sup>56,57</sup>.

The first-derivative of a zero-order spectrum measures the change in slope with wavelength. The second-derivative spectrum measures the slope of the first derivative spectral components.

Figure 2.2 shows the zero-order spectrum with peak (P) and its first (F) and second (S) differentials.

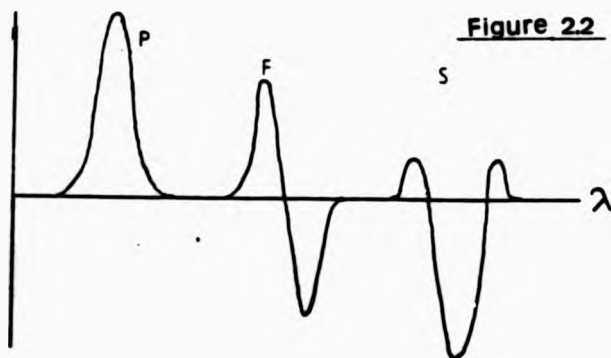


Figure 2.2

From Figure 2.2 it can be seen that the absorption maximum in the conventional spectrum appears as an absorption minimum in the second derivative spectrum.

## 2.4 <sup>1</sup>H NMR SPECTROSCOPY

### 2.4.1 Brief Theory

NMR spectroscopy is based upon the measurement of absorption of electromagnetic radiation in the radiofrequency region of the electromagnetic spectrum. In contrast to ultra-violet and infra-red absorption spectroscopy, the nuclei of atoms are involved rather than the outer electrons<sup>58</sup>.

The nuclei of certain atoms have properties of spin, magnetic moment and therefore spin angular momentum. Consequently, they behave as tiny bar magnets and can interact with an externally applied magnetic field,  $H_0$ . In the absence of a magnetic field the nuclear spins of magnetic nuclei are orientated randomly and the energy states ( $2I + 1$  discrete states, where  $I$  = spin angular quantum number) are degenerate. In the presence of a magnetic field, alignment of the nuclei occurs (with the field (more stable) or against the field (less stable since energy has to be absorbed to "flip" the proton magnet)), energy states are accessible and transitions can be induced by radiofrequency fields<sup>41</sup>.

However, the transitions only occur when the magnetic energy gap between the energy levels is exactly the same as the incoming radiofrequency i.e.  $E = h\nu$

$$\text{and } \nu = \frac{BH_0}{2\pi} \quad (2.10)$$

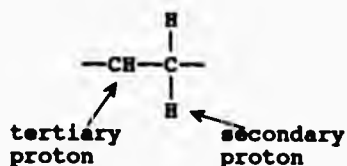
where  $h$  = Planck's constant

- $\nu$  = Frequency (Hz)  
 $H_0$  = Strength of magnetic field in gauss (G)  
 $B$  = Magnetogyric ratio, which for the proton is  
2.7927 nuclear magnetons.

In proton NMR spectroscopy, the absorption frequency is dependent on the magnetic and electronic environments of the nuclei. Protons of a given molecule have different electronic environments, and these environments generally determine the position of signals in a proton NMR spectrum<sup>59</sup>. In an applied magnetic field,  $H_0$ , the electrons surrounding the proton nucleus begin to circulate. This motion generates an induced magnetic field which opposes the applied field. Consequently, the net magnetic field at the proton nucleus is diminished, the proton is said to be shielded and absorption occurs upfield. If the induced magnetic field reinforces the applied field, the proton is deshielded and absorption is downfield. These changes in absorption are referred to as chemical shifts. Generally, as electronegativity of the surrounding atom increases, the electron density around the proton decreases resulting in deshielding<sup>59,60</sup>.

Furthermore, the appearance of a resonance in the  $^1\text{H}$  NMR spectrum of a particular chemical component is influenced by neighbouring hydrogen nuclei. The majority of  $^1\text{H}$  NMR spectra appear as doublets, triplets, quartets and so forth, i.e. "splitting" of peaks occurs. This phenomenon arises from the magnetic field associated with each individual spinning nearby proton<sup>60</sup>. For example, an NMR signal is split into a

doublet (two peaks) by one nearby proton and into a triplet by two nearby protons. Consider:



The magnetic field felt by the secondary proton is influenced by the spin of the neighbouring tertiary proton, i.e. slightly increased (when tertiary proton is aligned with the field) or decreased (when tertiary proton is aligned against the field). Consequently, absorption by the secondary proton is shifted slightly downfield for half the molecule, upfield for the other half and the signal is split into two peaks of 1:1 intensity<sup>60</sup>.

Similarly, the magnetic field "felt" by the tertiary proton is influenced by the spin of the two neighbouring secondary protons, and its  $^1\text{H}$  NMR signal is split into three peaks of 1:2:1 intensity. For three nearby protons, the  $^1\text{H}$  NMR signal is split into four peaks, i.e. a quartet.

The  $^1\text{H}$  NMR spectra of biological samples usually results in broad overlapping resonances attributable to relatively immobile macromolecular species such as proteins. Application of the Hahn spin-echo technique suppresses these broad peaks, resulting in an NMR spectrum containing well resolved resonances arising from low-molecular-mass components<sup>61</sup>.

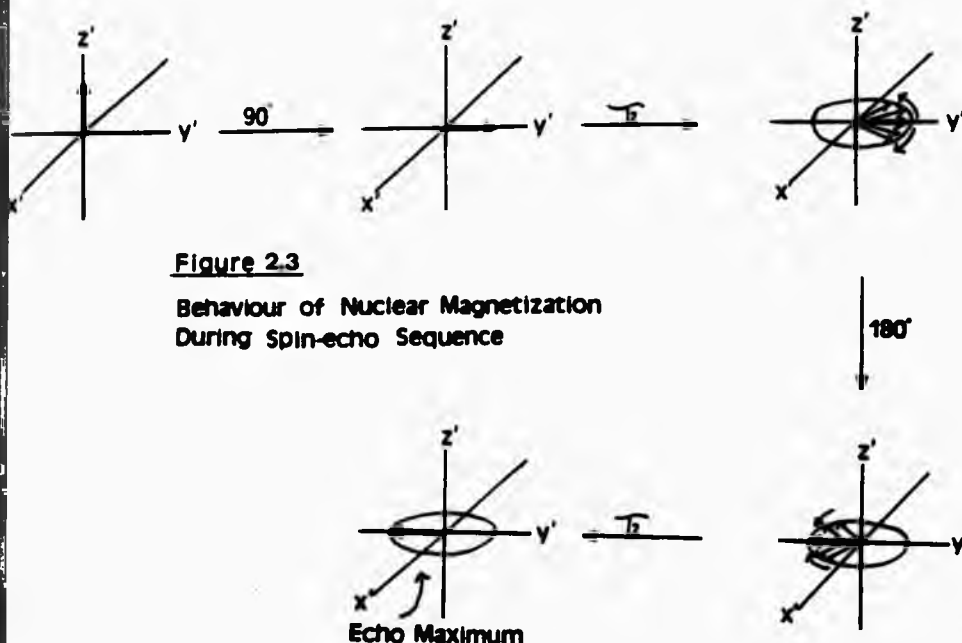
#### 2.4.2 The Proton Hahn Spin-echo Technique

The Hahn spin-echo sequence consists of a  $90^\circ$  pulse

followed by a delay interval of length  $\tau_2$ , and a pulse of  $180^\circ$  followed by a second time delay of  $\tau_2$ . It is commonly written as:

$$D[90^\circ x - \tau - 180^\circ y - \tau - \text{collect}]_n \quad (2.11)$$

A schematic representation of the Hahn spin-echo sequence is shown in Figure 2.3<sup>62</sup>.



Due to loss of phase coherence, the magnetisation vectors in the  $x'y'$  plane fan out following the  $90^\circ$  pulse. The main contributing factors are loss of phase coherence from spin-spin (transverse) relaxation and magnetic field ( $H_0$ ) inhomogeneity. Fanning out usually occurs because nuclei in

different parts of the sample precess at different rates, some slower and some faster than the average. Following the time delay  $\tau_2$ , the  $180^\circ$  pulse is applied. This has the effect of rotating all the magnetisation vectors by  $180^\circ$  about  $y'$ . The magnetisation vectors continue to precess at the same rate as before until after a time delay  $\tau_2$ , they converge and are again in phase in the  $y'$  direction. Using this technique the effect of field inhomogeneity,  $H_0$ , is eliminated.

Resolution is enhanced by the spin-echo pulse sequence due to differences in the relaxation times ( $T_2$ ) of different compounds. For example, a high-molecular-weight macromolecule usually has a short  $T_2$  value for its  $^1\text{H}$  resonances compared to those of smaller mobile molecules of higher mobility<sup>62,63</sup>. Hence by making  $\tau_2$  long enough in the spin-echo sequence, the large overlapping molecule resonances can be eliminated from the spectrum leaving a well resolved "clean" spectrum.

## 2.5 INSTRUMENTATION

Chromatography was performed on a Philips PU4015 Pye Unicam HPLC analytical system (Cambridge, England) using an Anachem S50DS1/7397 (Luton, Bedfordshire) reversed-phase column (25 cm x 4.6 mm) with an Anachem S50DS2/292 (Luton, Bedfordshire) guard column. A 20 µl injection loop (serial no. 7125, Rheodyne, California, USA) was employed.

Detection of phenols and phenolic acids was by electrochemical oxidation using an EC detector (EG+G Model 400, Princeton Applied Research, New Jersey) equipped with a glassy carbon working electrode and a Ag/AgCl reference electrode. A strip chart recorder (serial no. 196, Perkin Elmer) was used with a chart speed of 5 mm/min.

The mobile phase consisted of  $3.0 \times 10^{-2}$  mol dm<sup>-3</sup> sodium citrate/  $2.7 \times 10^{-2}$  mol dm<sup>-3</sup> sodium acetate buffer and methanol (% composition variable) and was continuously purged with helium gas during elution, (pH 4.75).

Ultra-violet/visible spectrophotometry was performed on a commercial single beam Philips PU8740 spectrophotometer (Cambridge, England).

Proton NMR measurements on prawn supernatants were conducted on a JEOL JNM-GSX 500 (University of London Intercollegiate Research Service, Biomedical NMR centre, Birkbeck College, London, U.K.) spectrometer operating at 500 MHz for <sup>1</sup>H (probe temperature 22°C). Proton NMR measurements of chemical model systems and standard amino acids were conducted on a Bruker WH 400 NMR spectrometer (University of London Intercollegiate Research Service, Queen Mary and



Westfield College, London. U.K.) equipped with a Bruker Aspect 3000 data system, operating in quadrature detection mode at 400 MHz for  $^1\text{H}$ .

## 2.6 MATERIALS

All solvents used were of HPLC or spectroscopic grade and purchased from BDH Chemicals Ltd. (Poole, Dorset). Standard phenolic acids, linoleic, linolenic, 2-thiobarbituric acids, L-methionine and DL-methionine sulphoxide were obtained from Sigma Chemical Company. All other reagents used were of the highest possible grade and obtained from commercially available sources. All food samples were purchased locally.

Standard solutions of the phenolic acids ( $1.0 \times 10^{-3}$  mol  $\text{dm}^{-3}$ ) gallic, protocatechuic, gentisic, salicylic, 4-hydroxybenzoic, catechol, vanillic, salicyluric, 3,4-dihydroxybenzaldehyde and ascorbic acid were prepared in HPLC-grade water containing  $0.05$  mol  $\text{dm}^{-3}$  HCl.

Oxidative degradation of linoleic and linolenic acids, and "Mazola" corn oil was initiated by a Fenton system containing EDTA. The final concentration of each reagent consisted of (1) EDTA ( $1.0 \times 10^{-3}$  mol  $\text{dm}^{-3}$ , 67  $\mu\text{l}$ ), (2)  $\text{H}_2\text{O}_2$  ( $3.3 \times 10^{-3}$  mol  $\text{dm}^{-3}$ , 22  $\mu\text{l}$ ) and (3)  $\text{FeSO}_4$  ( $1.0 \times 10^{-3}$  mol  $\text{dm}^{-3}$ , 67  $\mu\text{l}$ ) each added to the samples in the given order. This system initiates the peroxidation of PUFAs by generating the highly reactive  $\cdot\text{OH}$  radical.

All foodstuffs were gamma-irradiated using a Cobalt-60 source (Department of Immunology, Royal London Hospital Medical College). Samples were irradiated at doses of 2.8 and

5.0 kGy (dose rate 4.76 Gy/min.) and for each sample a non-irradiated control was also analysed.

## 2.7 EXPERIMENTAL PROCEDURES

### 2.7.1 Phenolic Acid Analysis in Celery and Strawberry : Extraction

Strawberry and celery samples were weighed and then homogenised with 10 ml water/methanol (80:20, (v/v)). The slurry was centrifuged for 30 minutes at 2500 r.p.m. After centrifuging, an internal standard (salicylic acid) at a fixed concentration, was added to aliquots (5 ml) of the aqueous layer. Each aliquot was then treated with sufficient HCl and the pH adjusted to approximately 2.0 and then extracted with three 2 ml portions of diethylether (HPLC-grade) for 10 minutes on a reciprocal shaker. The combined ether extracts were evaporated to dryness under nitrogen and the remaining residue reconstituted with water or 0.10 mol dm<sup>-3</sup> HCl prior to injection on the liquid chromatograph. A mixture of standard phenolic acids were also injected and the retention times for each determined. The electrochemical detector potential was set to +0.85 V. The extraction efficiency of the internal standard and aromatic compounds was also determined.

### 2.7.2 Calibration of Standards

A series of standard phenolic acids of increasing concentration were injected onto the column and their peak heights at each concentration noted. The internal standard

concentration in each mixture of phenolic acids was kept constant. Calibration curves were constructed by plotting the ratio of peak height of the standard to the peak height of the internal standard against the concentration of compound.

Hydrodynamic voltammograms were also constructed (plots of peak height versus electrochemical potential of the detector at a fixed concentration of compound) both for the standard phenolic acids and the sample components of strawberry and celery.

#### 2.7.3 Hydroxylation of Phenolic Acids

Phenolic acids (1 ml) of concentration  $5 \times 10^{-4} \text{ mol dm}^{-3}$  were subjected to hydroxyl radical attack generated by the Fenton system. The mixtures were incubated at room temperature for 1 hour after which an internal standard (at fixed concentration) was added. The mixture was then injected directly onto the column for analysis. The mobile phase composition was a citrate/acetate buffer and methanol mixture (95:5 v/v), and the electrochemical detector potential was set at + 0.85 V, (pH 4.75 buffer).

#### 2.7.4 Ascorbate (Vitamin C) Analysis in Irradiated Strawberry

Each strawberry sample was weighed, homogenised and centrifuged (as described in section 4.3.1). The aqueous layer (after centrifuging and acidifying) was directly injected onto the column and analysed for ascorbate. The electrochemical detector potential was set at +0.40 V.

#### 2.7.5 Determination of Conjugated Diene Species

Cyclohexane solutions of a commercial brand of corn oil (irradiated) and standard linoleic and linolenic fatty acids were analysed for conjugated diene signals using a Philips PU8740 spectrophotometer. The extracts were scanned in the 200-255 nm wavelength range and zero-order (absorbance) and second derivative (2D) spectra were recorded.

##### (a) Corn Oil Analysis

Control and irradiated samples of corn oil (10 $\mu$ l) were diluted quantitatively to 5 ml with cyclohexane (HPLC-grade) and analysed by ultra-violet/visible spectrophotometry. Since lipid peroxidation can also be stimulated by many other factors, samples of the corn oil were subjected to the following treatments:

- (a) a non-irradiated sample of corn oil was exposed to air at room temperature for a period of 24 hours
- (b) a non-irradiated sample of corn oil was heated to 60°C for 20 hours.

The nature and extent of peroxidation resulting from these three treatments was measured by monitoring conjugated diene signals over a period of time by UV spectroscopy. Each treatment was compared to a control sample kept at room temperature.

##### (b) Standard Fatty Acid Analysis

Peroxidation of linoleic and linolenic acids (of concentration  $6.40 \times 10^{-4}$  mol dm $^{-3}$ ) was initiated by hydroxyl radical generated by the Fenton system. Each fatty acid

(10ul) was sonicated with a 2 ml aliquot of water (HPLC-grade) and the Fenton reagents were added sequentially in the specified order. The solution was extracted with a 5 ml aliquot of chloroform (HPLC-grade). The chloroform extract (containing the fatty acids) was evaporated under nitrogen and the residue reconstituted with cyclohexane (5 ml).

The cyclohexane-reconstituted lipid/chloroform extracts of linoleic and linolenic fatty acids were analysed for conjugated diene signals.

#### 2.7.6 Thiobarbituric Acid (TBA) Test

##### (a) Polyunsaturated fatty acids (PUFAs)

The TBA test was performed on linoleic and linolenic fatty acids, and also on samples of the corn oil subjected to the various peroxidation treatments. In each case a control and a peroxidised sample was reacted with TBA.

Each sample (10  $\mu$ l) was sonicated with a 2 ml aliquot of water (HPLC-grade). The Fenton system reagents were then added. The mixture was treated with glacial acetic acid (3 ml) and 1% thiobarbituric acid (1 ml), and the mixture heated at 95°C for a period of 15-20 min. for the development of a pink-coloured chromogen. The spectrum of each sample was recorded in the 350-700 nm wavelength region.

##### (b) Carbohydrates

The TBA test was carried out on a range of sugars and compounds putatively derived from their radiolytic damage. The compounds investigated were glucose, fructose, sucrose, lactose, maltose, galactose, ribose, arabinose, 2-

Deoxyribose, glyoxal, gluconic acid, glyceraldehyde and glycollaldehyde. Solutions of concentration  $1.0 \times 10^{-3}$  mol  $\text{dm}^{-3}$  were prepared and 1.00 ml aliquots subjected to an OH radical flux generated by the Fenton system prior to analysis with TBA.

#### 2.7.7 Analysis of Prawn Supernatants by $^1\text{H}$ NMR Spectroscopy

##### **(a) Preparation of Prawn Sample Supernatants**

The prawn samples (either fresh shelled or frozen de-shelled) were weighed, homogenised in 10 ml of doubly-distilled water and then centrifuged at 3,800 r.p.m. for a period of 30 min. After centrifuging, a 7.0 ml aliquot of the clear supernatant was divided into ten 0.70 ml portions. All samples were labelled and five were subjected to gamma-irradiation treatment (5.0 kGy). The remaining five of these samples served as non-irradiated controls.

##### **(b) NMR Measurements on Prawn Supernatants**

0.60 ml of homogenised prawn supernatant (untreated or gamma-irradiated) were transferred to a 5 mm diameter NMR tube, to which was added 0.08 ml deuterium oxide ( $^2\text{H}_2\text{O}$ ). The Hahn Spin-echo sequence was repeated 128 times and chemical shifts were referenced to external sodium-3-(trimethylsilyl)-1-propanesulphonate (TSP,  $\delta = 0.00$  ppm).

##### **(c) NMR Measurements on Chemical Model Systems**

Standard solutions of L-methionine and DL-methionine sulphoxide of concentration  $0.10$  mol  $\text{dm}^{-3}$  were made up in doubly-distilled water. 0.60 ml of each sample was placed into a 5 mm diameter NMR tube, to which was added 0.07 ml of



$^2\text{H}_2\text{O}$ . Single-pulse  $^1\text{H}$  spectra were recorded and chemical shifts referenced to external TSP.

**CHAPTER 3**

**RADIOLYTIC DAMAGE TO**  
**AROMATIC COMPOUNDS**  
**AND VITAMIN C**



### 3.1 AROMATIC HYDROXYLATION

The hydroxyl radical (a primary radiolytic species) is an electrophilic reagent capable of attacking aromatic compounds. It may be produced chemically by reaction between two reagents (e.g.  $\text{Fe}^{2+}$  and  $\text{H}_2\text{O}_2$  in the Fenton reaction, equation 3.1), photochemically by UV light, or radiolytically by high energy ionising radiation<sup>4</sup>.



Homolytic fission of the O—O bond in the  $\text{H}_2\text{O}_2$  molecule (in the presence of a metal ion catalyst) produces the hydroxyl radical ( $\cdot\text{OH}$ ). In biological systems,  $\cdot\text{OH}$  radical production has been postulated to result from the interaction of the superoxide radical anion ( $\text{O}_2^{\cdot-}$ ) with hydrogen peroxide ( $\text{H}_2\text{O}_2$ ) in the presence of chelated metal ions, traces of which are present in certain biochemical systems<sup>64,65</sup>. The  $\cdot\text{OH}$  radical is extremely reactive and is capable of reacting with almost any molecule present in biological systems.

In unsaturated compounds free radicals are capable of initiating reactions such as polymerization or hydrogen abstraction. In aromatic compounds (e.g. phenols, phenolic acids and the amino acid phenylalanine), the  $\cdot\text{OH}$  radical reacts predominantly by addition to the ring resulting in the formation of a mixture of hydroxylated products<sup>66</sup>. The extent of the chemical reaction in any system depends upon the dose of gamma-radiation applied.

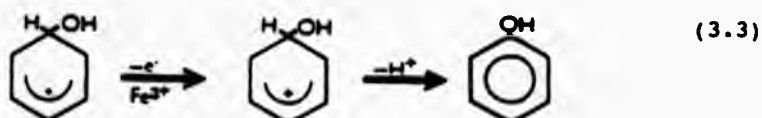
### 1.2 MECHANISM OF AROMATIC HYDROXYLATION

The mechanism of aromatic hydroxylation has been previously studied in some detail<sup>67</sup>. The reaction of the hydroxyl radical with aromatic compounds proceeds by an electrophilic substitution mechanism. The  $\cdot\text{OH}$  radical reacts with benzene and substituted benzenes by addition to the ring (a hydrogen atom is substituted and the reaction involves the rate-determining formation of an intermediate) and the pattern of  $\cdot\text{OH}$  attachment to the ring is dependent upon the electron-donating/withdrawing properties of the substituents<sup>67</sup>.

The reaction with benzene illustrates the general behaviour of unsaturated and aromatic molecules. The reaction of the hydroxyl radical with an aromatic nucleus (a reaction characteristic of the primary species) initially yields the hydroxycyclohexadienyl radical<sup>67</sup>, (equation 3.2).

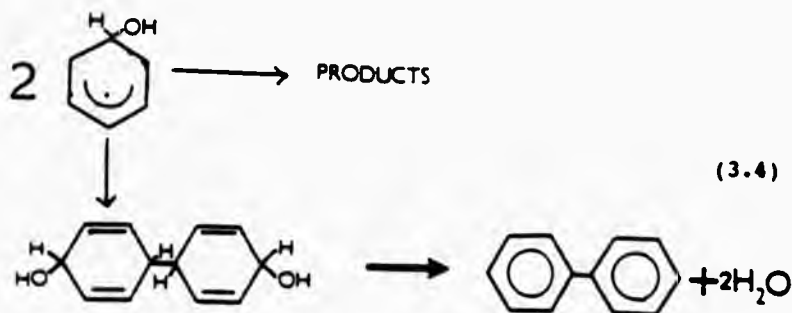


This radical is rapidly oxidised to phenol in the presence of a suitable oxidant, e.g. a transition metal ion complex, (equation 3.3).



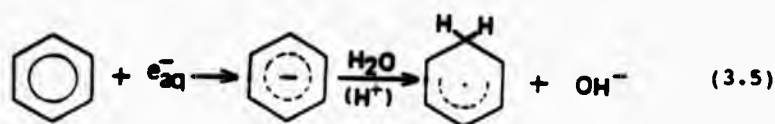
The hydroxyl radical reacts with benzene at a diffusion-limited rate of  $k_2 = 8 \times 10^9 \text{ mol}^{-1} \text{ dm}^3 \text{ s}^{-1}$  (where  $k_2$  is the second-order rate constant i.e. rate =  $k_2 [\text{OH}] [\text{benzene}]$ ) and with phenol ( $k_2 = 1.4 \times 10^{10} \text{ mol}^{-1} \text{ dm}^3 \text{ s}^{-1}$ ). The presence of the -OH group in phenol directs the polar  $\text{OH}$  radical to the *para*, *ortho* (predominantly) and *meta* positions in a ratio of 9:6:1 to initially form dihydroxycyclohexadienyl radicals<sup>67</sup>.

Dimers of hydroxycyclohexadienyl radicals can also form from  $\text{OH}$  radical attack on benzene by recombination, eliminating water to yield biphenyl (equation 3.4).

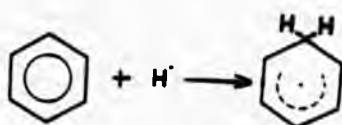


A series of complex reactions are therefore initiated. Hydrated electrons and hydrogen atoms also react with aromatic compounds (equations 3.5 and 3.6).

For example,



$$k_2 = 1.3 \times 10^4 \text{ mol}^{-1} \text{ dm}^3 \text{ s}^{-1}$$



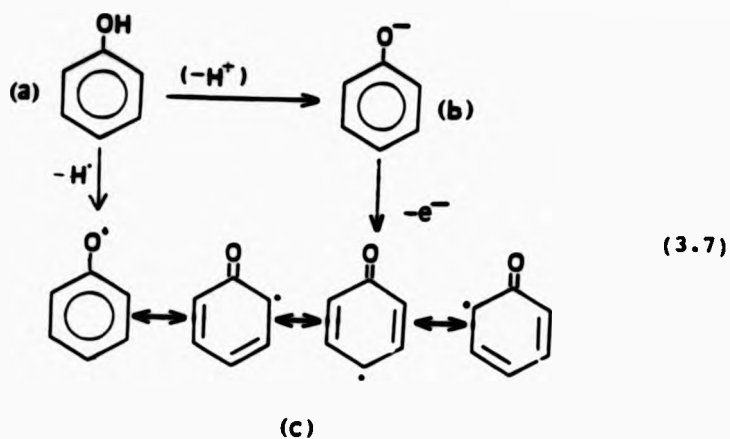
(3.6)

$$k_2 = 9.1 \times 10^5 \text{ mol}^{-1} \text{ dm}^3 \text{ s}^{-1}$$

The products formed by the cyclohexadienyl radicals generated above (equations 3.5 and 3.6) include cyclohexadienes and reduced biphenyls<sup>3</sup>. Discussion here however, has been limited to the reactivity of the hydroxyl radical.

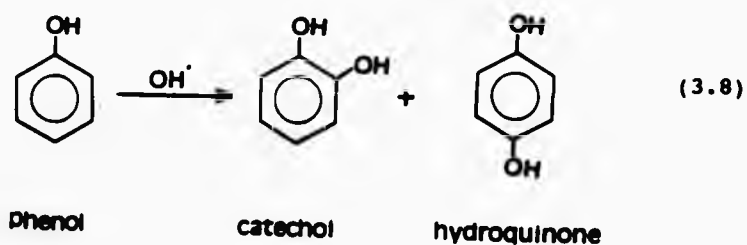
### 3.3 ELECTROCHEMICAL OXIDATION OF PHENOLS

Hydroxylated aromatic species are readily identified and separated from other phenolic constituents present in extracts of plant-derived foodstuffs by reversed phase HPLC and detected by electrochemical oxidation<sup>68,69,70</sup>. One major characteristic property of phenols and phenolic components is their facile oxidative conversion to quinone species. As the number of hydroxyl groups increase and hence the polarity of the compound, phenolic compounds become more susceptible to oxidation. Oxidation occurs by a one-electron abstraction. For example, for phenol itself oxidation results in the generation of a phenoxy radical. One pathway involves the initial formation of a phenoxide anion (by heterolytic cleavage of the O-H bond in phenol (a) equation 3.7), and the phenoxy radical, (c) results either from the loss of hydrogen atom or the loss of an electron from the corresponding phenoxide anion<sup>71</sup>, (b).

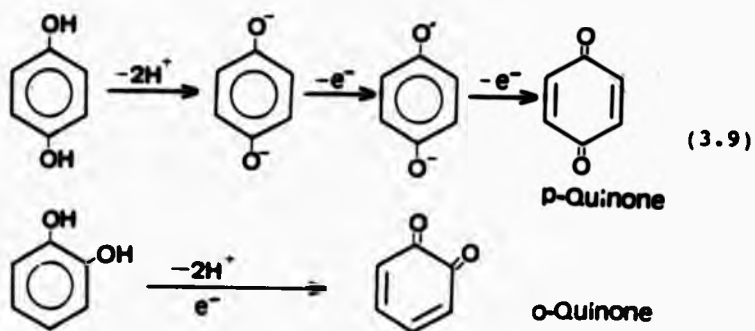


The phenoxide anion is resonance stabilised by delocalisation of the unpaired electron over the aromatic ring.

The hydroxylation of phenol takes place almost exclusively at the *o*- and *p*- positions (i.e. the -OH group is *o/p* directing<sup>72</sup>), and to a lesser extent at the *m*- position (9:6:1 for *p*:*o*:*m* product concentration ratio).



Both catechol and hydroquinone undergo oxidation and in so doing are converted to the corresponding *o*- and *p*- quinones. The reaction generally consists of a one-electron transfer with the formation of a semiquinone radical (equation 3.9).



All phenols and phenolic acids have a characteristic optimum redox potential at which oxidation occurs, and thus the technique of electrochemical detection has the necessary selectivity required in the detection of these compounds.

#### 1.4 DETECTION OF 'OH RADICAL IN BIOLOGICAL SYSTEMS

Since hydroxyl radicals are very highly reactive, proving their radiolytic generation in biochemical systems is correspondingly difficult. The formation of the 'OH radical has been previously investigated in a number of studies by investigating its reactions with a range of compounds, including its ability to degrade tryptophan<sup>73</sup>, convert methional to ethene<sup>74</sup> and deoxyribose to thiobarbituric acid-reactive material<sup>75</sup>.

An alternative approach in which 'OH radicals can be conveniently detected is by their ability to hydroxylate aromatic compounds, of which salicylic acid and phenol are the most extensively studied. The hydroxylated products have been detected by colorimetry<sup>64</sup>, gas-liquid chromatography (a method for the separation of hydroxylated products of phenol involving pre-column derivatisation<sup>76</sup>) and more conveniently by high performance liquid chromatography (HPLC) coupled with electrochemical detection (ECD)<sup>77,78</sup>. In the majority of systems studied, 'OH radical production was achieved by the Fenton reaction or by a superoxide radical-generating system.

Furthermore, the technique of aromatic hydroxylation has been employed in medically-orientated studies as a means of measuring 'OH radical production *in vitro*<sup>79,80</sup> and *in vivo*<sup>81</sup>.

The reaction of 'OH radical with a range of biomolecules in foodstuffs may also result in the formation of hydroxylated products. Some of these products may be unique to irradiated foods and consequently may be useful as marker molecules for their detection.

A wide range of aromatic compounds are found to occur in various foodstuffs (Table 3.1). For example, foods containing or derived from plant tissues contain phenols such as catechol, and phenolic acids such as salicylic, 4-hydroxybenzoic, gallic and gentisic acids, some of which have been identified in plant materials and commercial beverages by HPLC coupled with ECD<sup>82-84</sup>. The suitability of these species as aromatic detector molecules for irradiated foods depends primarily upon the nature and extent of the products generated by  $\cdot\text{OH}$  radical attack.

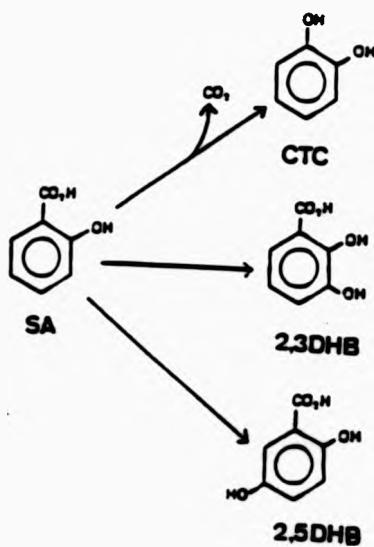
Attack of  $\cdot\text{OH}$  radical may result in hydroxylation, decarboxylation or dehydrogenation of aromatic compounds. For example, attack of  $\cdot\text{OH}$  radical on salicylic acid produces 2,3-dihydroxybenzoate (49%), 2,5-dihydroxybenzoate (40%) by hydroxylation and catechol (11%) by decarboxylation<sup>78,85</sup> (Figure 3.1). 2,3-dihydroxybenzoate has been proposed as a marker of  $\cdot\text{OH}$  radical production *in vivo*.

Another compound which has been studied extensively as an aromatic detector molecule is the naturally occurring amino acid phenylalanine, present in proteins of various meat products. Hydroxylation of phenylalanine results in the formation of 3 isomers: *para*-, *ortho*- and *meta*- tyrosine, and hydroxylation of *p*-tyrosine leads to the formation of 3,4-dihydroxyphenylalanine (DOPA<sup>86,87</sup>). *P*- Tyrosine and DOPA are found to occur naturally in non-irradiated meat tissues and are therefore not used as radiolytic markers<sup>87</sup>. However, *o*- and *m*- tyrosine isomers of phenylalanine have been proposed



as markers of irradiation<sup>88</sup>, although very small levels of these isomers have been reported to occur naturally in non-irradiated meat<sup>89</sup>. This may be attributable to the presence of the enzyme tyrosine hydroxylase which is known to produce small quantities of these compounds<sup>90</sup>. Radiolytic modifications of other aromatic amino acids such as tryptophan and tyrosine have also been studied<sup>91</sup>.

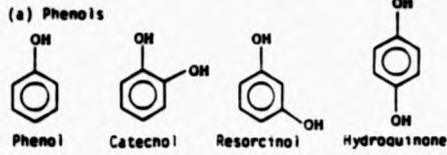
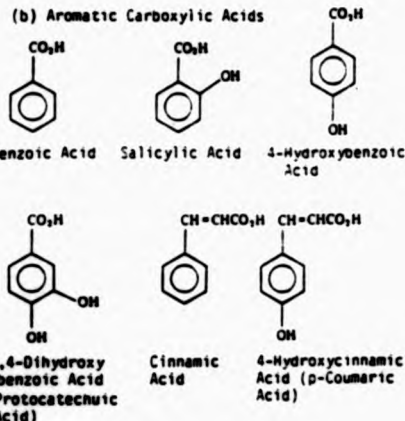
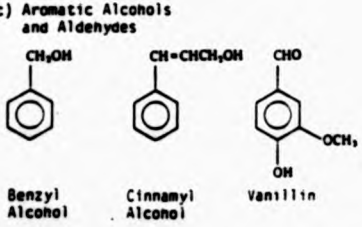

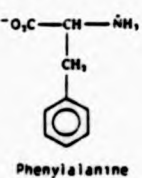
Figure 3.1



**'OH RADICAL ATTACK ON SALICYLIC ACID**

**Table 3.1**

**AROMATIC COMPOUNDS OCCURRING IN FOODSTUFFS**

<p>(a) Phenols</p>  <p>Phenol      Catechol      Resorcinol      Hydroquinone</p>	<p>present in the free state and as monoglucosides in plant-derived foodstuffs, e.g. tea</p>
<p>(b) Aromatic Carboxylic Acids</p>  <p>Benzoic Acid      Salicylic Acid      4-Hydroxybenzoic Acid</p> <p>3,4-Dihydroxybenzoic Acid (Protocatechuic Acid)      Cinnamic Acid      4-Hydroxycinnamic Acid (p-Coumaric Acid)</p>	<p>present in plant tissues (e.g. strawberries, lettuce, celery, onions, potatoes and coffee beans) as simple salts or as esters, the latter occurring in essential oils, gums and resins.</p>
<p>(c) Aromatic Alcohols and Aldehydes</p>  <p>Benzyl Alcohol      Cinnamyl Alcohol      Vanillin</p>	<p>present in the free state and as esters in foodstuffs of plant origin</p>
<p>(d) Aromatic Amines</p>  <p>Tyramine</p>	<p>present in large amounts in cheese and yeast extract</p>
<p>(e) Aromatic Amino Acids</p>  <p>Phenylalanine</p>	<p>naturally occurring amino acid that is present in proteins in a variety of meat and fish products.</p>

#### 1.4.1 'OH Radical Attack on DNA

DNA is an important target for attack of 'OH radical and is found to occur in a large number of foodstuffs. For example, it is present in calf thymus (2.3%), meat and liver (0.2-0.4%), and fish (0.2%).

DNA is a long chain polymer built up by the extended repetition of deoxyribonucleotides, each composed of a purine and pyrimidine base, a 5-Carbon sugar (2-deoxy-D-ribose) and a phosphate group. The preferential site of attack of radiolytically-generated hydrated electrons ( $e^-_{aq}$ ) and hydrogen atoms (H) is with the base moieties. However, for the 'OH radical, 25% of the reaction is with the sugar component although the major reaction occurs with the base moieties<sup>92</sup>.

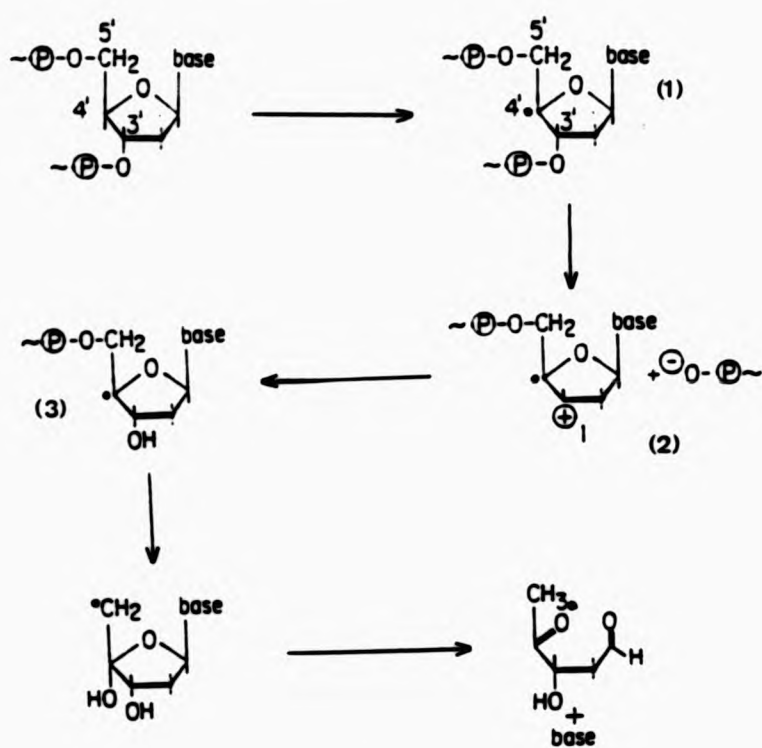
'OH attack on DNA results in a number of chemical modifications, in particular free radical-induced base damage to DNA. In previous studies, the 'OH radical has been generated by ferric ion chelates in the presence of hydrogen peroxide<sup>29</sup>. Damage to DNA results in the release of a large number of modified purine and pyrimidine base products which have been identified by the use of gas chromatography and mass spectrometry (GC-MS<sup>31,32</sup>).

The free radicals generated may also cause oxidation of the deoxyribose moiety in DNA. Oxidation results in the formation of malondialdehyde (MDA) which reacts with thiobarbituric acid (TBA) to form the 2:1 TBA-MDA adduct. This adduct can be identified by chromatographic techniques

together with absorbance or fluorescence spectroscopy<sup>93</sup>. MDA is also a product of the lipid peroxidation process<sup>94</sup>.

In addition, the  $\cdot\text{OH}$  radical can also cause single and double strand breakages in the DNA molecule (i.e. scission of the sugar-phosphate bond occurs, an event probably induced by the sugar radicals<sup>35</sup>). These sugar radicals are formed by hydrogen abstraction, which can occur at all five positions of the sugar molecule (Figure 3.2). The sugar radical (1) eliminates the phosphate ester anion at the C-3 and C-5 positions, thereby breaking the chain and forming a radical cation (2). This radical cation forms another radical (3) and elimination of a second phosphate group then occurs. The radical is eventually terminated in disproportionation reactions with other radicals. Ring opening occurs followed by the elimination of the base leading to DNA strand breakage<sup>92</sup>.

Figure 3.2



Sugar Radical Formation in DNA Leading to Strand Breakage

### 1.5 ·OH RADICAL ATTACK ON VITAMIN C

Aromatic compounds are not the only species attacked by ·OH radicals. Indeed, certain compounds of nutritional significance may also be affected, for example, vitamins. These are generally divided into water- or fat-soluble vitamins, i.e. the medium in which they are soluble determines the possible types of radical reactions in which they participate. The two most studied vitamins are vitamin C (water-soluble) and vitamin E (or tocopherols, fat-soluble) as both are extremely radiation sensitive and are chemically modified following irradiation<sup>68,95</sup>.

Vitamin C (ascorbic acid) is abundant in fruits and vegetables (for example strawberries contain 50mg of vitamin C per 100g weight of fruit). Some is also found in animal products including milk, liver and kidney at concentrations of 10-300ug/g<sup>95</sup>. The ascorbate ion is an important naturally occurring radical scavenger and consequently offers some protective mechanism against radical species (for example, the superoxide radical anion,  $O_2^-$  and the ·OH radical) which may form in biochemical systems. In addition, it is a powerful electron donor (reducing agent) and is readily destroyed due to its ability to act as a powerful antioxidant<sup>96</sup>. It reacts rapidly with ·OH radical (produced by radiolysis of water) to form the semi-dehydroascorbate radical which disproportionates to ascorbate and dehydroascorbate. Dehydroascorbate is itself unstable and breaks down to L-threonic and oxalic acid by a complex

mechanism (Figure 3.3).

Many studies have shown that irradiating fruits and vegetables causes substantial depletion of vitamin C content<sup>40,97</sup>. The extent of loss is dependent upon the dose of irradiation and its pre-irradiation concentration<sup>98</sup>.

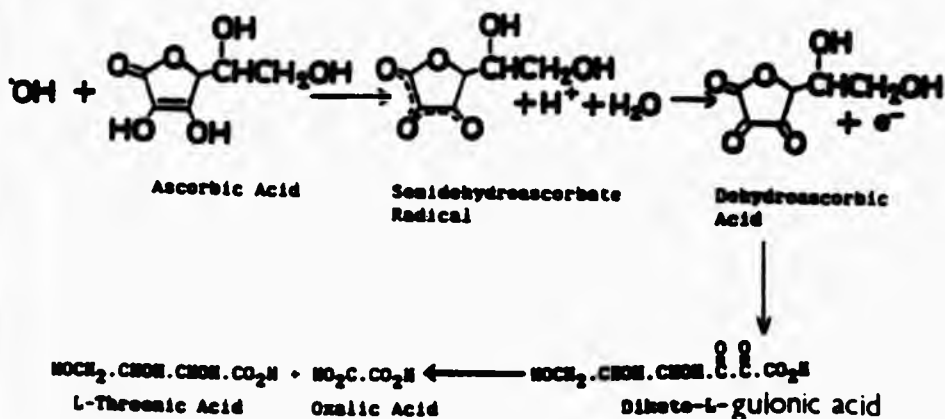


Figure 3.3

HPLC in combination with ECD has been utilised for the identification and quantification of phenolic constituents present in extracts of celery and strawberry homogenates prior and subsequent to gamma-irradiation.

The hydroxylated products produced by  $\cdot\text{OH}$  radical attack on standard phenolic acids have also been analysed by these techniques. The results obtained are outlined and discussed in the next section. Additionally, the vitamin C content of fresh strawberries prior and subsequent to gamma-irradiation treatment has also been determined.

## 3.6 RESULTS

### 3.6.1 Hydroxylation of Standard Phenolic Acids

A wide range of phenolic acids are known to occur in fruits and vegetables. Exposure of these species to a source of ionising radiation results in the formation of hydroxylated phenolic components. Prior to the analysis of irradiated samples of plant-derived foodstuffs, standard solutions of naturally occurring phenolic acids were treated with a hydroxyl radical flux generated by the Fenton system. The products of hydroxyl radical attack on each phenolic acid were determined by comparisons of their relative retention times to those of standard phenolic acids.

#### (a) Attack of 'OH Radical on 4-Hydroxybenzoic and Protocatechuic Acids

Figure 3.4 shows the chromatogram of a mixture of standard phenolic acids (including salicylic as the internal standard (IS) at a concentration of  $2.00 \times 10^{-4} \text{ mol dm}^{-3}$ ). Their relative retention times (under the experimental conditions stated) are shown in Table 3.2. Figures 3.5(a) and (b) show the chromatograms of a standard control sample of 4-hydroxybenzoic acid (4-HB) and a corresponding sample subjected to the 'OH radical generating system.

A comparison of Figures 3.5(a) and (b) demonstrates that as a consequence of 'OH radical attack, the concentration of 4-HB decreases from  $440 \mu\text{M}$  to  $6.0 \mu\text{M}$ , with the formation of a new peak "b", the relative retention time of which is 0.372. This peak is attributable to protocatechuic acid (for



standard PCA the relative retention time is 0.370). Its calculated concentration in the  $\cdot\text{OH}$  radical-modified sample is  $62 \mu\text{M}$ , (typical chromatogram for  $n=10$  determinations).

Consequently, attack of  $\cdot\text{OH}$  radical on 4-HB yields protocatechuic acid (PCA). Peak "a" in Figure 3.5(b) is attributable to hydrogen peroxide utilised in the Fenton reaction system. PCA may be further attacked by  $\cdot\text{OH}$  radical resulting in the production of 1,2,4-trihydroxybenzene (1,2,4-THB). Although there is no direct evidence for this reaction, 1,2,4-THB is an expected product arising via a decarboxylation mechanism. These reactions are depicted in Figure 3.5(c).

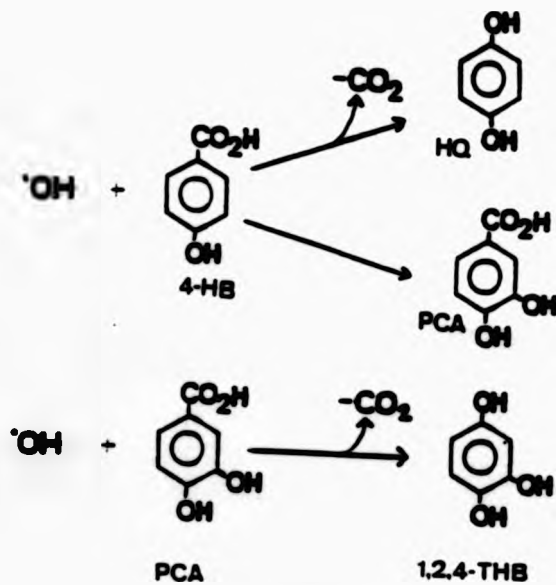
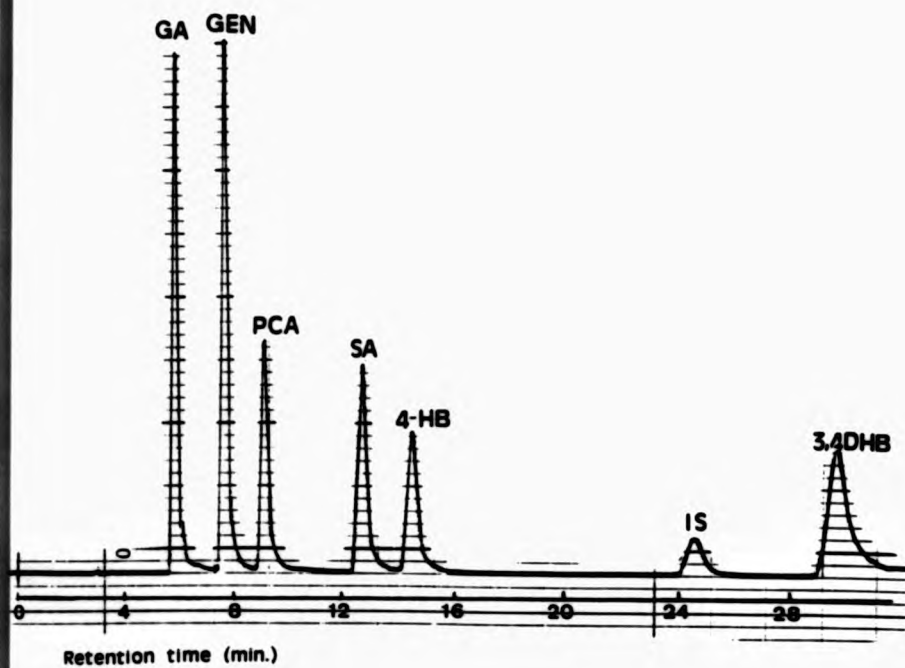


Figure 3.5(c)

**Figure 3.4**



Reversed phase HPLC chromatogram of a standard mix of phenolic acids (500  $\mu\text{M}$ ). Mobile phase composition 95:5 citrate/acetate buffer: methanol. ECD potential +0.85v and sensitivity 1.0  $\mu\text{A}$ .

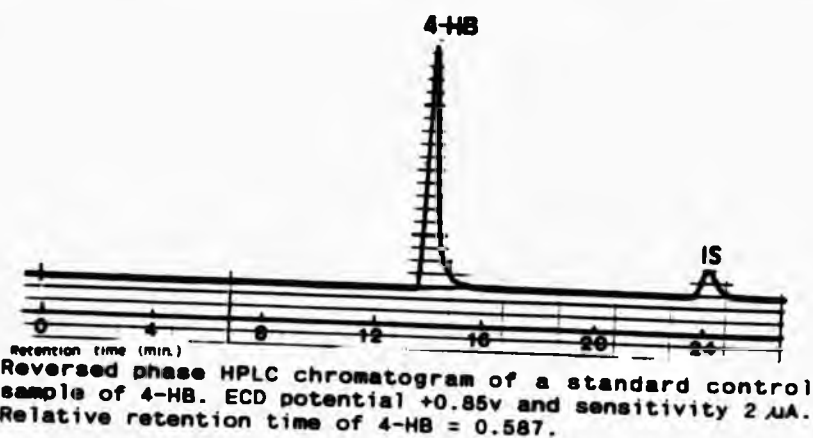
**TABLE 3.2**

**Relative Retention Times of Standard Phenolic Acids in Figure 3.4**

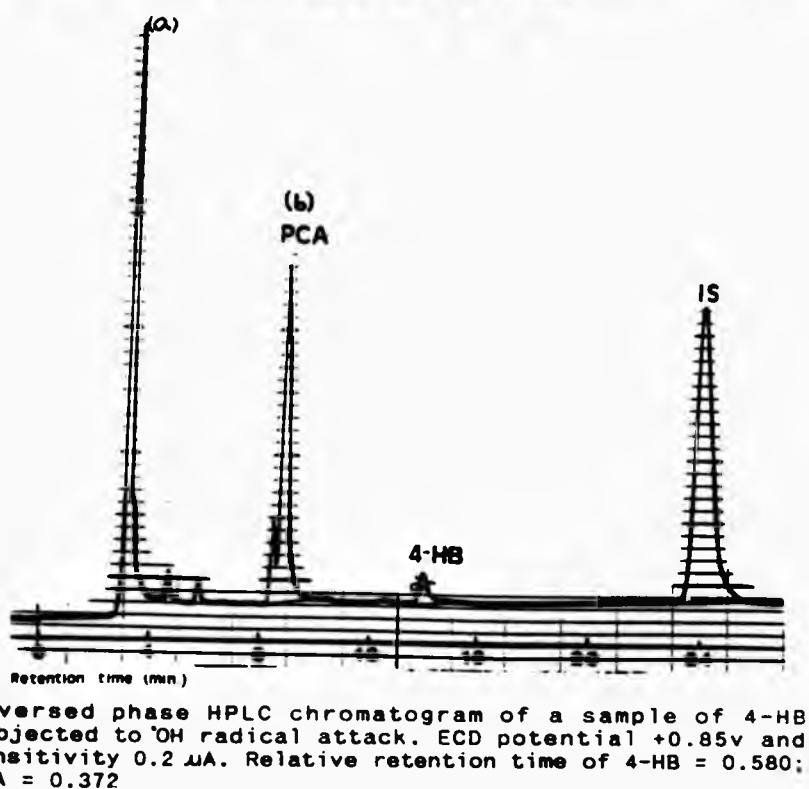
Phenolic Acid	Relative Retention Time
GA = Gallic	0.236
GEN = Gentisic	0.309
PCA = Protocatechuic	0.370
SA = Salicylic	0.521
4-HB = 4-Hydroxybenzoic	0.585
IS = Internal Standard	1.000
3,4- DHB = 3,4-Dihydroxybenzaldehyde	1.203

**Figure 3.5**

(a)



(b)



(b) Attack of  $\cdot\text{OH}$  Radical on Salicylic Acid

A suitable and most studied aromatic compound frequently used as a detector molecule for  $\cdot\text{OH}$  radical activity is salicylic acid (SA)<sup>76,78,85</sup>. Figures 3.6(a), (b) and (c) show chromatograms of standard control SA, (a) and a sample subjected to  $\cdot\text{OH}$  radical attack, the products of which were detected at an oxidation potential of +0.85 V, (b) and at +0.65 V, (c). The products of hydroxyl radical attack on SA include 2,3- and 2,5- dihydroxybenzoates (2,3 and 2,5-DHB) and catechol<sup>70</sup> (CTC), (Figure 3.6(d)). Both CTC and SA have the same retention time (under the experimental conditions specified in Figure 3.6(b)) and are therefore distinguished by their difference in oxidation potential. Table 3.3 shows the comparison of Figures 3.6(a), (b) and (c) and Figure 3.7 shows the chromatogram of a standard mix of phenolic acids containing 2,3-DHB and CTC.

As a consequence of  $\cdot\text{OH}$  radical attack, the concentration of SA decreases from 310  $\mu\text{M}$  in the control sample to 64.5  $\mu\text{M}$  in the treated one (Figures 3.6(a) and (b)). Figure 3.6(c) shows the chromatogram of the treated SA sample run at an oxidation potential of 0.65V. At this potential SA is not detectable and peak "d" corresponds to CTC only.

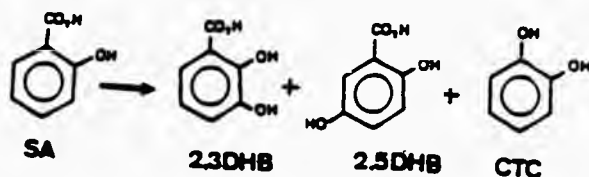
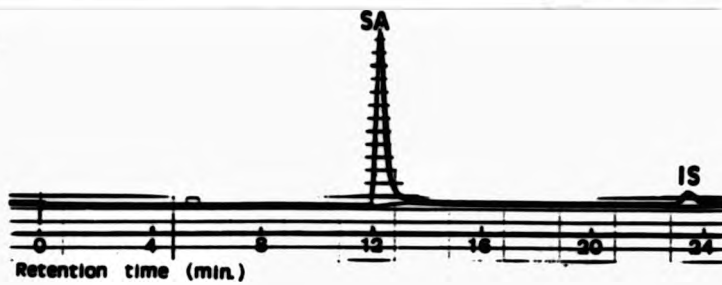


Figure 3.6(d)

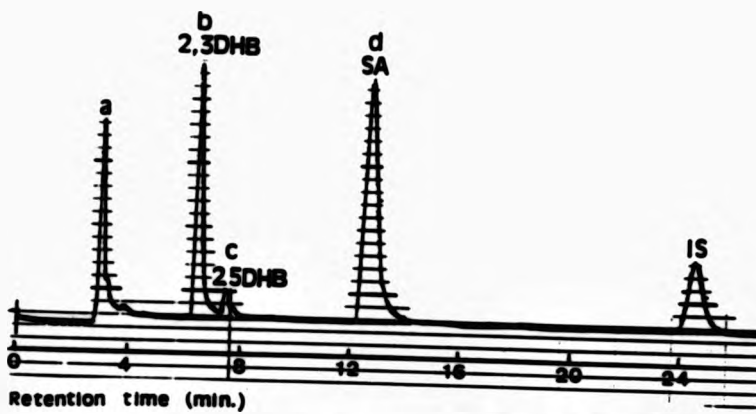
**Figure 3.6**

(a)



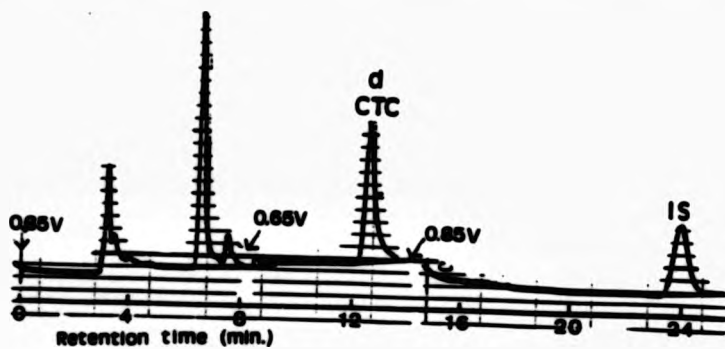
Reversed phase HPLC chromatogram of a standard control sample of salicylic acid. ECD potential +0.85v and sensitivity 5  $\mu$ A.

(b)



Reversed phase HPLC chromatogram of a sample of salicylic acid subjected to  $^{\bullet}$ OH radical attack. ECD potential +0.85v and sensitivity 0.5  $\mu$ A. Mobile phase composition: 95% (v/v) 30 mmol.  $\text{dm}^{-3}$  sodium citrate/ 27.7 mmol.  $\text{dm}^{-3}$  sodium acetate buffer, pH 4.75 and 5% (v/v) methanol at a flow rate of 1.0  $\text{ml min}^{-1}$ .

(c)



Reversed phase HPLC chromatogram of a sample of salicylic acid subjected to  $^{\bullet}$ OH radical attack. ECD oxidation potential at +0.85v and +0.65v. ECD sensitivity: 0.5  $\mu$ A.

**TABLE 3.3 Hydroxylation Products Generated From the Reaction of Salicylic acid with  $\cdot\text{OH}$  Radical: A Comparison of the Chromatograms of Figures 3.6(a), (b) and (c)**

**Figure 3.6 (a) - Salicylic control detected at +0.85 v**

Components	Relative retention time	Concentration of Acid (Maximum Sensitivity 0.5 $\mu\text{A}$ )
SA	0.521	310 $\mu\text{M}$
IS	1.000	25 $\mu\text{M}$

**Figure 3.6 (b) - Salicylic hydroxylated detected at +0.85 v**

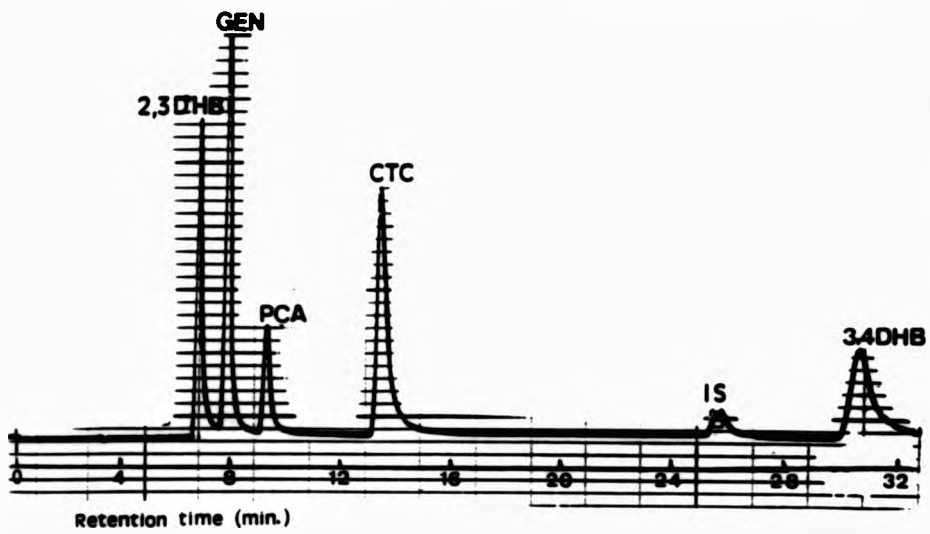
Components	Relative retention time	Concentration of Acid (Maximum Sensitivity 0.5 $\mu\text{A}$ )
a= $\text{H}_2\text{O}_2$	0.132	36 $\mu\text{M}$
b= 2,3DHB	0.262	45.5 $\mu\text{M}$
c= 2,5DHB	0.307	6.0 $\mu\text{M}$
d= SA	0.516	64.5 $\mu\text{M}$
IS	1.000	26.0 $\mu\text{M}$

**Figure 3.6 (c) - Salicylic hydroxylated detected at +0.65 v**

Components	Relative retention time	Concentration of Acid (Maximum Sensitivity 0.5 $\mu\text{A}$ )
peak d	0.525	25.0 $\mu\text{M}$
IS	1.000	26.0 $\mu\text{M}$

Peak d = CTC = catechol

**Figure 3.7**



Reversed phase HPLC chromatogram of a standard mix of phenolic acids. Relative retention time for 2,3-DHB = 0.260 and for CTC = 0.523. ECD potential at 0.65v.



**(c) Attack of  $\cdot\text{OH}$  Radical on 3,4-Dihydroxybenzaldehyde**

Attack of  $\cdot\text{OH}$  radical on 3,4-dihydroxybenzaldehyde (3,4-DHB) results in the formation of a compound with a relative retention time of 0.37 (Figures 3.8(a) and (b)). Although the precise identity of this compound is unclear, it appears that from HPLC relative retention time data and the "spiking" technique (data not shown) that this compound is likely to be PCA.

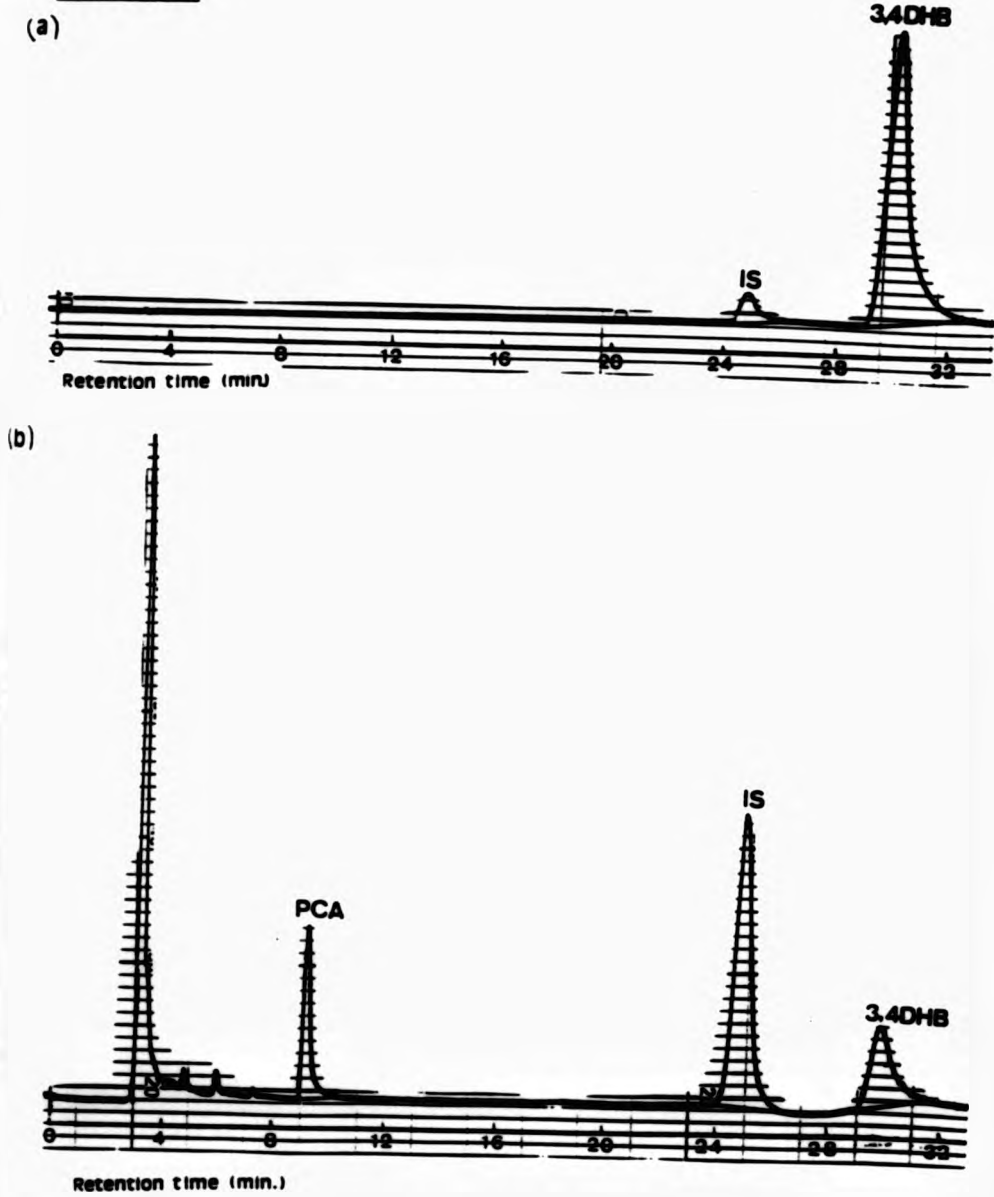
Proton and carbon-13 nuclear magnetic resonance (NMR) spectra of 3,4-DHB before and after exposure to an  $\cdot\text{OH}$  radical generating system provided further evidence that PCA may indeed be a product derived from  $\cdot\text{OH}$  radical attack on 3,4-DHB.

Figures 3.9(a), (b) and (c) show the  $^{13}\text{C}$  NMR spectra obtained for control samples of (a) 3,4-DHB and (b) PCA and (c) a sample of 3,4-DHB following treatment with the  $\text{Fe(II)/EDTA/H}_2\text{O}_2$  radical-generating system. The chemical shift values for the functional groups in the samples studied are listed in Table 3.4. The resonance at 197 ppm (Figures 3.9(a) and (c)), attributable to the aldehyde group carbon in 3,4-DHB, markedly decreases in intensity following treatment of 3,4-DHB with an  $\cdot\text{OH}$  radical. In addition, the signal at 126 ppm (marked by the arrow, Figure 3.9(b)) in control PCA, is also present in the spectrum of treated 3,4-DHB (Figure 3.9(c)), indicating the formation of PCA from 3,4-DHB subsequent to  $\cdot\text{OH}$  radical attack. This resonance was absent in spectra of control 3,4-DHB.

Figures 3.9(d), (e) and (f) show the proton NMR spectra

obtained for the three samples. The proton of the aldehyde group (in 3,4-DHB) absorbs far downfield at 9.63 ppm. The intensity of this resonance was found to decrease substantially following attack of  $\cdot\text{OH}$  radical attack on 3,4-DHB. These signals are broad, a consequence of iron (III) chelation by 3,4-DHB and any products derived from the interaction of  $\cdot\text{OH}$  on this molecule.

**Figure 3.8**

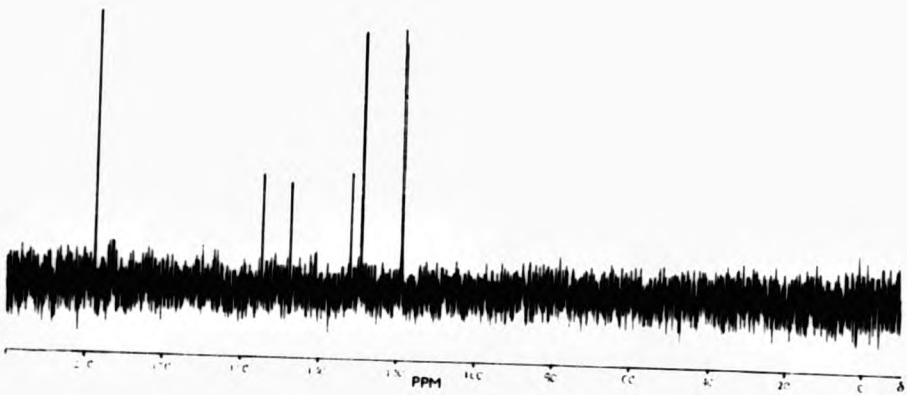


Reversed phase HPLC chromatogram of standard 3,4-dihydroxybenzaldehyde (a) before (ECD sensitivity 2  $\mu$ A) and (b) after exposure to an  $\cdot$ OH radical generating system (ECD sensitivity 0.2  $\mu$ A). ECD potential = 0.85 V.

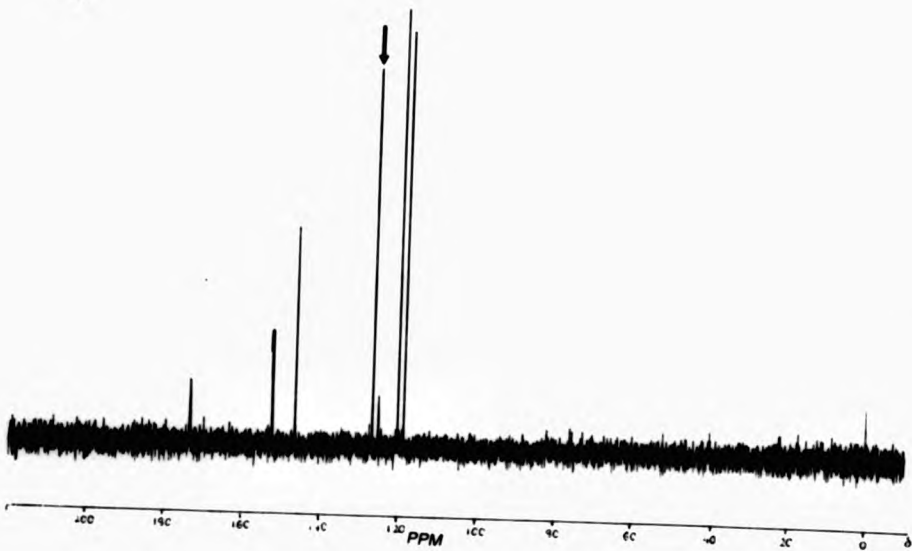


Figure 3.9

(a)



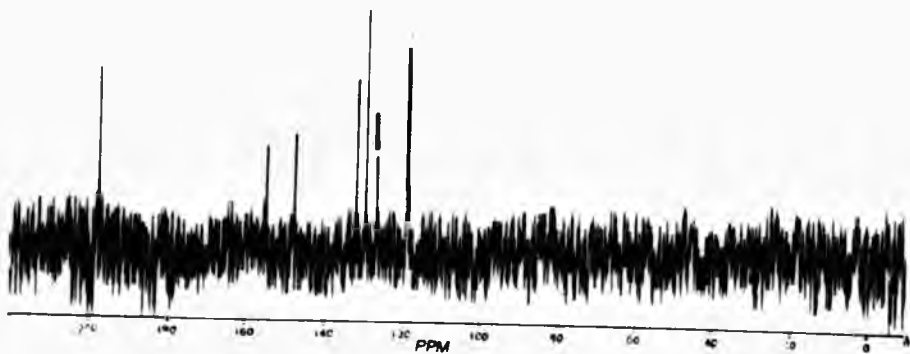
(b)



Carbon-13 magnetic resonance spectra of control samples of (a) 3,4-DHB and (b) PCA



(c)



Carbon-13 magnetic resonance spectrum of 3,4-DHB obtained after exposure to an 'OH radical generating system

**TABLE 3.4**

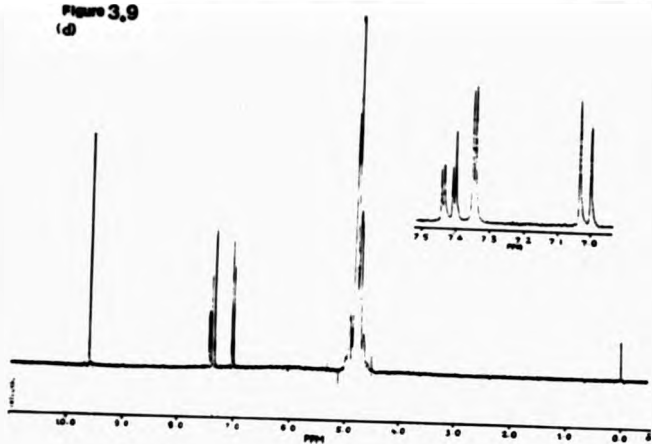
**Chemical Shift Values for Compounds Studied**

Compound	Resonances ( $\delta = \text{ppm}$ )			
	197	173	140-160	120-140
3,4-DHB control and hydroxylated	aldehyde group	absent	carbon atom attached to OH- group	aromatic carbon atom
PCA control	absent	carboxylic acid group	carbon atom attached to OH- group	aromatic carbon atom

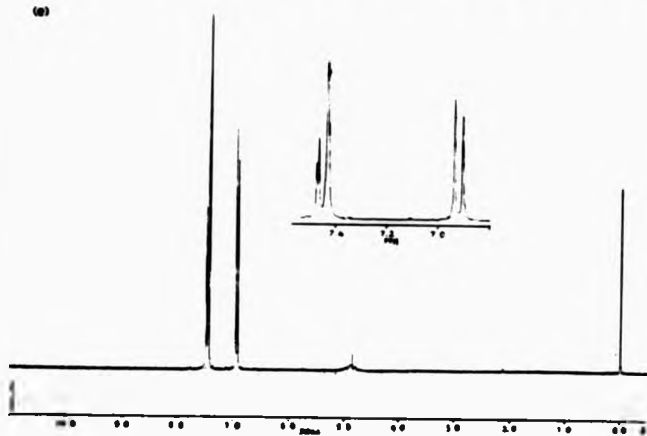
Data collected from Figures 3.9(a), (b) and (c)



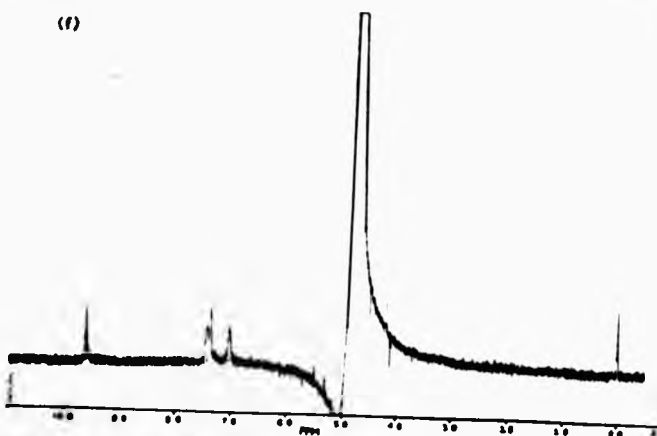
Figure 3.9  
(d)



(e)



(f)



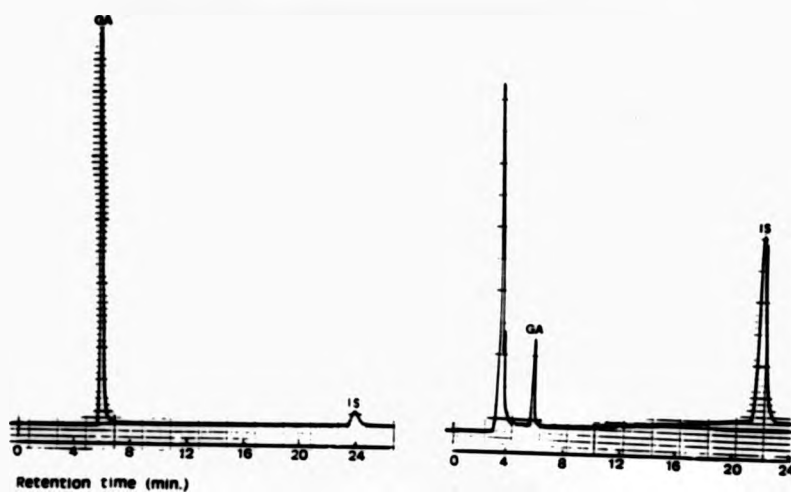
Proton magnetic resonance spectra of (d) control 3,4-DHB, (e) control PCA and (f) 3,4-DHB after exposure to an  $\cdot\text{OH}$  radical generating system

**(d) Attack of  $\cdot\text{OH}$  Radical on Gallic and Gentisic Acids**

For gallic and gentisic acids,  $\cdot\text{OH}$  radical-mediated hydroxylation resulted in a decrease in concentration of each acid (Figures 3.10 (a) and (b)) with no further electrochemically-active components detectable under these experimental conditions.

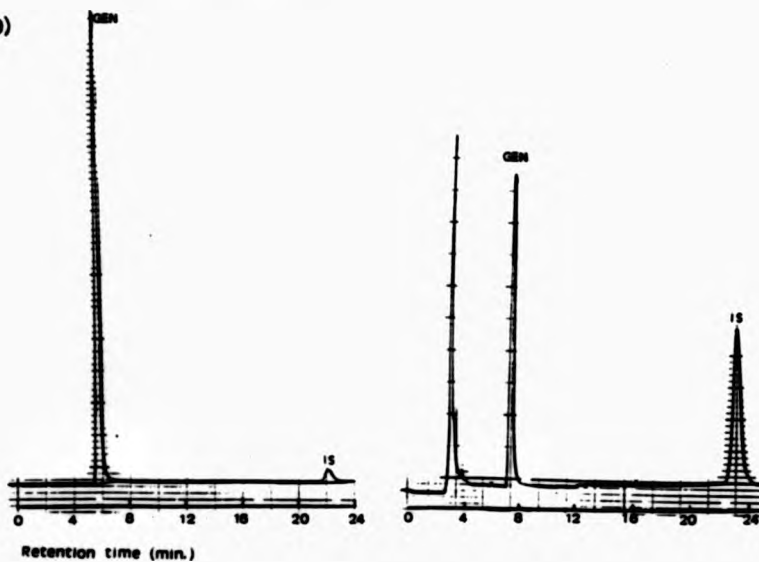
**Figure 3.10**

(a)



Reversed phase HPLC chromatogram of standard gallic acid (a) before (ECD sensitivity  $2.0 \mu\text{A}$ ) and (b) after exposure to an  $\cdot\text{OH}$  radical generating system (ECD sensitivity  $0.2 \mu\text{A}$ ). ECD oxidation potential  $+0.85 \text{ V}$ .

(b)



Reversed phase HPLC chromatogram of standard gentisic acid (a) before (ECD sensitivity  $2.0 \mu\text{A}$ ) and (b) after exposure to an  $\cdot\text{OH}$  radical generating system (ECD sensitivity  $0.2 \mu\text{A}$ ). ECD potential  $+0.85 \text{ V}$ .



3.6.2 HPLC/EC Detection of Phenolic Constituents in Celery Homogenates Subjected to Gamma-Irradiation Treatment

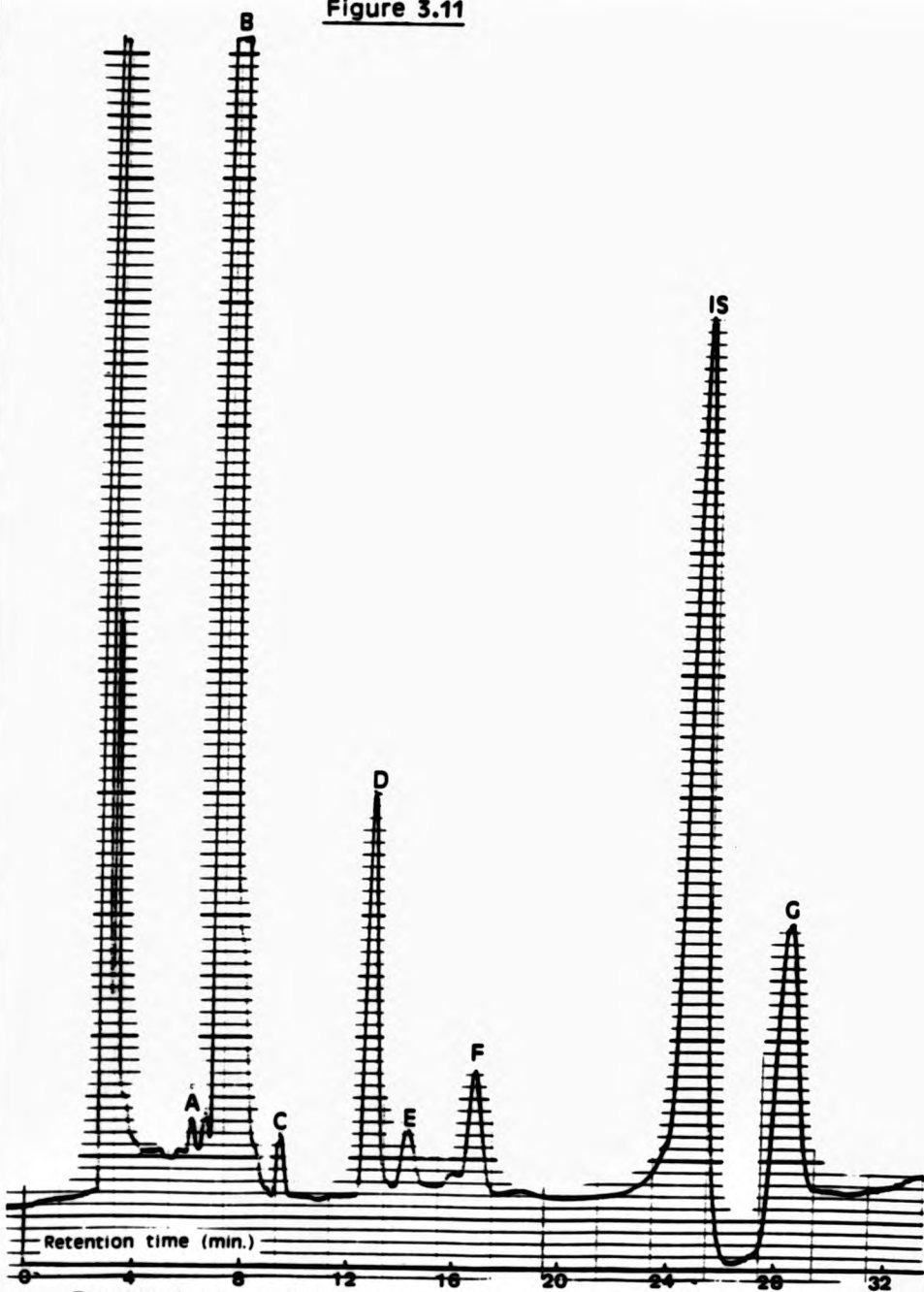
(a) Preliminary Constituent Identification in Celery

(i) On the Basis of Relative Retention Times (k')

Figure 3.11 shows the high performance liquid chromatogram of phenolic constituents extracted from a non-irradiated celery sample. Initially, steps were taken to complete the preliminary identification of the chromatographic peaks in Figure 3.11. The first step was a comparison of the retention times of sample constituents and a mixture of standard phenolic compounds that were putative sample components. Figure 3.12 shows the HPLC chromatogram of a standard mixture of phenolic acids and Table 3.5 lists the corresponding retention time data for the standard mixture and a typical celery sample. Six of the peaks present in the chromatogram obtained from the non-irradiated sample of celery had retention times which matched those of standard phenolic compounds.

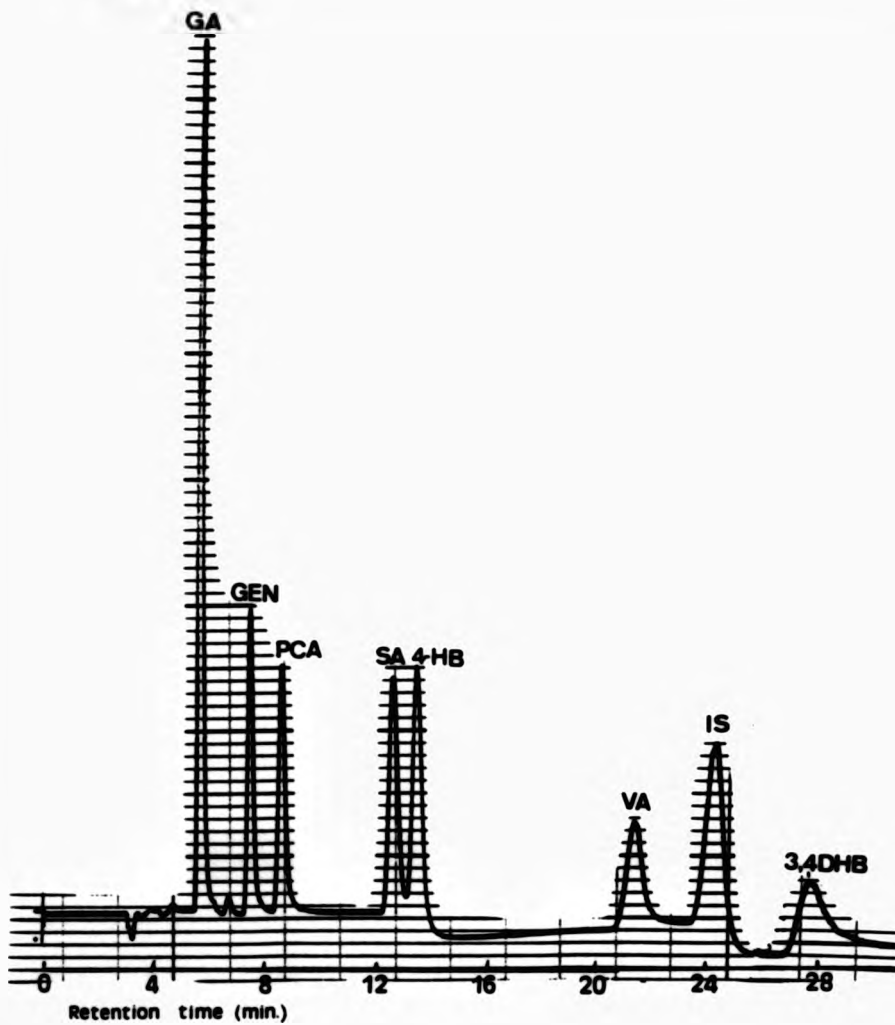
These peaks were tentatively assigned to gallic, gentisic, protocatechuic, salicylic and 4-hydroxybenzoic acids together with 3,4-dihydroxybenzaldehyde. These compounds may frequently be found in foods containing or derived from plant tissues. Indeed, the phenolic constituents arising in commercial beverages and plant extracts have been previously identified utilising HPLC coupled with ECD or UV detection<sup>84,99</sup>.

Figure 3.11



Reversed phase HPLC chromatogram of phenolic components present in celery. IS = internal standard (salicylic acid). ECD detector potential: + 0.85v, Sensitivity: 0.2 $\mu$ A. Mobile phase composition 95:5 citrate/acetate buffer:methanol, flow rate: 1ml min<sup>-1</sup>. (All chromatograms run under these conditions unless stated otherwise).

Figure 3.12



Reversed phase chromatogram of a standard mixture of phenolic acids (100 $\mu$ M). Abbreviations: GA, gallic acid; GEN, gentisic acid; PCA, protocatechuic acid; SA, salicylic acid; 4-HB, 4-hydroxybenzoic acid; VA, vanillic acid; IS, internal standard; 3,4-DHB, 3,4-dihydroxybenzaldehyde. ECD detector sensitivity 1.0  $\mu$ A.

**TABLE 3.5**

**Retention Time Data For a Standard Mixture of Phenolics and a Celery Sample**

Components in celery	Relative Retention Time (k')	Standard Mixture	Relative Retention Time (k')
Component A	0.25	GA	0.24
Component B	0.30	GEN	0.31
Component C	0.38	PCA	0.37
Component D	0.51	SA	0.52
Component E	0.57	4-HB	0.58
Component F	0.67	VA	0.92
IS	1.00	IS	1.00
Component G	1.14	3,4-DHB	1.15

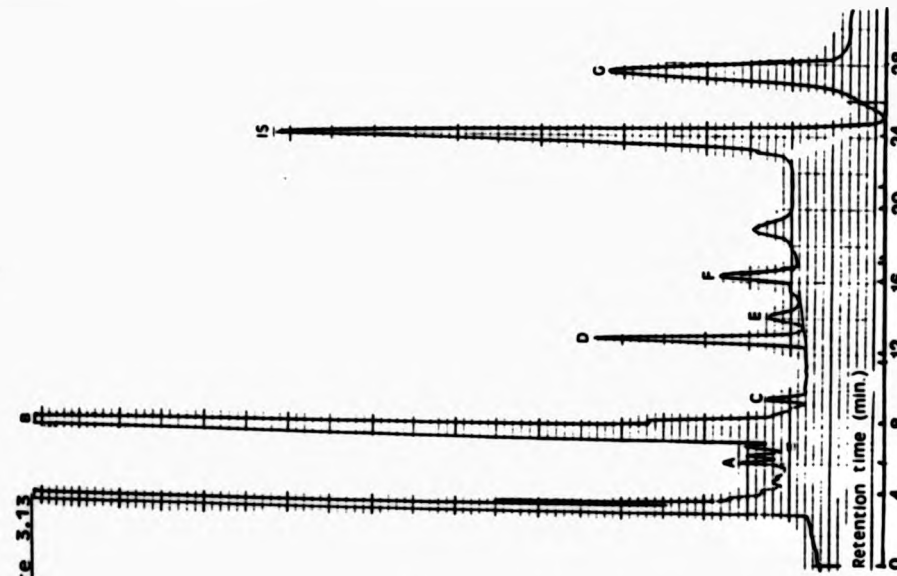
$$k' = \frac{\text{Retention time (mm) of compound}}{\text{Retention time (mm) of IS}}$$

IS = Internal Standard = Salicylic acid

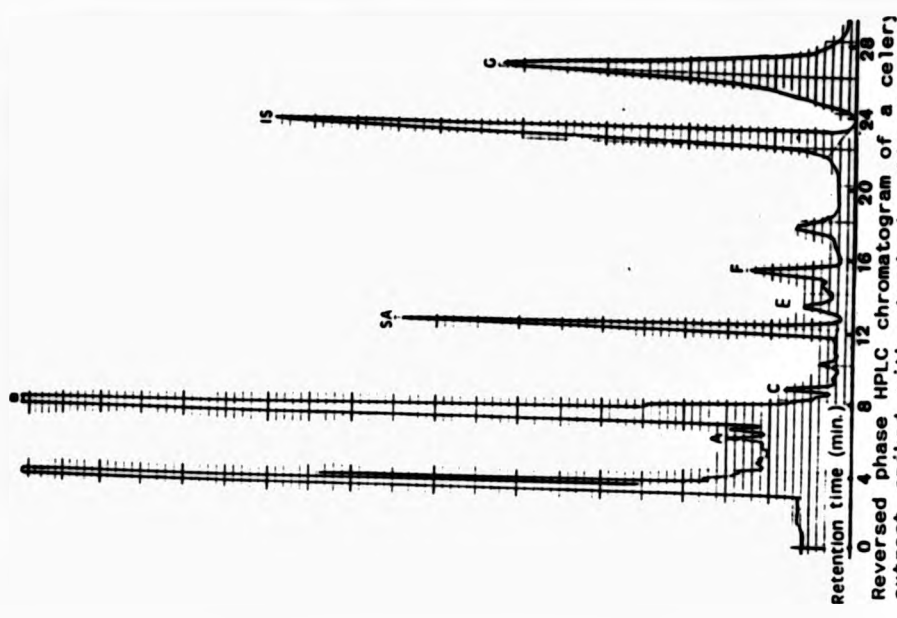
**(ii) Technique of "Spiking"**

Confirmation of the presence of these phenolic components in celery was completed by the technique of "spiking" the suspected component at a concentration which is exactly equal to that estimated from its peak height or area in the chromatogram. It was found that the identity of each putative peak was the same as that of the suspected component, since each spiked sample gave a chromatogram with an increase in the peak height of the putative component, the peak remaining perfectly symmetrical. Figures 3.13(a) and (b) show the corresponding HPLC chromatograms for two of the identified phenolic acids (salicylic and gentisic acids).

FIGURE 3.13  
(a)

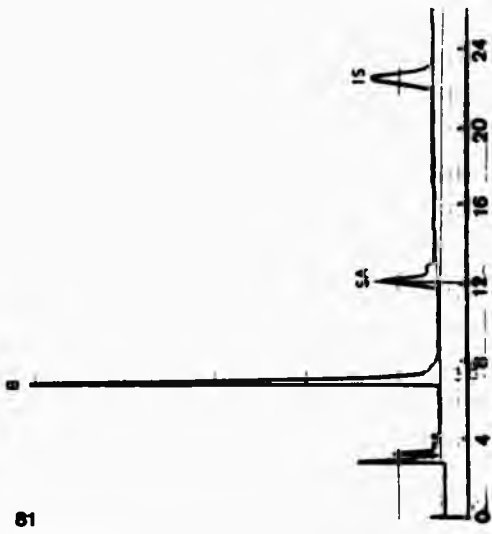


Reversed phase HPLC chromatogram of a celery extract (half dilution). ECD sensitivity 0.1 uA and oxidation potential +0.85V.

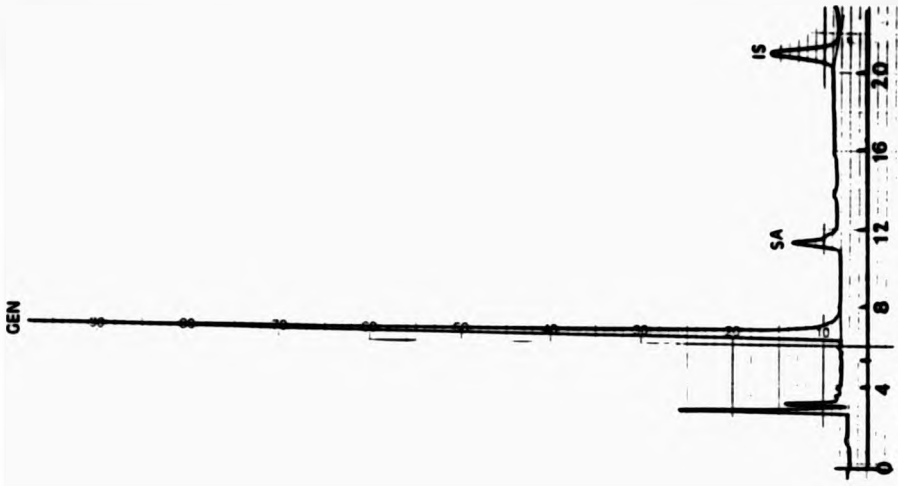


Reversed phase HPLC chromatogram of a celery extract spiked with standard salicylic acid (concentration:  $3.0 \times 10^{-4}$  mol. dm<sup>-3</sup>). ECD sensitivity: 0.1 uA and oxidation potential: +0.85V.  $k'$  for salicylic acid = 0.52.

Figure 3.13 (b)



Reversed phase HPLC chromatogram of a celery extract. ECD sensitivity 1.0  $\mu\text{A}$  and oxidation potential +0.85v. Peak "B" is now on scale.



Reversed phase HPLC chromatogram of a celery extract spiked with standard gentisic acid (concentration:  $7.5 \times 10^{-4} \text{ mol. dm}^{-3}$ ). ECD sensitivity: 1.0  $\mu\text{A}$ .  $k'$  for gentisic acid = 0.32.

#### (iii) Hydrodynamic Voltammograms

The final preliminary constituent identification involved the construction of hydrodynamic voltammograms (i.e. a plot of relative peak height or area versus electrochemical detector potential). In this method, the electrochemical detector was employed to obtain a voltammetric characterisation of each eluting species<sup>78,84</sup>, and these were compared with the voltammograms of the standard phenolic components. Figure 3.14 shows the hydrodynamic voltammograms for standard phenolic acids and suspected components in the control celery sample. A typical identifying feature is the general shape of the response-voltage curve. The three initial assignment procedures undertaken confirmed the identity of the phenolic species present in the celery sample.



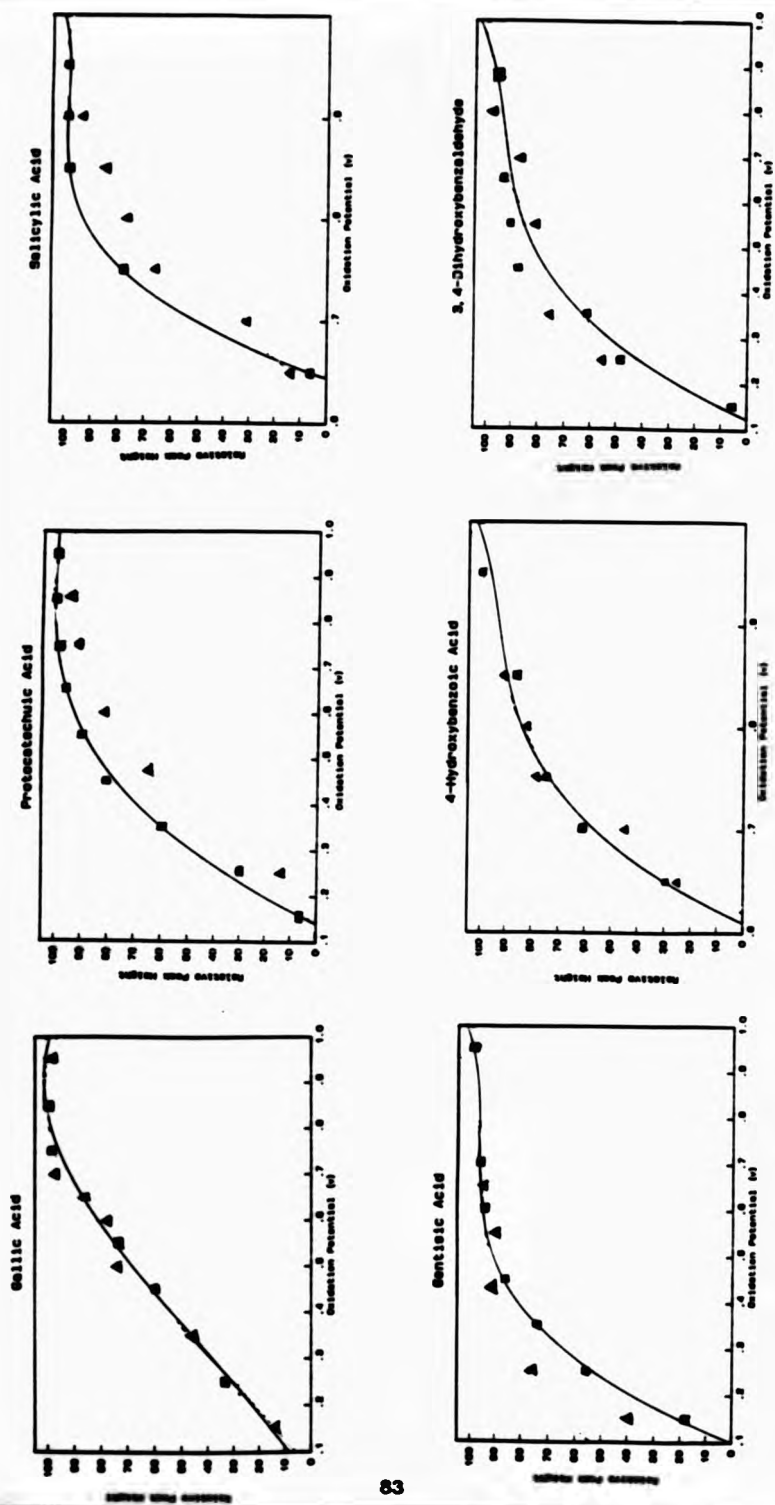


Figure 3.14. Hydrodynamic voltammograms for the standard phenolic acids (□) and those occurring in a control celery sample (▲)

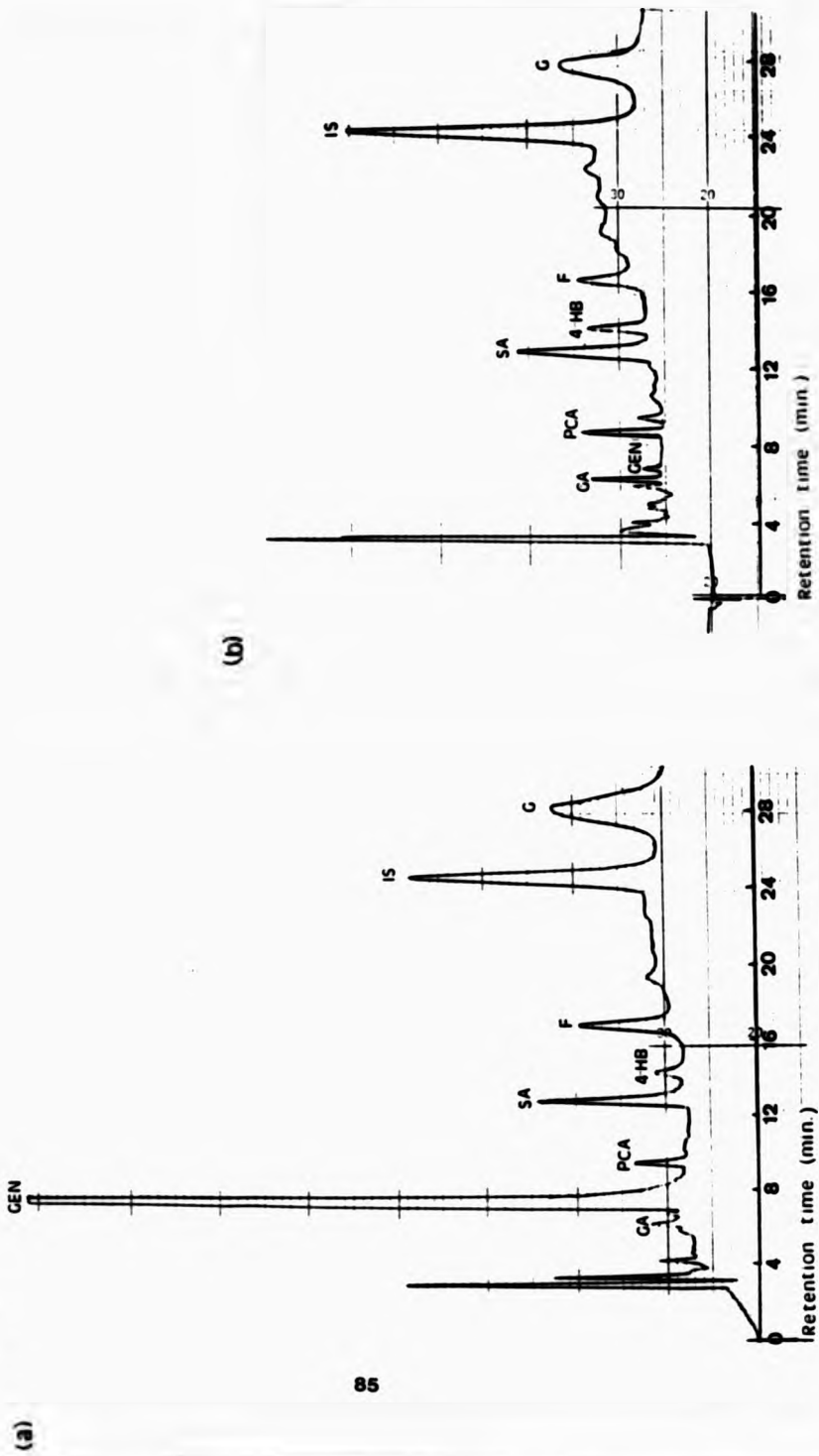
### 3.6.3 Comparison of Celery Homogenates Prior and Subsequent to Irradiation Treatment

Figures 3.15(a) and (b) show high performance liquid chromatograms of acidic diethyl ether extracts of homogenates obtained from celery samples prior and subsequent to irradiation at a dose of 5.0 kGy. Table 3.6 shows the relative retention time data for standard phenolic acids and the phenolic components of celery samples before and after irradiation. As previously (for the control samples), preliminary identification steps were undertaken to confirm the presence of the phenolic acids in the irradiated sample. Figure 3.16 shows the hydrodynamic voltammograms constructed for phenolic constituents identified in irradiated celery.

Comparison of the chromatogram of the irradiated sample with that of the non-irradiated sample reveals a number of differences. Subsequent to irradiation treatment, the intensities of a number of peaks in the irradiated sample increase or decrease as a consequence of the attack of radiolytically-generated  $\cdot\text{OH}$  radical on the phenolic components.

The most striking modification is the marked depletion of gentisic acid (which upon  $\cdot\text{OH}$  radical attack is destroyed with no further electrochemically-detectable product formation) following irradiation treatment. Different celery samples were also irradiated and similar results were obtained throughout, demonstrating the reproducibility of the result (n=8).

Figure 3.15



Reversed phase HPLC chromatogram of acidic diethyl ether extracts of celery homogenates before (a) and after, (b) irradiation at a dose of 5.0 kGy. ECD sensitivity: 0.2  $\mu$ A and oxidation potential + 0.85 volts.

**TABLE 3.6**

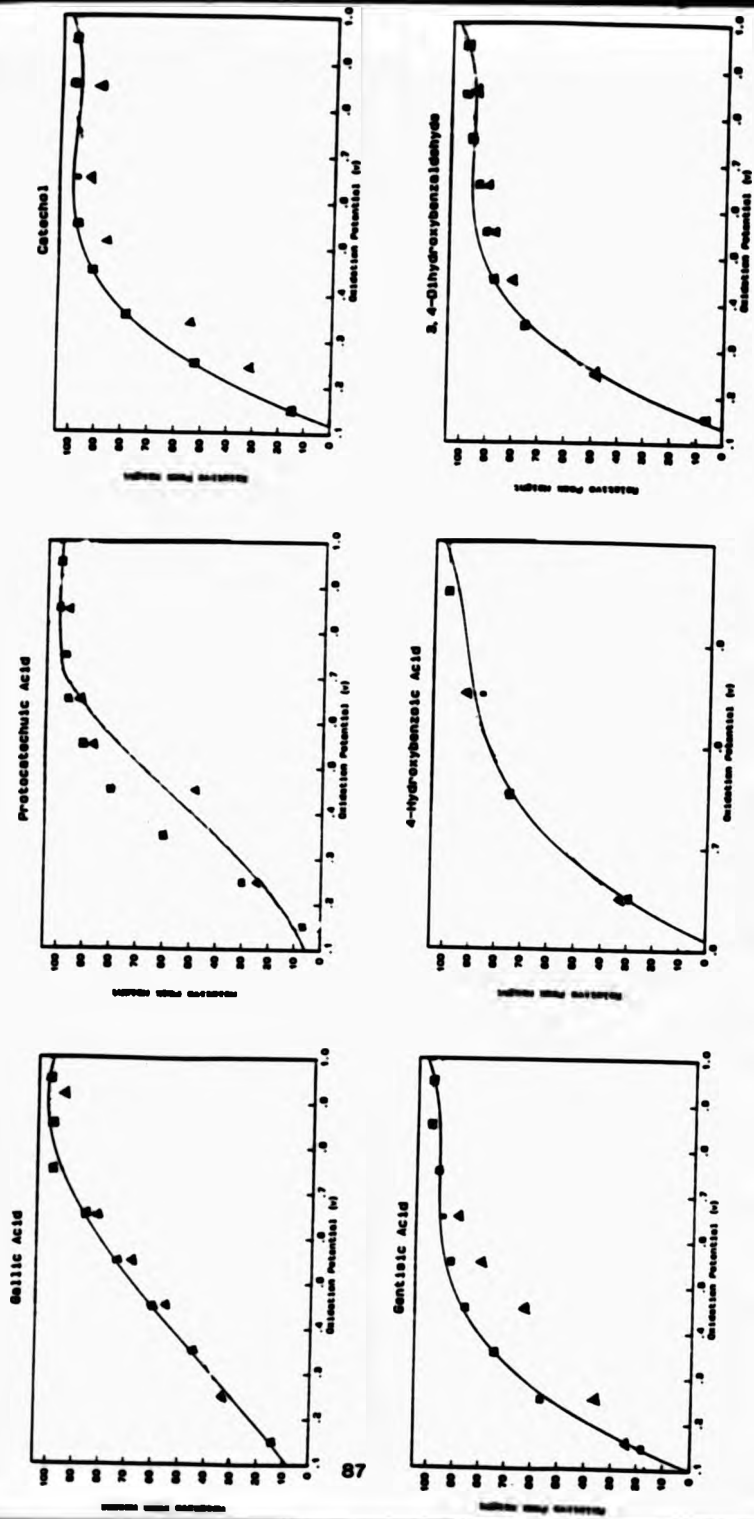
**Retention Time Data for Standard Phenolic Acids and Components in Celery**

Relative Retention Times of Phenolic Acids in Celery C	Relative Retention Times of Phenolic Acids in Celery I	Relative Retention Times of Standard Phenolic Acids
GA 0.25	GA 0.25	GA 0.24
GEN 0.30	GEN 0.28	GEN 0.30
PCA 0.39	PCA 0.36	PCA 0.37
SA 0.52	SA 0.53	SA 0.52
4HB 0.58	4HB 0.58	4HB 0.57
F 0.68	F 0.68	
IS 1.00	IS 1.00	IS 1.00
G 1.14	G 1.14	3,4DHB 1.15
		VA 0.91

Celery C = Celery control

Celery I = Celery irradiated at a dose of 5.0 kGy

(mean of n=8 determinations).




**Figure 3.16** Hydrodynamic voltammograms for the standard phenolic acids (■ ■ ■) and those occurring in an irradiated celery sample (▲ ▲ ▲).

The peak attributable to salicylate does not appear to be significantly altered subsequent to irradiation treatment and its intensity (reflecting concentration) in both control and irradiated celery samples appears unchanged. However, when the irradiated celery sample was chromatographed with the ECD detector potential set at +0.60 volts (a potential at which salicylic is not detectable) this peak was still detectable (Figure 3.17(b)). Therefore it is possibly attributable to catechol (a hydroxylation product of salicylate<sup>85</sup>). Since catechol and salicylic co-elute (i.e. have the same retention time under the experimental conditions stated<sup>70</sup>) the only way to distinguish between the two is by their difference in oxidation potential.

The control celery sample was also run with the detector set at an operating potential of +0.60 volts, but catechol was undetectable (Figure 3.17(a)). Consequently, attack of radiolytically-generated OH radical on salicylate results in the formation of catechol formed by decarboxylation. This compound is present only in the celery sample subjected to irradiation.

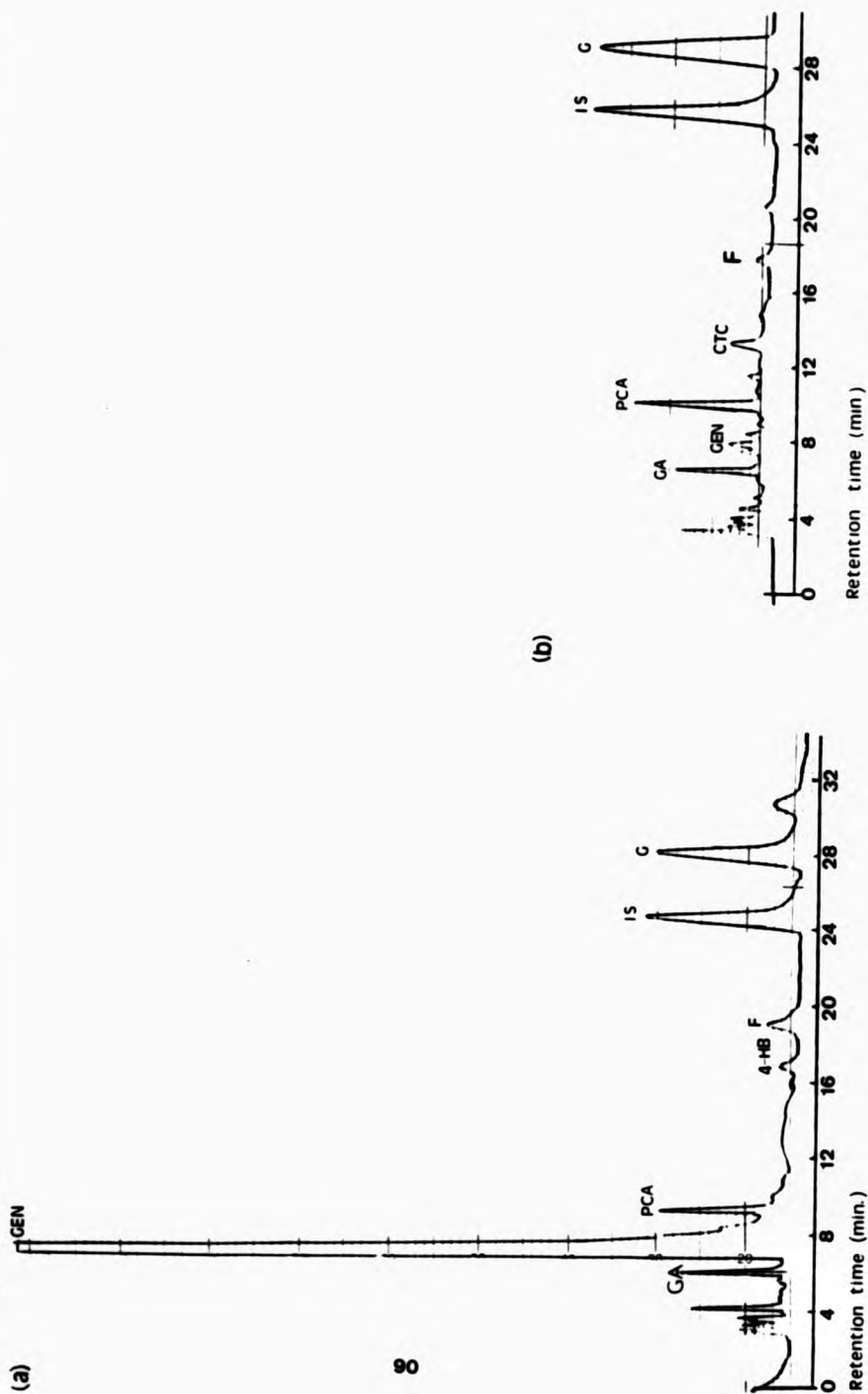
The intensity of the peak attributable to 3,4-dihydroxybenzaldehyde (3,4-DHB), decreases following irradiation treatment. OH radical attack on 3,4-DHB (from chemical model systems) may result in the formation of a compound whose identity may be PCA. However, the concentration of PCA did not significantly increase in intensity subsequent to gamma-irradiation treatment. This is



probably attributable to the PCA itself being further attacked by  $\cdot\text{OH}$  radical to produce the expected product, 1,2,4-THB (cf. Figure 3.5(c), p. 58, Section 3.4.1).

In addition to irradiation, a celery sample was subjected to hydroxyl radical attack (generated by the Fenton reaction) and similar results were obtained, thus demonstrating that it is  $\cdot\text{OH}$  radical which is responsible for hydroxylation of the phenolic constituents. Figures 3.18(a) and (b) show the HPLC chromatogram of a celery sample before and after treatment with the Fenton system.

Figure 3.17



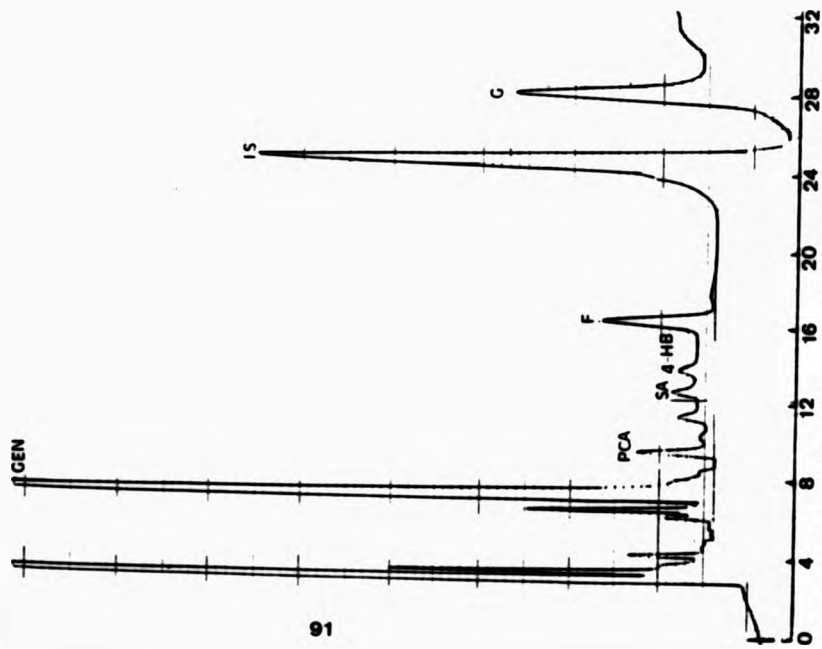
Reversed phase HPLC chromatogram of a control celery extract. ECD sensitivity: 0.2  $\mu$ A and oxidation potential + 0.60 volts (potential at which salicylate is not detectable).

Reversed phase HPLC chromatogram of an irradiated (5kGy) celery extract. ECD sensitivity: 0.2  $\mu$ A and oxidation potential + 0.60 volts. CTC: Catechol.



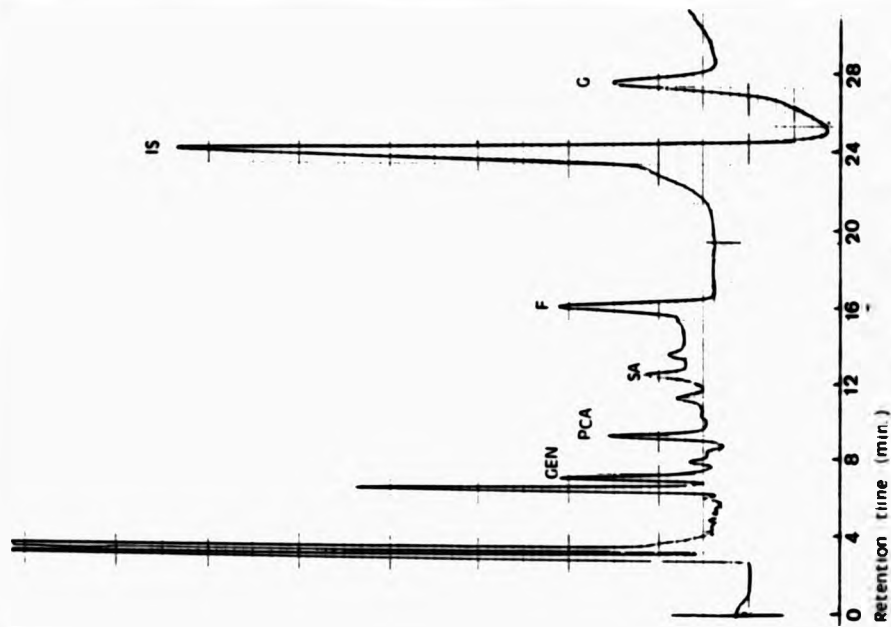
Figure 3.18

(a)



Reversed phase HPLC chromatogram of a celery extract before exposure to an  $\cdot\text{OH}$  radical flux generated by a Fenton system. ECD sensitivity: 0.2  $\mu\text{A}$  and oxidation potential  $+0.85\text{V}$

(b)



Reversed phase HPLC chromatogram of a celery extract subjected to  $\cdot\text{OH}$  radical attack using a Fenton system. ECD sensitivity: 0.2  $\mu\text{A}$ .

### 3.6.4 Quantification of Phenolic Constituents Present in Celery

#### (a) Calibration Curves for Standard Phenolic Acids

Calibration curves for the individual phenolic acids (at a range of different concentrations, with the internal standard concentration constant at  $1.00 \times 10^{-4} \text{ mol dm}^{-3}$ ) were constructed (Figure 3.19). Each plot of the ratio of the peak height of the individual phenolic standard to that of the internal standard versus component concentration was linear. The regression parameters ( $b$ , regression coefficient (slope) and  $y_I$ ,  $y$  intercept) and correlation coefficient for these data are given in Table 3.7.

The line of regression,  $y$  and correlation coefficient,  $r$ , are given by the following equations<sup>100</sup>

$$y = y_I + bx$$

and

$$r = \frac{\sum xy - n\bar{x}\bar{y}}{\sqrt{(\sum x^2 - n\bar{x}^2)(\sum y^2 - n\bar{y}^2)}}$$

The regression parameters determined from the calibration curves were used to calculate the concentration (micromoles  $\text{dm}^{-3}$ ) of each phenolic acid in the celery samples. Consequently, the concentration of phenolic acids in the entire homogenised celery sample (before and after irradiation) was calculated and results expressed as parts per billion (ppb) of wet weight. Results for at least six different samples of celery have been tabulated in Table 3.8.

From Table 3.8, celery samples not subjected to irradiation contain between 1000-3000 ppb of gentisic acid.

The concentration of the component attributable to salicylic increases in all samples following irradiation treatment, indicating the generation of catechol. Therefore, in irradiated celery samples the concentration of the component measured corresponds to catechol.

**TABLE 3.7**  
**Calibration Curve Data For Standard Phenolic Acids**

Phenolic Acids Standards	Slope (b)	Intercept ( $y_1$ )	Correlation Coefficient (r)
Gallic acid	0.02055	-0.1795	0.9976
Gentisic	0.00877	-0.0052	0.9979
Protocatechuic	0.00574	-0.0603	0.9964
Salicylic	0.00967	-0.0294	0.9966
4-hydroxybenzoic	0.01612	-0.0928	0.9966
3,4-dihydroxy-benzaldehyde	0.00753	-0.0004	0.9965

Mobile Phase Composition 95% (v/v) 30 mmol dm<sup>-3</sup> sodium citrate/ 27.7 mmol dm<sup>-3</sup> sodium acetate buffer and 7% (v/v) methanol. Electrode potential: +0.85 V.

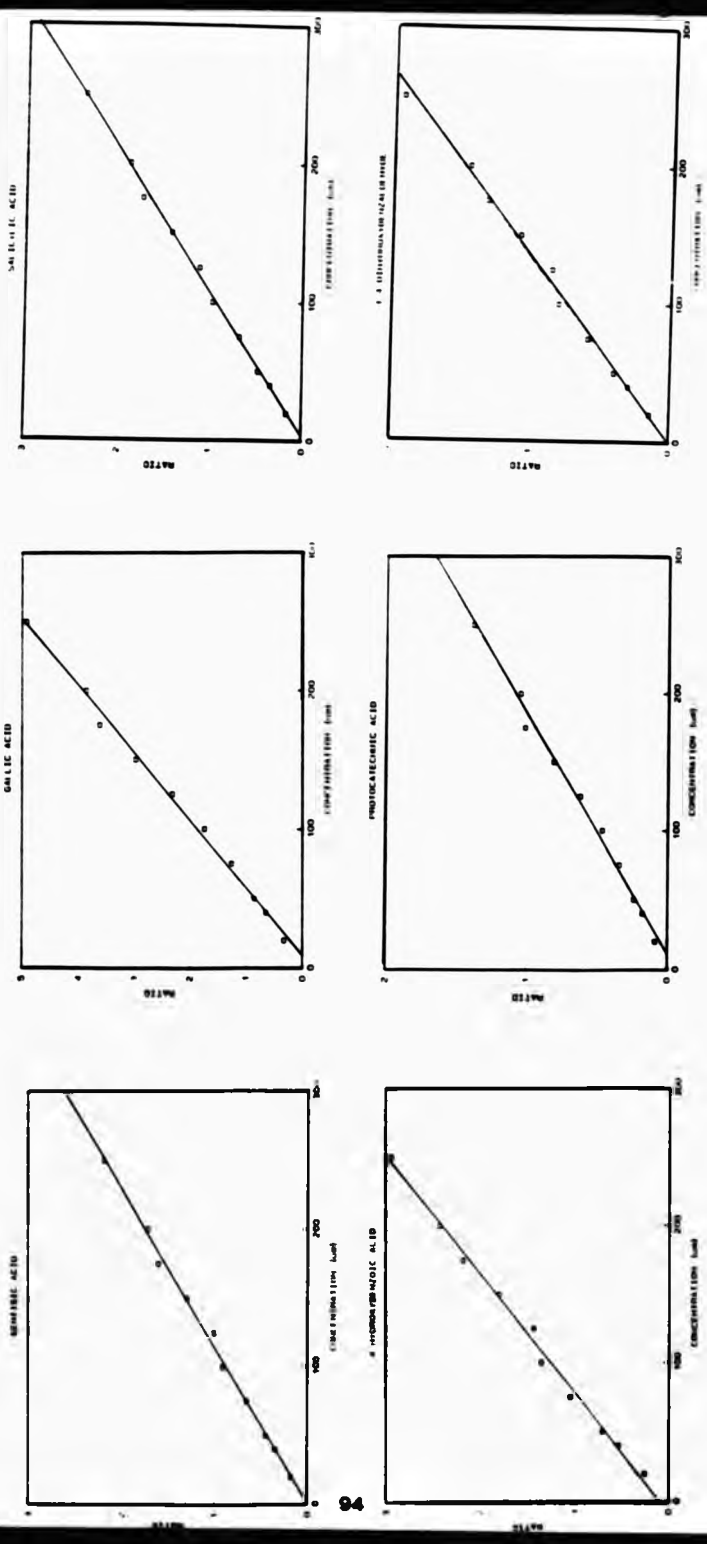


Figure 3.19 Calibration curves for standard phenolic acids



**TABLE 1.2**

**Calculated Concentrations (in parts per billion) of Phenolic  
Constituents Identified in Samples of Celery Before and After  
Irradiation Treatment**

Data 1			Data 2		
Weights: 10.5g      9.80g			Weights: 8.50g      7.50g		
Acids	Celery C	Celery I	Celery C	Celery I	
GA	83	107	138	149	
GEN	2562	47	2968	62	
PCA	154	141	239	363	
SA	79	63 (CTC)	97	99 (CTC)	
4-HB	98	89	136	155	
3,4-DHB	515	451	304	223	
Data 3			Data 4		
Weights: 10.7g      9.10g			Weights: 9.00g      9.55g		
Acids	Celery C	Celery I	Celery C	Celery I	
GA	157	112	96	85	
GEN	1097	51	2800	85	
PCA	267	183	113	106	
SA	62	159 (CTC)	35	52 (CTC)	
4-HB	66	73	74	56	
3,4-DHB	366	154	552	255	
Data 5			Data 6		
Weights: 9.50g      10.0g			Weights: 8.50g      7.50g		
Acids	Celery C	Celery I	Celery C	Celery I	
GA	78	55	100	95	
GEN	2855	44	2650	37	
PCA	175	285	196	206	
SA	109	135 (CTC)	93	155 (CTC)	
4-HB	74	104	78	54	
3,4-DHB	431	205	395	215	

Celery C = Celery Control  
 Celery I = Celery Irradiated (5.0 kGy)  
 CTC = Catechol

### 3.6.5 HPLC/EC Detection of Phenolic Constituents in Strawberry Homogenates Subjected to Gamma-Irradiation Treatment

#### (a) Preliminary Constituent Identification in Strawberry

As with celery, the naturally occurring components in strawberry were initially identified using the preliminary techniques described previously.

Figure 3.20(a) shows the high performance liquid chromatogram of the phenolic constituents extracted from a typical non-irradiated strawberry sample and Figure 3.20(b) exhibits the corresponding chromatogram of a standard mixture of phenolic acids (mobile phase composition was 95% (v/v) 30 mmol. dm<sup>-3</sup> sodium citrate/ 27.7 mmol. dm<sup>-3</sup> sodium acetate buffer and 5% (v/v) methanol). Table 3.9 shows the relative retention time data for the standard mixture and the strawberry sample.

From the initial identity assignment, six of the phenolic components had retention times which matched those of standard phenolic acids in the mixture: gallic, gentisic, protocatechuic, salicylic, 4-hydroxybenzoic and vanillic acids. Confirmation of these assignments was achieved by "spiking" each suspected component with standard phenolic acid, and by the construction of hydrodynamic voltammograms.

Figures 3.21(a) and (b) show the chromatograms obtained subsequent to "spiking" two of the identified phenolic acids, salicylic and 4-hydroxybenzoic acid respectively into the extract. Figure 3.22 shows the hydrodynamic voltammograms of

four standard phenolic acids and those acids suspected to be present in the control strawberry extract. A reasonably good agreement exists in the shapes of the response-voltage curve for the standard phenolic acids and those acids suspected to be present in the strawberry extract, thereby providing additional information for the confirmation of their identities.

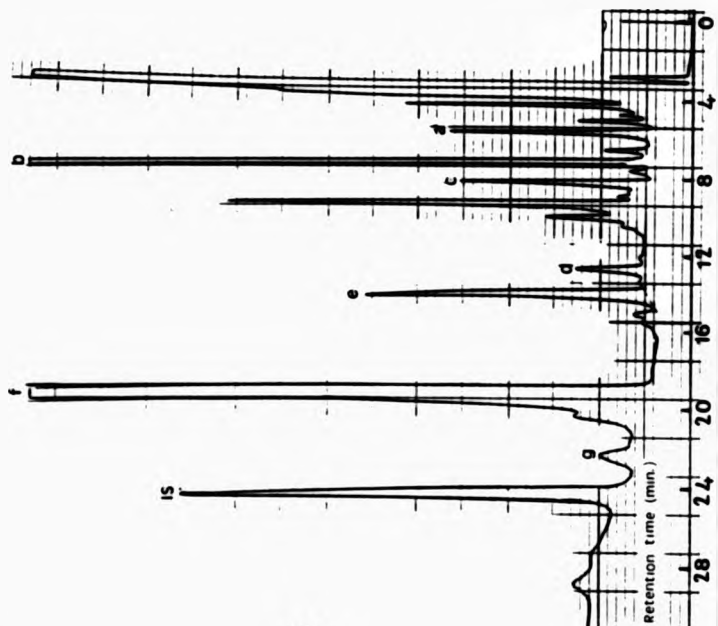
**TABLE 3.9**  
**Retention Time Data for a Standard Mixture of Phenolic Acids**  
**and a Strawberry Sample**

Components in Sample	Relative Retention Time (k')	Standard mixture	Relative Retention Time (k')
Component a	0.23	GA	0.23
Component b	0.30	GEN	0.30
Component c	0.34	PCA	0.36
Component d	0.52	SA	0.52
Component e	0.58	4-HB	0.58
Component f	0.80		
Component g	0.92	VA	0.94
IS	1.00	IS	1.00

IS = Internal Standard = Salicylic acid  
 (For n=8).

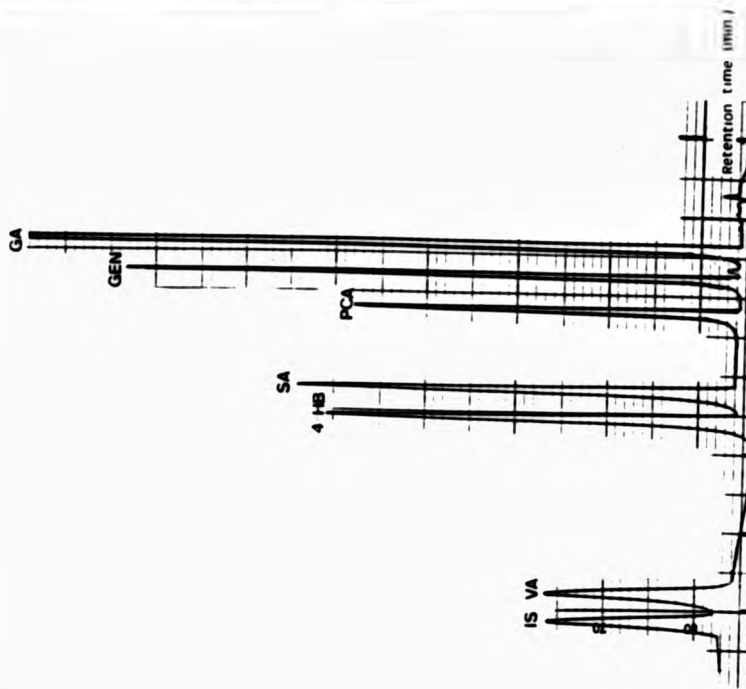
Figure 3-20

(a)



Reversed phase HPLC chromatogram of phenolic constituents (a to e) naturally occurring in a strawberry diethylether extract. Mobile phase composition 95:5 citrate/acetate buffer: methanol. ECD detector sensitivity/oxidation potential at 1  $\mu$ A and +0.85v. Flow rate 1 ml/min (for all chromatograms).

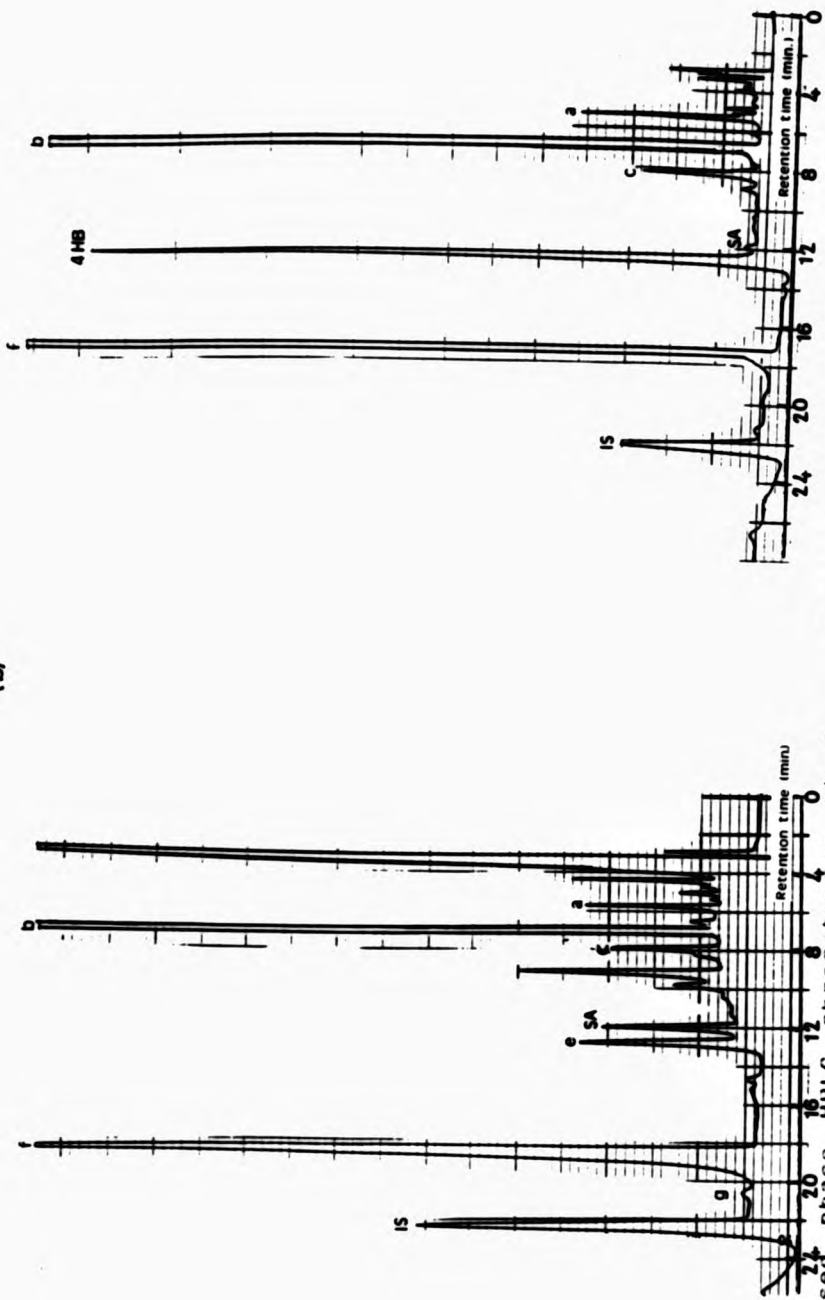
(b)



Reversed phase HPLC chromatogram of a standard mixture of phenolic acids. Mobile phase composition 95:5 citrate/acetate buffer: methanol. ECD sensitivity and oxidation potential at 2  $\mu$ A and +0.85v. Abbreviations: GA, gallic acid; GEN, gentisic acid; PCA, protocatechuic acid; SA, salicylic acid; 4-HB, 4-hydroxybenzoic acid; VA, vanillic acid and IS, internal standard (salicylic acid).

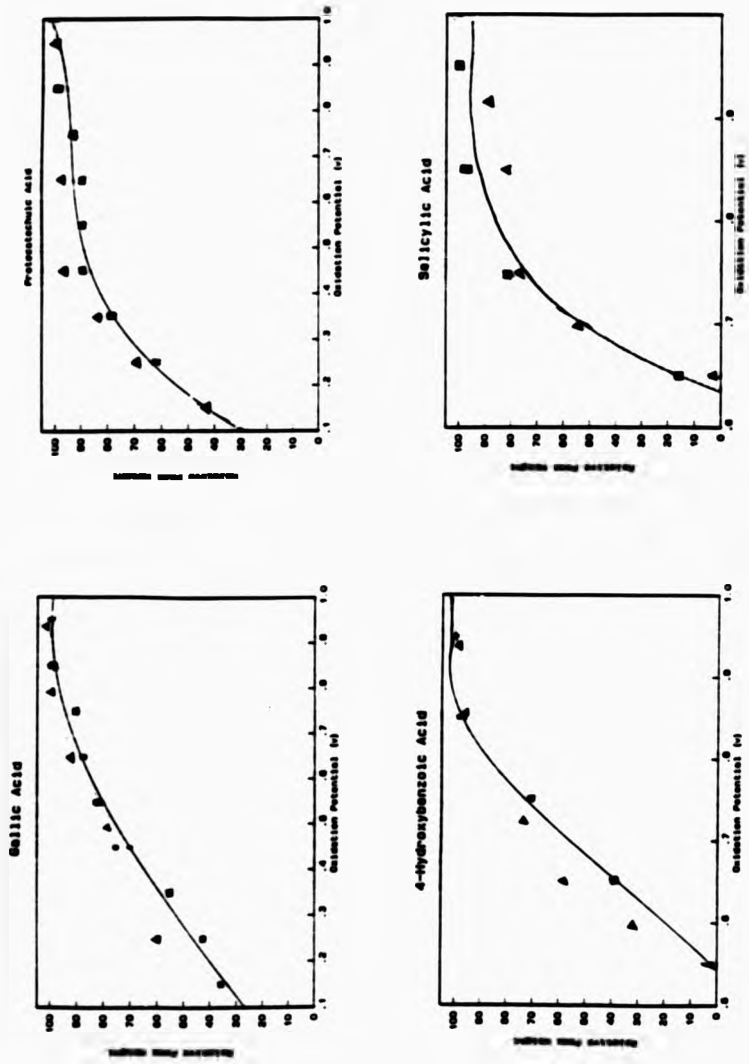


(b)



Reversed phase HPLC chromatogram of a strawberry extract spiked with standard 4-hydroxybenzoic acid.  $k'$  for 4-HB = 0.57. Mobile phase composition 93:7 citrate/acetate buffer: methanol. ECD sensitivity and potential at 1  $\mu$ A and +0.85V.

Reversed phase HPLC chromatogram of a strawberry extract spiked with standard salicylic acid.  $k'$  for SA = 0.53. Mobile phase composition 95:5 citrate/acetate buffer: methanol. ECD sensitivity and potential at 1  $\mu$ A and +0.85V.



**Figure 3.22** Hydrodynamic voltammograms for the standard phenolic acids (□) and those occurring in a control strawberry sample (▲)

#### 3.4.6 Comparison of Strawberry Homogenates Prior and Subsequent to Irradiation Treatment

Figures 3.23(a), (b) and (c) show high performance liquid chromatograms of acidic diethyl ether extracts of strawberry homogenates (a) before irradiation (b) after irradiation at a dose of 1.0 kGy and (c) at a dose level of 5.0 kGy. Table 3.10 shows the relative retention time data for standard phenolic acids and the phenolic components of strawberry samples before and after irradiation. Figure 3.23(d) shows the same HPLC chromatograms for the control and irradiated samples obtained at a lower detector sensitivity.

Comparison of the irradiated sample with the non-irradiated sample shows a number of differences. Following treatment with irradiation, the intensities of several peaks decrease. The peaks attributable to gallic and protocatechuic acids decrease in intensity as the irradiation dose increases from 1.0 to 5.0 kGy. The peak attributable to 4-hydroxybenzoic acid decreases in intensity to a small extent following irradiation at 1.0 kGy. At low doses of irradiation,  $\cdot\text{OH}$  radical attacks 4-HB resulting in the formation of protocatechuic acid<sup>68,69</sup>.

However, as the dose of irradiation increases from 1.0 to 5.0 kGy, the concentration of 4-HB increases substantially. The concentration of the unknown peak "f" however, decreases substantially with an increase in the irradiation dose.

The identity of the unknown component peak "f" has not been successfully determined, but it appears that  $\cdot\text{OH}$  radical

attack on this unknown component (at a high radiation dose) may result in the formation of 4-HB.

The peak attributable to gentisic acid gradually decreases in intensity as the irradiation dose is increased, i.e. from 1323 ppb (in the control) to 1000 ppb in the sample irradiated at 1.0 kGy and then to 950 ppb in the sample irradiated at 5.0 kGy, c.f. Table 3.11 (p. 108).

**TABLE 3.10**  
**Retention Time Data for Standard Phenolic Acids and Components in Control and Irradiated Strawberry Homogenates**

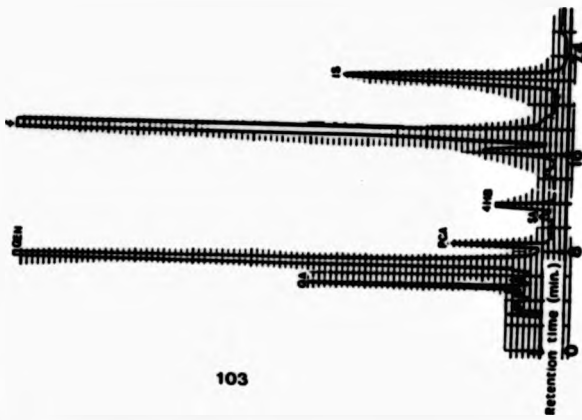
Relative Retention Times of Phenolics in Control Sample	Relative Retention Times of Phenolics in Irrad. (1.0 kGy)	Relative Retention Times of Phenolics in Irrad. (5.0 kGy)
GA 0.23	GA 0.24	GA 0.24
GEN 0.32	GEN 0.32	GEN 0.31
PCA 0.38	PCA 0.36	PCA 0.35
SA 0.50	SA n.d.	SA 0.51
4-HB 0.54	4-HB 0.56	4-HB 0.55
"f" 0.80	"f" 0.80	VA 0.88
IS 1.00	IS 1.00	IS 1.00

n.d. = not detectable  
(For n=8 determinations)

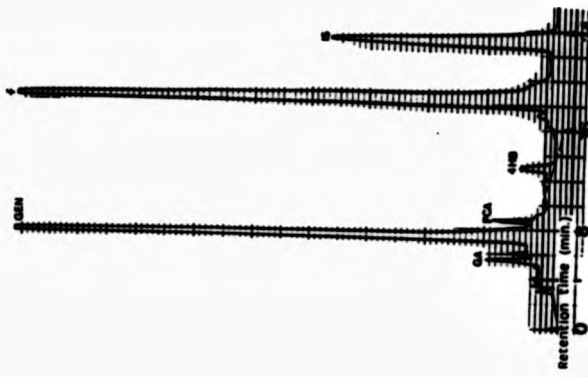
Identity of the unknown component "f" was investigated by testing a wide range of standard aromatic compounds including benzoic and hydroxycinnamic acids. However, retention times of all acids tested did not match retention time of component "f". Isolation of component "f" and subsequent analysis by NMR spectroscopy did however reveal the presence of an aromatic functional group.

Figure 2.2a,b,c

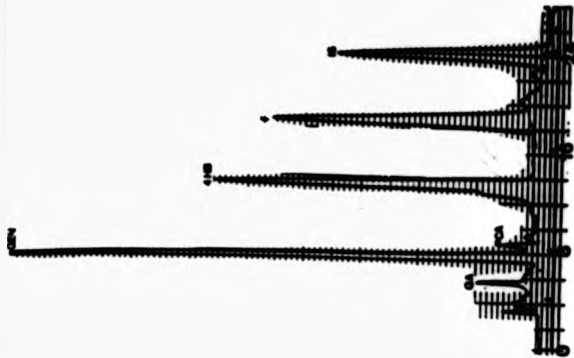
(a) control



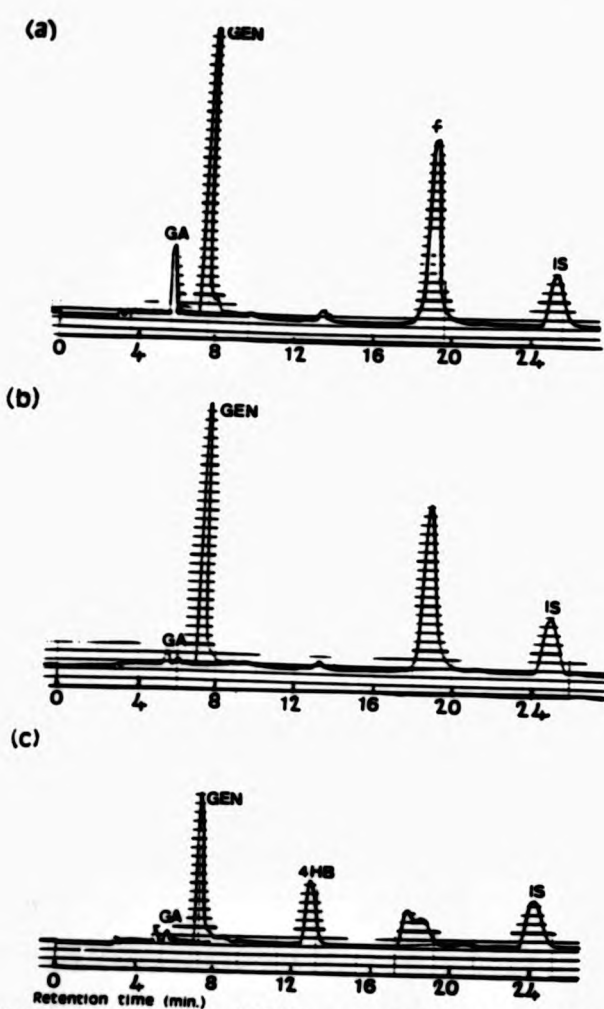
(b) 1.0kGy



(c) 5.0kGy



**Figure 3.23(d)**



Reversed phase HPLC chromatogram of a strawberry extract (a) before irradiation, (b) after irradiation at a dose of 1.0 kGy, and (c) at a dose of 5.0 kGy. ECD sensitivity and operating potential were  $5 \mu\text{A}$  and  $+0.85\text{V}$  respectively.

The reproducibility of these results was tested. A number of strawberry samples were subjected to irradiation treatment and in each case similar results were obtained (i.e. n = 8). Figures 3.24(a) and (b) show the HPLC chromatograms of a strawberry extract from an alternative batch, subjected to irradiation at a dose of 5.0 kGy and compared to a control sample. The results obtained are comparable to those obtained in Figures 3.23(a) and (b).

**3.6.7 Quantification of Phenolic Constituents in Strawberry Calibration Curves for Standard Phenolic Acids**

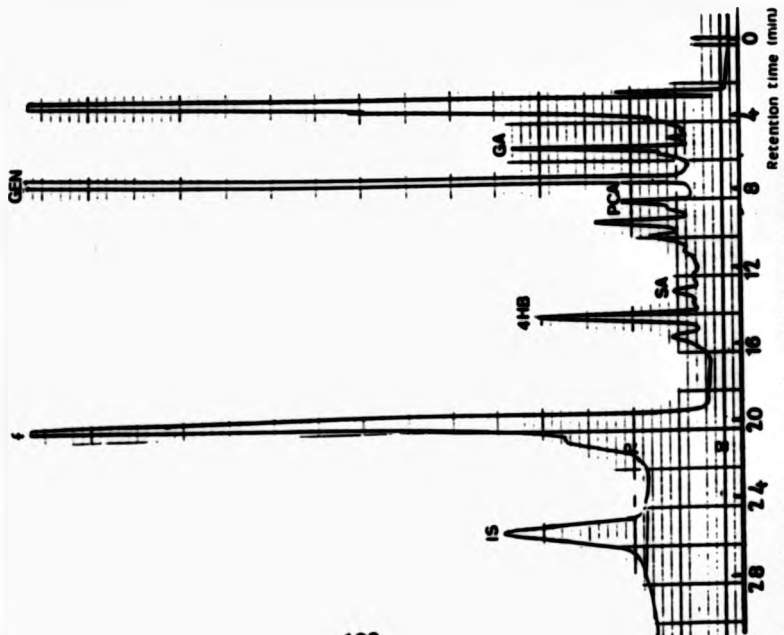
Calibration curves were also constructed for standard phenolic acids at a range of concentrations (as previously determined for celery) and results quantified. Figure 3.25 shows the individual calibration curves for standard phenolic acids found occurring in the strawberry extract. Table 3.12 shows the values of slope and intercept determined from the straight line plots together with the correlation coefficient (r). The concentration of phenolic components identified in different strawberry samples before and after irradiation treatment has been calculated in parts per billion and the results are tabulated in Table 3.11.

**TABLE 3.12 Calibration Curve Data for Standard Phenolic Acids**

Phenolic Acids Standards	Slope (b)	Intercept ( $y_I$ )	Correlation Coefficient (r)
Gallic acid	0.02414	-.02129	0.9971
Gentisic acid	0.01050	0.01460	0.9979
Protocatechuic	0.00620	0.01880	0.9992
Salicylate	0.01035	0.01598	0.9993
4-Hydroxybenzoic	0.02438	0.00900	0.9971

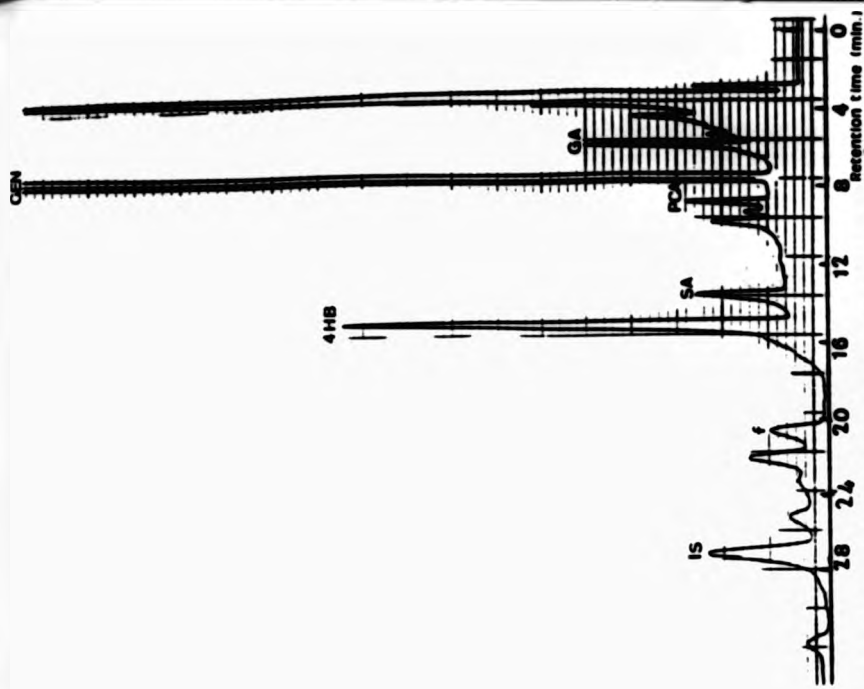
Figure 3-24

(a)



Reversed phase HPLC chromatogram of the naturally occurring phenolic constituents present in a strawberry extract before irradiation (mobile phase composition 95:5 citrate/acetate buffer: methanol). The ECD sensitivity and electrode potential were 1  $\mu$ A and +0.85v respectively.

(b)



Reversed phase HPLC chromatogram of the phenolic constituents present in a strawberry extract after irradiation at a dose of 5.0 kGy (mobile phase composition 95:5). The ECD sensitivity and electrode potential were 1  $\mu$ A and +0.85v respectively.



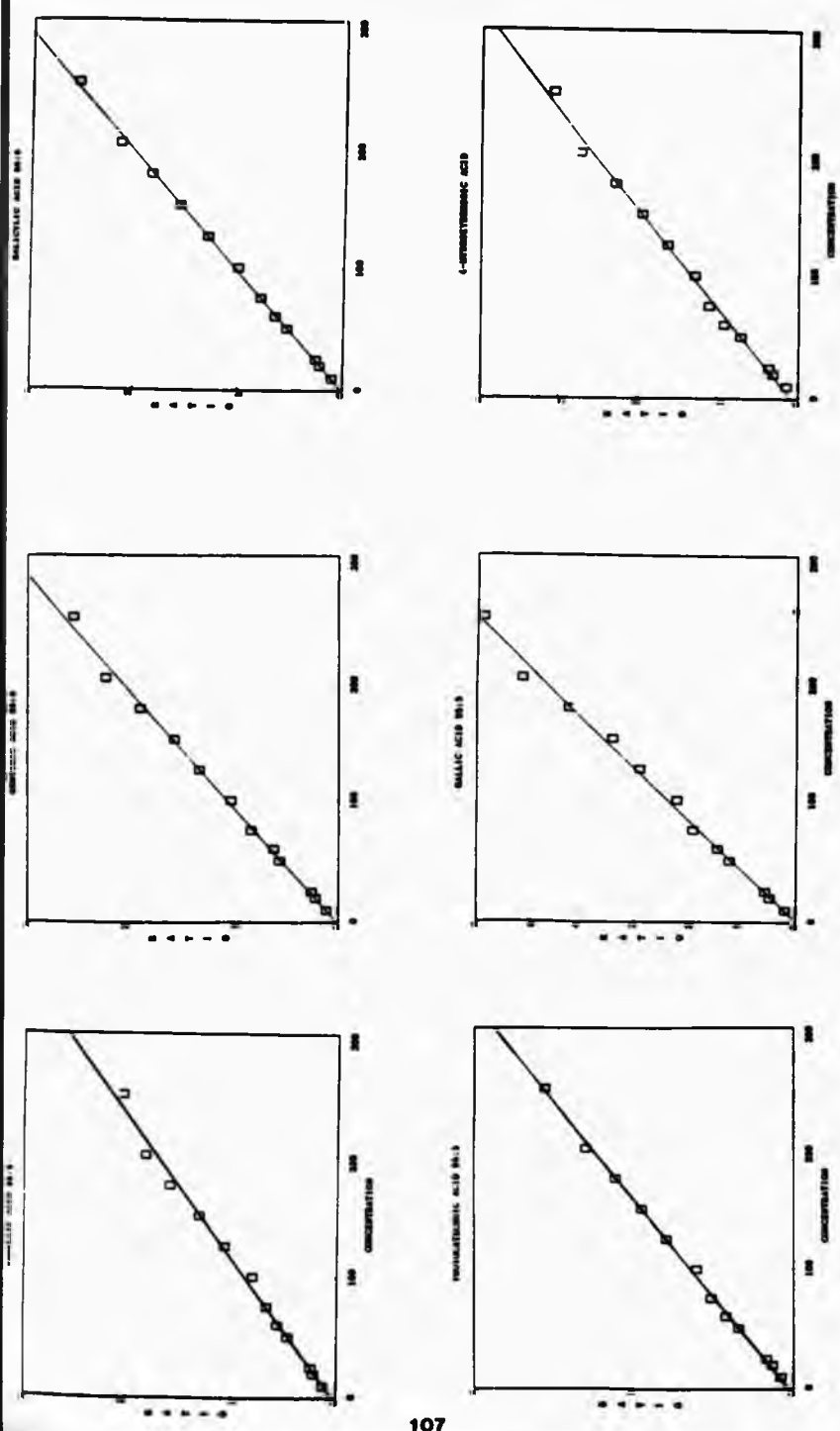


Figure 3.25 Calibration curves for standard phenolic acids



**TABLE 3.11**  
Calculated Concentrations (in parts per billion) of Phenolic  
Constituents Identified in Samples of Strawberry Before and  
After Irradiation Treatment

	DATA 1		DATA 2	
	Weights 10.0g	10.5g	Weights 17.27g	15.46
Strawberry C	I		Strawberry C	I
GA	113	105	100	58
PCA	122	43	77	60
SA	36	40	20	33
4-HB	261	1033	89	471
	DATA 3			
	Weights 13.58g	16.03g	10.0g	
Strawberry C	Irrad (1kGy)	Irrad (5kGy)		
GA	135	31	53	
GEN	1323	1000	950	
PCA	157	40	36	
SA	12	n.d.	n.d.	
4-HB	44	2.0	715	

Strawberry C = strawberry control  
 Strawberry I = strawberry irradiated  
 n.d. = not detectable

### 3.6.8 Vitamin C (Ascorbic Acid) Analysis of Control and Gamma-irradiated Strawberry Homogenates

The effect of ionising radiation on the ascorbic acid content of fresh strawberries has been determined by HPLC/ECD. Since ascorbic acid is detectable at a low oxidation potential, the ECD detector potential was set to +0.40 V. At this potential, no other electrochemically-active compound is detectable and hence the assay has a high degree of specificity<sup>68</sup>.

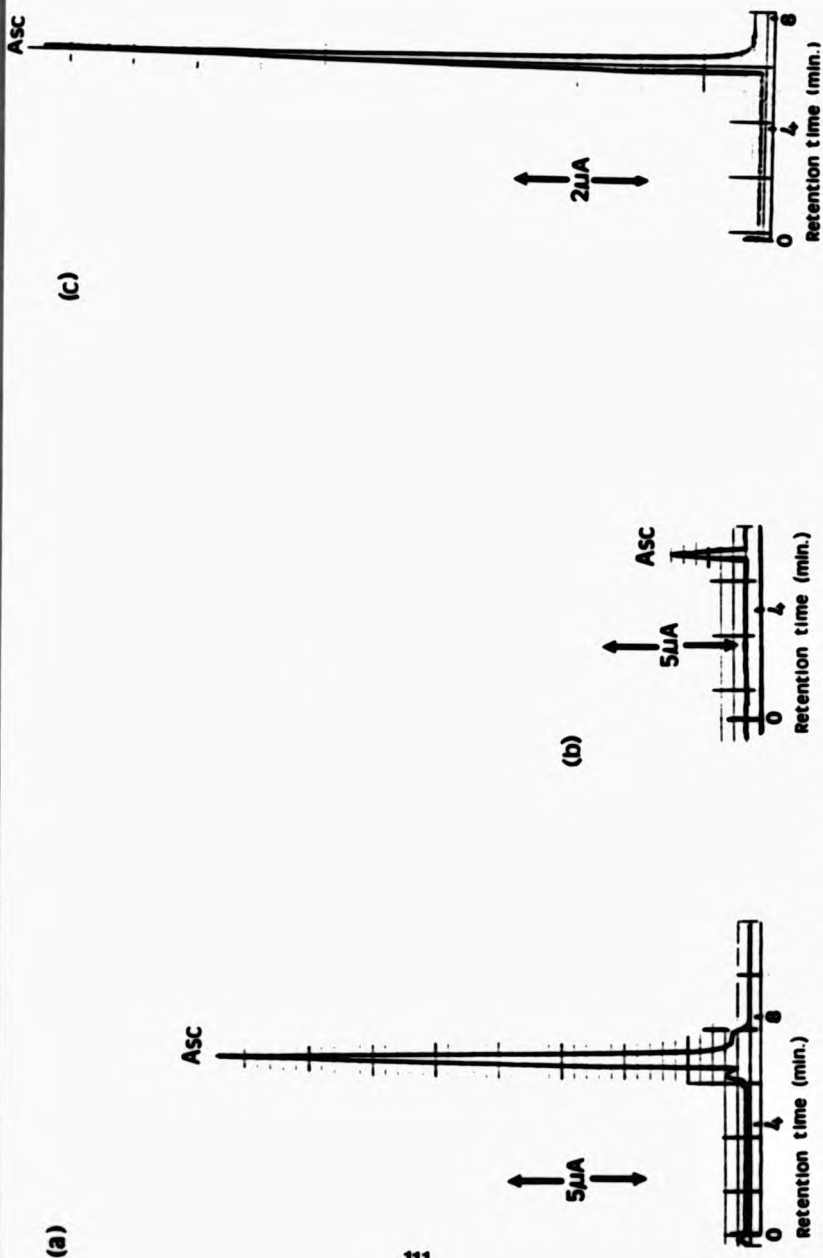
Figures 3.26(a), (b) and (c) exhibit liquid chromatograms of ascorbic acid in strawberry homogenates before, (a) and after, (b), treatment with gamma-radiation at a dose level of 5.0 kGy. The chromatogram of a standard solution of ascorbic acid at a concentration of  $2.0 \times 10^{-4} \text{ mol dm}^{-3}$  is shown in Figure 3.26(c). A calibration curve of standard ascorbic acid at a range of concentrations was constructed, and the ascorbic acid content of the strawberry samples determined. Figure 3.27 shows the calibration curve for standard ascorbic acid and Table 3.13 gives the ascorbic acid contents of the strawberry samples.

As expected, irradiation results in a reduction of the ascorbic level, and from this data the ascorbic acid content in irradiated strawberry is reduced to approximately 80% of its original level at a dose of 5.0 kGy.

Ascorbic acid is very prone to oxidation and generally a large number of food processes result in its rapid degradation. Moreover, ascorbic acid is itself an antioxidant and is rapidly oxidised to dehydroascorbate<sup>96</sup>. Consequently,

although radiation treatment results in the degradation of ascorbic acid, its determination in fruits and vegetables cannot be employed as a useful marker of irradiation. However, it is important to note that the ascorbic acid content of irradiated strawberries is significantly less than that in strawberries not subjected to irradiation.

Additionally, since ascorbic acid is a very good radical scavenger (its second order rate constant for reaction with OH radical,  $k_2 = 1.1 \times 10^{10} \text{ mol. dm}^{-3} \text{ s}^{-1}$ , pH 1.5)<sup>7</sup>, its presence in strawberries (60-90 mg/100 gm fresh weight<sup>101</sup>) offers much protection for phenolic components against radiolytic damage.

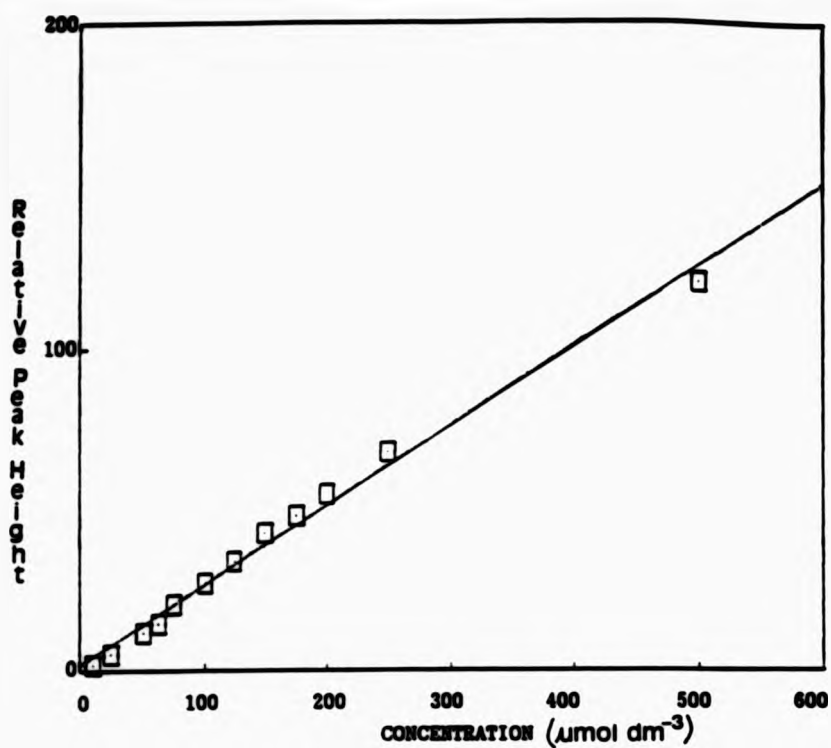


**Figure 326** Reversed phase HPLC determination of ascorbic acid in strawberry samples before (a), and after irradiation at a dose of 5.0 kGy (b), together with a standard solution of ascorbic acid, (c). Mobile phase composition 95:5 citrate/acetate buffer and methanol at a flow rate of 0.5 ml min<sup>-1</sup>. The electrochemical detector potential was set to +0.40V. Asc = ascorbic acid.



Figure 3.27

ASCORBIC ACID 98:5



Correlation Coefficient ( $r$ ) = 0.9957  
Slope ( $b$ ) = 0.2487  
Intercept ( $y_1$ ) = 1.7532

TABLE 3.13

Calculated Ascorbic Acid Content of Strawberry Samples Before and After Treatment with Gamma-Irradiation

Dose of Irradiation (kGy)	Ascorbic Acid Content (mg/10g wet wt. sample)
0	0.70
5.0	0.08

### 3.7 SUMMARY/CONCLUSION

The aromatic compounds present in a variety of fruits and vegetable-derived foodstuffs react extremely rapidly with OH radical to form the corresponding hydroxylated compounds<sup>68,69</sup>. These are readily separated by HPLC and detected by electrochemical detection (ECD)<sup>68,79,81,84</sup>. The phenolic acid components occurring in celery and strawberry have been identified prior and subsequent to irradiation treatment and their concentrations determined.

In this study, celery samples subjected to ionising radiation or treated with Fentons reagent, resulted in the formation of catechol (formed from naturally-occurring salicylate). Catechol was not detected in the control celery sample. Additionally, as a consequence of irradiation there was a marked depletion of gentisic acid from samples subsequent to gamma-irradiation treatment.

Strawberry samples treated with ionising radiation also exhibited a number of differences from those not treated. These differences were attributable to the reaction of OH radical with the phenolic components. In addition, strawberries contain large quantities of vitamin C (60-90 mg/100 gm fresh weight) in comparison to celery (7 mg/100 gm fresh weight<sup>101</sup>). Vitamin C in strawberries may offer protection to phenolic components against radiolytic damage. This may explain why the concentration of gentisic acid in irradiated strawberries was fairly high and yet was virtually destroyed in irradiated celery homogenates. In general, for both celery and strawberry, results were reproducible and

showed consistency.

Consequently, the applicability of naturally-occurring phenolic compounds in plant-derived materials as suitable "target" molecules for radiolytically-generated  $\cdot\text{OH}$  radical is largely dependent upon the nature of their chemical modifications, i.e. hydroxylation and/or decarboxylation. Furthermore, the concentration of phenolic constituents present in foodstuffs increase or decrease as a result of irradiation treatment and significant differences between control and irradiated samples were readily detectable.

Hence, aromatic hydroxylation utilising HPLC in combination with EC detection appears to be a highly sensitive method for measuring radiolytically-generated  $\cdot\text{OH}$  radical-mediated damage to aromatic components present in plant-derived foodstuffs subjected to ionising radiation. The vitamin C content of strawberry homogenates prior and subsequent to gamma-irradiation has also been successfully determined by the combination of these two analytical techniques. Gamma-irradiation treatment of strawberries at a dose of 5.0 kGy resulted in the reduction of vitamin C content to approximately 80% of its original level. However, measurement of vitamin C in fruits and vegetables is not a very useful marker of gamma-irradiation treatment since vitamin C itself is extremely prone to oxidative degradation.



**CHAPTER 4**

**LIPID PEROXIDATION**

#### 4. LIPID PEROXIDATION

##### 4.1 Introduction

Lipid peroxidation is one of the major degradative processes responsible for loss in quality of foodstuffs containing polyunsaturated fatty acids (PUFAs). Common PUFAs contain two or more double bonds, generally separated by a single methylene group. The lipids most susceptible to oxidative degradation are the unsaturated fatty acid moieties present in oleic, linoleic and linolenic acids which are found to occur in most plants and animals<sup>102</sup>.

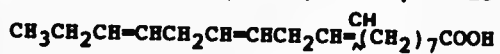
**OLEIC ACID** (*cis*-9-Octadecanoic acid)



**LINOLEIC ACID** (*cis*-9,*cis*-12-Octadecadienoic acid)



**LINOLENIC ACID** (*cis*-9,*cis*-12,*cis*-15-Octadecatrienoic acid)



The oxidative deterioration of food lipids involves primary autoxidation reactions which are accompanied by various secondary reactions. PUFAs are particularly sensitive to oxidative damage due to the facile abstraction of an allylic hydrogen atom from their methylene (-CH<sub>2</sub>-) carbon atoms by radiolytically-generated OH radical together with secondary alkoxy and peroxy radicals<sup>103-104</sup>. Their susceptibility to oxidative deterioration increases as the number of double bonds present increases<sup>102</sup>.

The OH radical combines with the abstracted hydrogen atom (H) to form water (Figure 4.1). The carbon-centred radical (R) so produced generates a conjugated diene species which

interacts with dioxygen to produce a conjugated diene peroxy radical (ROO $\cdot$ ). This radical abstracts another hydrogen atom from an adjacent PUFA to form a conjugated diene lipid hydroperoxide, resulting in a self-perpetuating autocatalytic chain reaction. *Cis,trans* -(c,t)- and *trans,trans*-(t,t)-conjugated diene hydroperoxides are the primary products formed in linoleate autoxidation<sup>104,105</sup>, as illustrated in Figure 4.2.

These intermediary compounds, although stable at ambient temperatures, are degraded to a wide variety of so-called "end-products" (cf. Figure 4.3 for hydroperoxide decomposition<sup>106</sup>). The degradation is catalysed by traces of redox-active transition metal-ion complexes (e.g. those of iron and copper<sup>107</sup>). The secondary and tertiary end-products formed during oxidation of unsaturated fatty acid components consist of saturated and unsaturated aldehydes, di- and epoxyaldehydes, lactones, furans, ketones, oxo- and hydroxy-acids, and saturated and unsaturated hydrocarbons. The aldehydes are believed to contribute to the "off smell" and flavours characteristic of rancidity in edible oils and fats<sup>108</sup>.

**Figure 4.1**

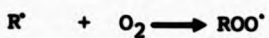
**Autoxidation of PUFAs by a Free Radical Chain Mechanism  
Involving Three Stages**

**INITIATION: HYDROGEN ATOM ABSTRACTION**



where, RH = unsaturated lipid

**PROPAGATION: FREE RADICAL CHAIN REACTIONS**



**TERMINATION: FORMATION OF NON-RADICAL PRODUCTS**



**Figure 4.2**

AUTOXIDATION OF LINOLEIC ACID

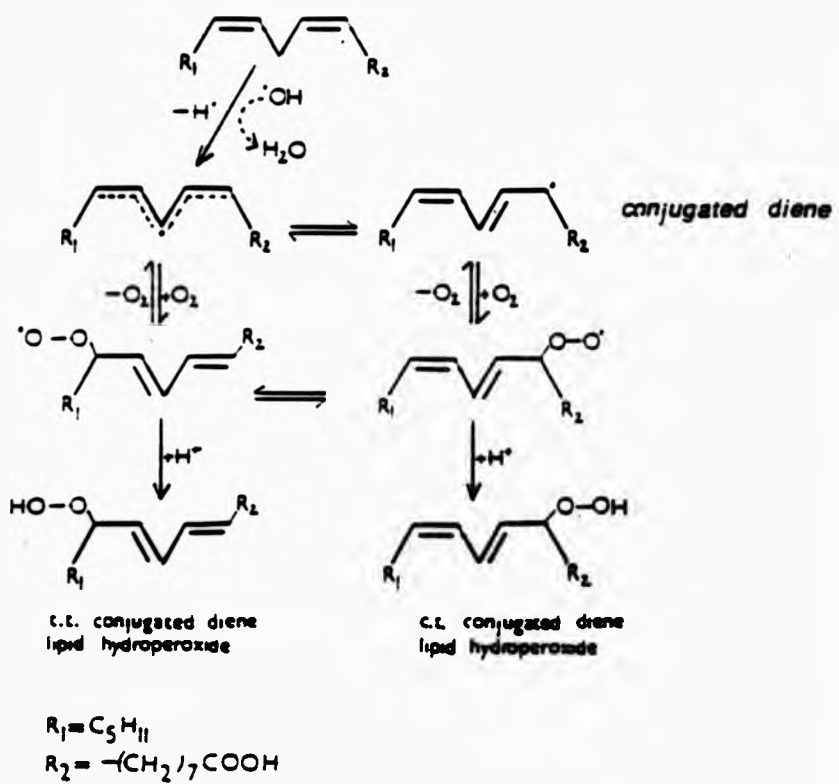
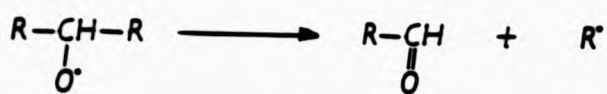
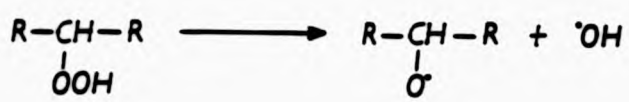


Figure 4.3

Hydroperoxide Decomposition



Generally, autoxidative degradation in fat-containing foods is prevented by the addition of specific compounds called antioxidants. These function by reducing the rate of chain initiation and causing chain breakage. The antioxidant provides a readily available hydrogen atom for abstraction by peroxy radicals. Active antioxidants commonly used in the food industry include  $\alpha$ -tocopherol and gallates such as BHA (t-butyl hydroxy-anisole) and BHT (di-t-butyl-hydroxy-toluene). These are sometimes used in combination with synergists such as citric and ascorbic acids which may act by binding trace metal ions or by regenerating the antioxidant respectively<sup>108,109</sup>.

#### 4.2 METHODS FOR MEASUREMENT OF LIPID PEROXIDATION

The identification and quantification of specific "end-products" resulting from OH radical-initiated attack on lipids may have some application to the assessment of radiolytic damage to foodstuffs containing PUFAs. The peroxidation process may also be initiated by factors other than irradiation. These include exposure of lipids to heat, light, oxygen and catalysts (i.e. traces of metal-ions, haemoproteins, or other iron-containing proteins in tissues<sup>106</sup>). Consequently, non-irradiated samples may also contain lipid peroxidation end-products similar to those found in irradiated food lipids. It is therefore essential to ensure that the end-products monitored do not occur widely in non-irradiated foodstuffs.

#### 4.2.1 Identification of Conjugated Diene Maxima by UV Spectroscopy

One possible method for monitoring the course of free radical-mediated damage to PUFAs is the identification of conjugated diene adducts, including diene lipid hydroperoxides and their isomers in appropriate extracts of irradiated foodstuffs<sup>68,69</sup>. These primary products and the conjugated ketodienes arising from their degradation absorb light strongly in the UV region of the electromagnetic spectrum at wavelengths in the range 230-270 nm<sup>110-112</sup>.

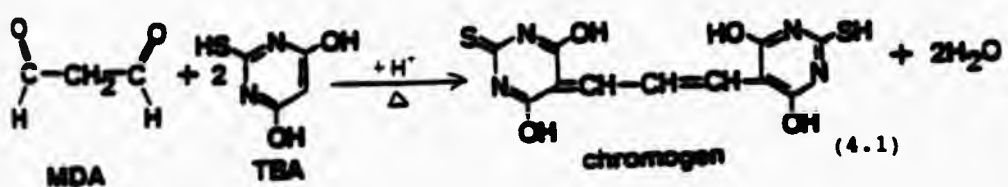
Although the lipid peroxidation end-products are readily isolated from food samples by a simple chloroform extraction process, direct measurement in this wavelength region is of limited utility. This is because the conjugated diene maxima appear as a poorly defined shoulder superimposed on the high absorbance of other food components also present in the lipid/chloroform extract. The conjugated diene absorption maxima can, however, be clearly identified and resolved by monitoring minima present in corresponding second-derivative (2D) spectra of lipid extracts (an absorption maximum in the zero-order spectrum appears as a minimum in the 2D spectrum). The technique of 2D spectrophotometry has previously been applied to the measurement of diene conjugates (specifically *cis,trans* and *trans,trans* isomers produced from the autoxidation of arachidonic acid) produced in microsomal PUFAs following exposure of rats to carbon tetrachloride<sup>112</sup>. However, it has not been applied to food lipid studies and



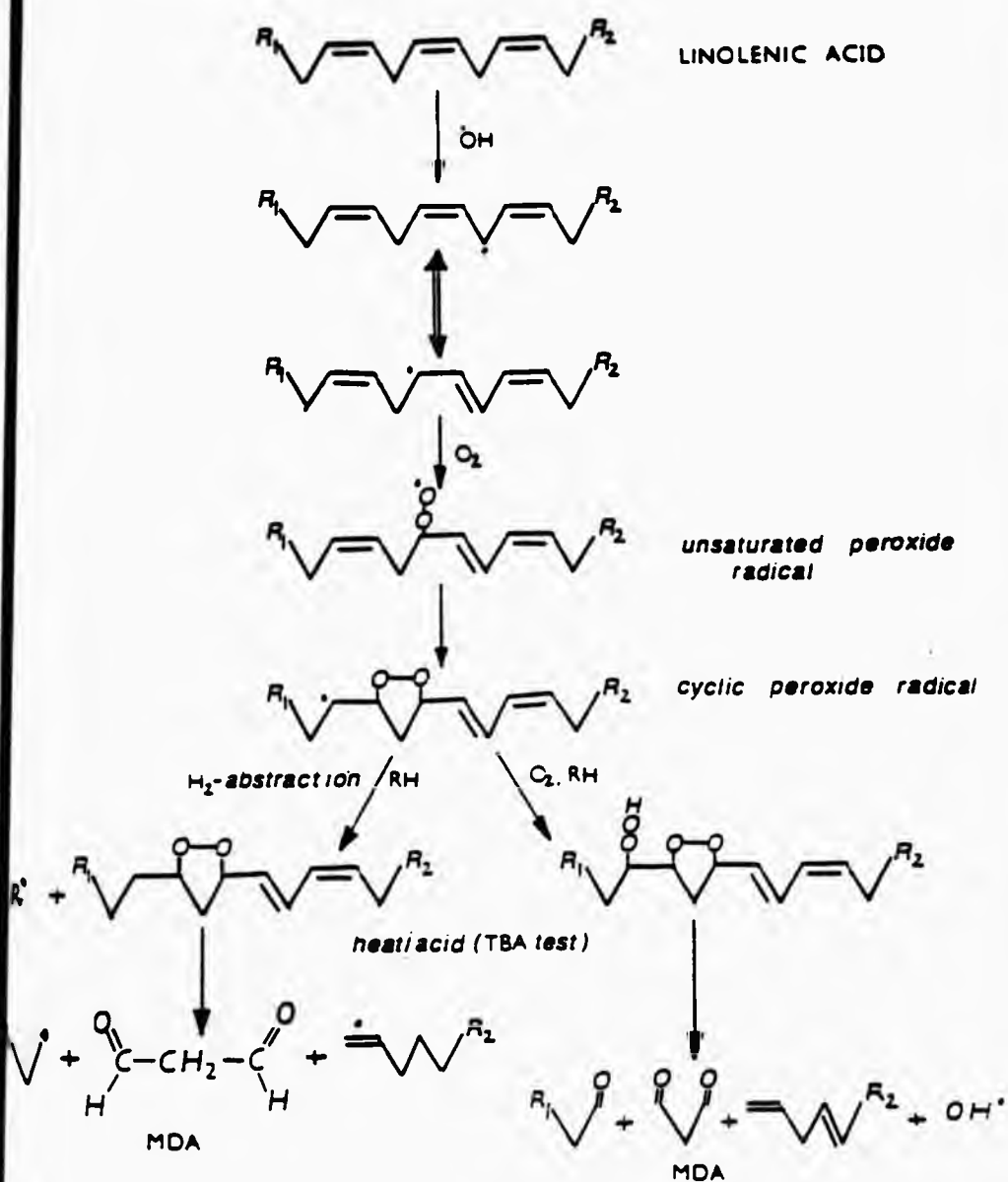
may therefore serve as a potential method for monitoring conjugated diene lipid hydroperoxide species (specifically *cis,trans*-( $\lambda_{\text{max}}$  242 nm) and *trans,trans*-( $\lambda_{\text{max}}$  232 nm) isomers) in peroxidised samples of corn oil (which consists mainly of linoleic with smaller quantities of linolenic acid).

#### 4.2.2 The Thiobarbituric Acid (TBA) Test

The TBA test has been widely used for measuring oxidative rancidity in fat-containing foods<sup>113</sup>. The primary products generated during peroxidation of PUFAs consist of a complex mixture of peroxides which are further degraded to produce a range of products including carbonyl compounds, eg. malondialdehyde (MDA<sup>108</sup>), as shown in Figure 4.4. The TBA test is a colorimetric analytical technique and involves the reaction of aldehydes in the sample with TBA under acidic conditions to produce a pink-coloured chromogen (generally attributable to the 2:1 TBA-MDA adduct) which absorbs light strongly at a wavelength of 532 nm (equation 4.1).



**Figure 4.4**  
**FORMATION OF MDA FROM LINOLENIC ACID<sup>108</sup>**



Although the major TBA-reactive component is MDA, it is now clear that a number of other compounds e.g. unsaturated carbonyls and other aldehydes, proteins and sugars, together with those resulting from 'OH radical attack on these species also react with TBA under the test conditions to form products which absorb at wavelengths close to 532 nm<sup>107</sup>. Indeed, reaction of the aldehydes, alkenals, alk-2-enals and alka-2,4-dienals with TBA produces yellow (absorption at 455 nm), orange (absorption at 495 nm) and red (absorption at 532 nm)- absorbing chromogens<sup>114</sup>. Moreover, since only a small amount (1-2%) of the lipid peroxidation end-products is actually MDA, a large quantity of the chromogen produced is due to further decomposition of lipid hydroperoxides during the acid/heating stage of the assay.

Although MDA is associated with rancidity, it has also been shown to occur in non-rancid foods including meat, herring and vegetable oil<sup>115</sup>. Although simple and relatively sensitive, the TBA test is non-specific as a method for the identification of lipid peroxidation products.

The application of 2D spectrophotometry to the analysis of TBA-reactive material in a peroxidised sample of a commercial brand of corn oil (and PUFAs i.e. linoleic and linolenic acids) is reported here. The 2D technique has not been previously applied in combination with the TBA test for foodstuffs susceptible to lipid peroxidation.

### 4.3 RESULTS

#### 4.3.1 Second-derivative (2D) Spectrophotometric Analysis of TBA-Reactive Material in Peroxidised Samples of Corn Oil

The 2D spectrophotometric technique was employed in order to resolve overlapping absorption maxima present in visible spectra obtained from the reaction of corn oil with TBA. The peroxidation of corn oil was previously induced by various treatments including (i) the Fe(II)/EDTA/H<sub>2</sub>O<sub>2</sub> system, (ii)  $\gamma$ -irradiation at a dose of 5.0 kGy and (iii) by heating the oil at 60°C as described in the experimental section. In all cases, a control sample was included.

Figure 4.5(a) shows typical zero-order and corresponding 2D visible absorption spectra obtained subsequent to the exposure of corn oil to an 'OH radical flux generated by the Fenton system. The resulting 2D spectra obtained from all treated samples of corn oil exhibited minima located at 452, 496 and 532 nm, (Figures 4.5(b) and (c)). Figure 4.5(d) shows the control sample of corn oil reacted with TBA.

The absorption band located at 532 nm can be assigned to the TBA-MDA adduct<sup>103</sup> since MDA is largely derived from the breakdown of isomeric linoleate hydroperoxides during the stringent acid/heating stage of the assay. Indeed, the percentage composition of linoleic acid in corn oil is approximately 55%, the rest comprising oleic acid (26%), linolenic acid (9%) and palmitic acid (11%)<sup>116</sup>.

The origin of the absorption bands at 452 and 496 nm was not further investigated. However, they are likely to arise

from the TBA-reactivity of alternative secondary oxidation products in the sample.

Table 4.1 shows the intensities of the 2D signals at 452, 496 and 532 nm obtained from corn oil samples subjected to the different peroxidation treatments. The intense 2D signal and increased zero-order absorption bands (Figure 4.5(a)) of the Fe(II)/EDTA/H<sub>2</sub>O<sub>2</sub>- treated sample demonstrates the ability of this system to enhance the lipid peroxidation process, a result of its 'OH radical producing and catalytic nature.

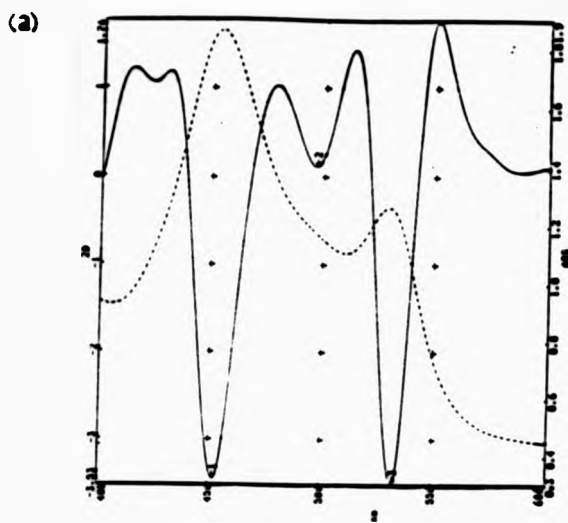
The 2D signals for the irradiated sample are more intense than those of the sample subjected to heating. A control sample of corn oil shows the absence of the 2D signals at 452 and 496 nm, although a very small signal is present at 532 nm indicating that peroxidation could have been initiated in the control sample by exposure to U.V. light or air<sup>105</sup>.

**TABLE 4.1**

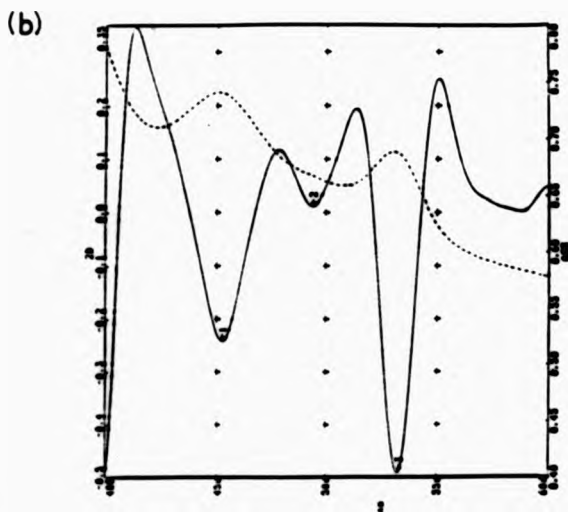
**Table Showing the Intensities of the 2D Signals at 452, 496 and 532 nm in Peroxidised Samples of Corn Oil Subjected to Various Treatments**

Wavelength in nm	INTENSITY OF 2D SIGNAL ( $d^2A/d\lambda^2$ )			
	Corn Oil Peroxidised by Fenton System	Corn Oil Irrad.	Corn Oil Heated	Corn Oil Control
452	3.71	0.46	0.23	n.d.
496	0.92	0.13	0.05	n.d.
532	4.20	0.72	0.32	0.11

**Figure 4.5**



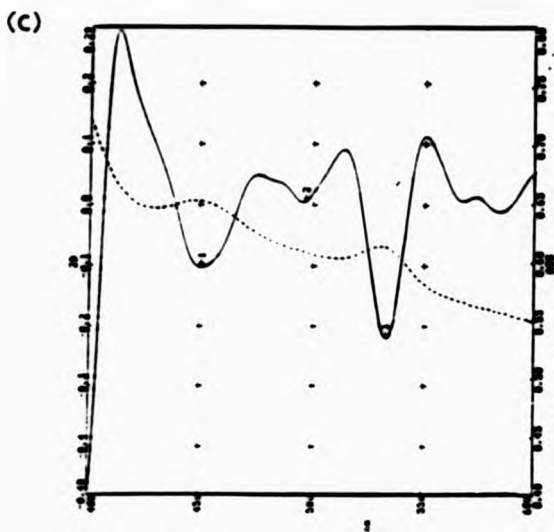
Zero-order (---) and corresponding 2D visible absorption spectra (—) of corn oil subjected to peroxidation by a Fe(II)/EDTA/H<sub>2</sub>O<sub>2</sub> system following reaction with TBA.



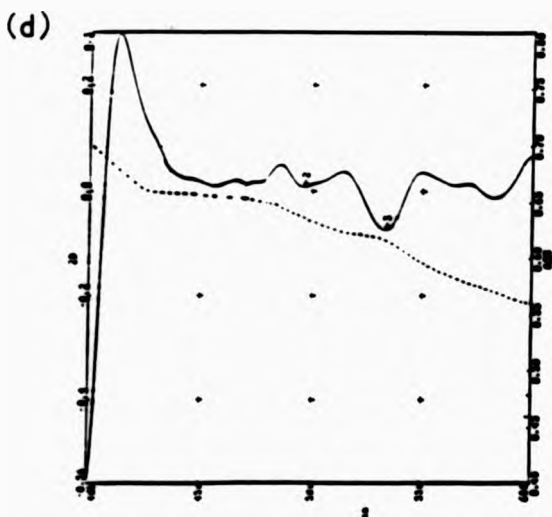
Zero-order (---) and corresponding 2D visible absorption spectra (—) of corn oil subjected to peroxidation by irradiation at a dose of 5.0 kGy following reaction with TBA.



**Figure 4.5**



Zero-order (---) and corresponding 2D visible absorption spectra (—) of corn oil subjected to peroxidation by heating at 60°C following reaction with TBA.



Zero-order (---) and corresponding 2D visible absorption spectra (—) of a control sample of corn oil following reaction with TBA.

#### 4.3.2 Application of 2D Spectrophotometry to Thiobarbituric Acid Reactivity in Peroxidised Commercially-Available PUFAs

The susceptibility to peroxidation of linoleic and linolenic fatty acids (both of which are present in corn oil) was evaluated by spectrophotometric analysis by using the TBA method. Figure 4.6(a) exhibits the zero-order and corresponding 2D electronic absorption spectra of linoleic acid before and after being subjected to the Fe(II)/EDTA/H<sub>2</sub>O<sub>2</sub> system, both recorded after reacting with TBA. The concentrations of both linoleic and linolenic fatty acids used was 0.64 mM.

The 2D spectrum of the peroxidised sample of linoleic acid exhibits relatively intense maxima centred at 452, 495 and 532 nm respectively. The control sample, however, shows only a very weak absorption band at 452 nm. The absorption band at 532 nm is solely attributable to the TBA-MDA adduct (as found previously with corn oil) and the bands at 452 and 495 nm are attributable to alternative secondary oxidation products which react with TBA.

Figure 4.6(b) shows the zero-order and corresponding 2D electronic absorption spectra obtained from the reaction of OH radical-damaged linolenic acid (generated by the Fenton system) with TBA. A control sample not subjected to this treatment is also shown. The 2D spectrum of the peroxidised sample exhibits maxima located at 453, 495 and 532 nm.

The corresponding 2D spectra obtained from the peroxidised sample of linoleic acid is analogous to that of linolenic



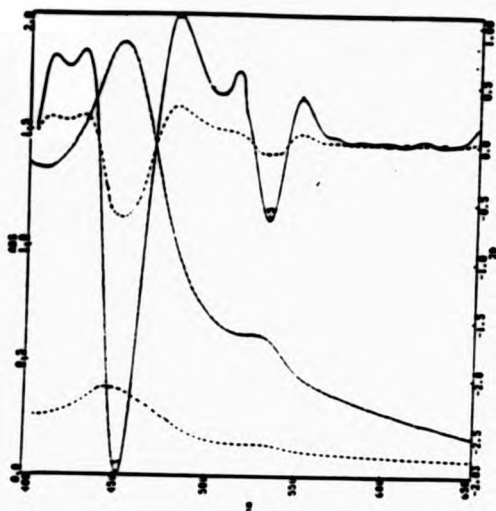
acid, but the absorption band at 532 nm (attributable to the TBA-MDA adduct) in linolenic acid is of much greater intensity. This observation is probably a consequence of the fact that linolenic acid has a faster rate of oxidative degradation than linoleic acid since it possesses one additional double bond i.e. susceptibility to peroxidation increases with the number of double bonds present. Indeed, the relative rates of peroxidation for oleic, linoleic and linolenic fatty acids with one, two and three double bonds respectively have been shown to be in the ratio 1:12:25<sup>102,117</sup>.

In section 4.3.1 it was concluded that the absorption band located at 532 nm was of high intensity relative to the other absorption bands (at 452 and 496 nm) for all peroxidised samples of corn oil, suggesting that the major contributor of the chromogen is attributable to linoleic and linolenic hydroperoxides which decompose to give MDA<sup>108</sup>.



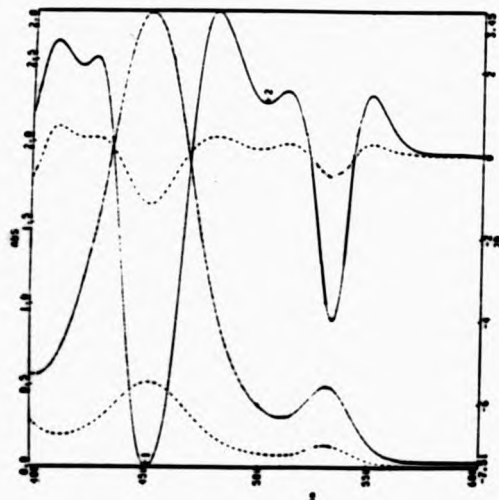
**Figure 4.6**

(a)



Zero-order and corresponding second-derivative (2D) electronic absorption spectra obtained after allowing both control (—) and Fe(II)/EDTA/H<sub>2</sub>O<sub>2</sub>- treated (---) samples of linoleic acid to react with TBA under acidic conditions.

(b)



Zero-order and corresponding second-derivative (2D) electronic absorption spectra obtained after allowing both control (—) and Fe(II)/EDTA/H<sub>2</sub>O<sub>2</sub>- treated (---) samples of linolenic acid to react with TBA under acidic conditions.

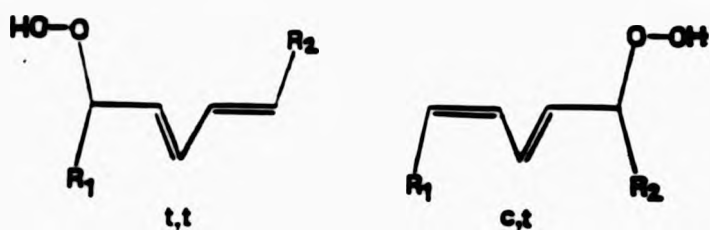
#### 4.3.3 Determination of Conjugated Diene Species in Peroxidised Commercially-Available PUFAs

Figure 4.7(a) shows the zero-order absorption spectra of samples of linolenic acid obtained before (control) and after oxidation induced by exposure to a Fe(II)/EDTA/H<sub>2</sub>O<sub>2</sub> system. The peroxidised sample shows a relatively large overlapping absorption band in the 220-250 nm region. These overlapping absorption bands are readily resolved by 2D electronic absorption spectrophotometry and Figures 4.7(b) and (c) show the zero-order and corresponding 2D spectra for the control and the peroxidised samples of linolenic acid.

The 2D spectra of the peroxidised sample exhibit minima located at 230, 236, 241 and 247 nm respectively. The 2D minima in peroxidised linolenic acid located at 236 and 241 nm are conceivably attributable to *trans,trans-* (*t,t*)- and *cis,trans-* (*c,t*)- conjugated diene hydroperoxydiene or hydroxydiene isomers<sup>112</sup>. The 2D spectra of the control sample exhibits relatively weak bands located at 230 and 235 nm respectively.

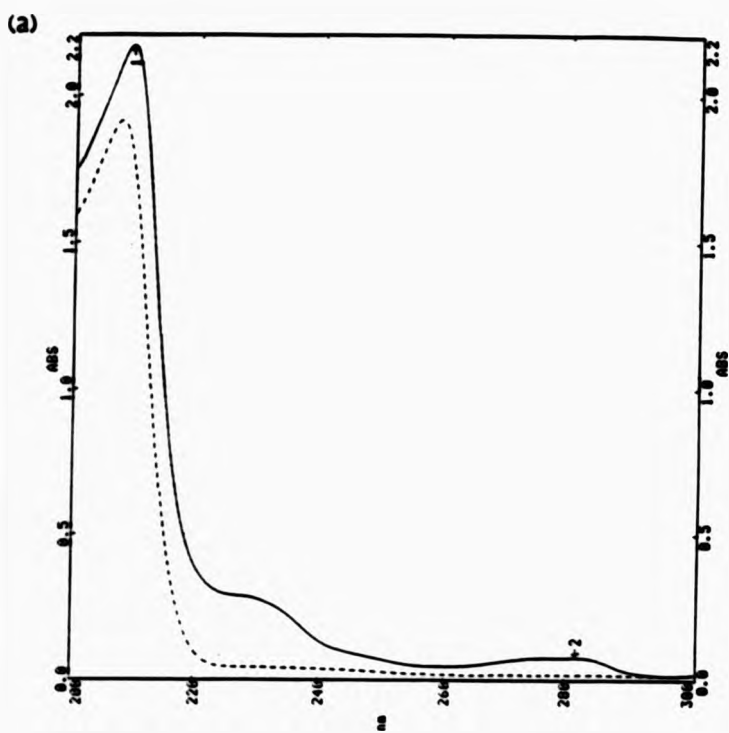
The conjugated diene species arising from autoxidised linoleic acid were also investigated following its exposure to an Fe(II)/EDTA/H<sub>2</sub>O<sub>2</sub> system. Figure 4.7(d) shows the zero-order spectra of linoleic acid before and after attack by OH radical generated by the Fenton reaction system. Figures 4.7(e) and (f) show the zero-order and the corresponding 2D spectra for a control and peroxidised sample of linoleic acid.

The 2D spectra shown in Figure 4.7(f) exhibit minima located at 230, 235 and 245 nm which correspond to conjugated diene absorption maxima in the zero-order spectrum. The minima located at 235 and 245 nm are attributable to *t,t*- and *c,t*- conjugated hydroperoxydienes or hydroxydienes<sup>110,112</sup>.



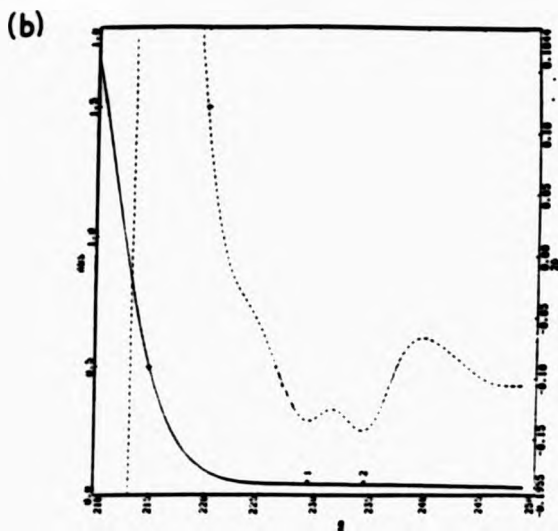
CONJUGATED DIENE ISOMERS OF  
LINOLEIC ACID

**Figure 4.7**

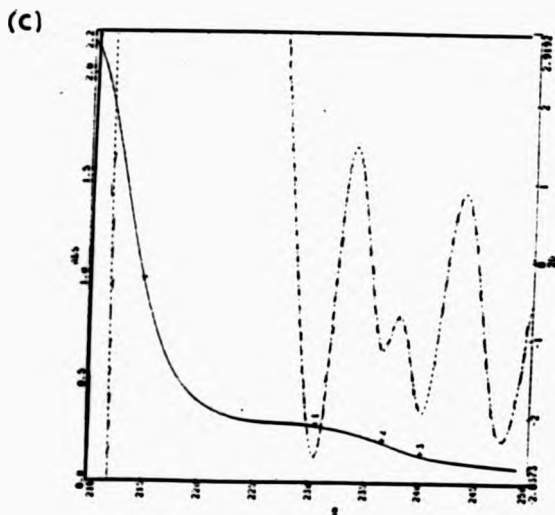


Zero-order absorption spectra of cyclohexane extracts of linolenic acid before (----) and after (——) exposure to a catalytic Fe(II)/EDTA/H<sub>2</sub>O<sub>2</sub>- system.

**Figure 4.7**

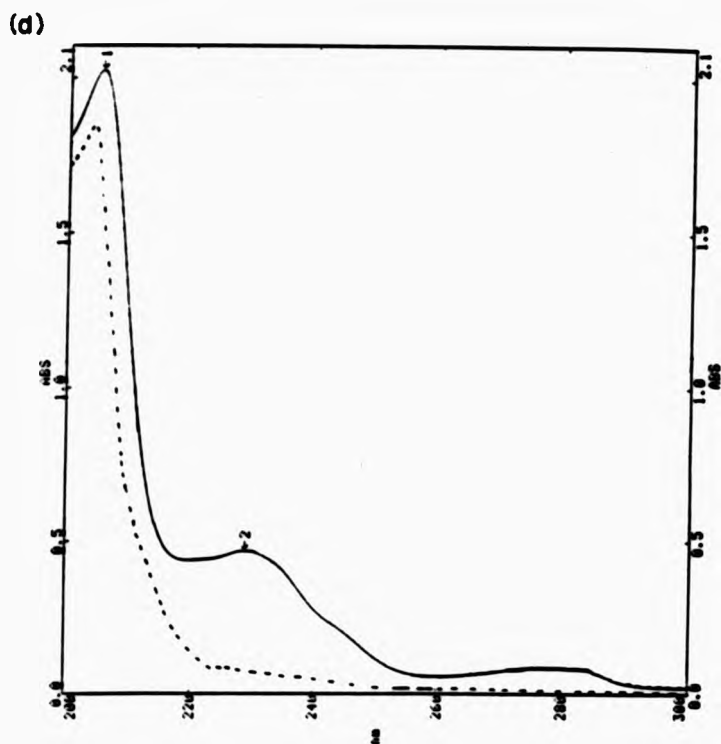


Zero-order (—) and corresponding second-derivative (2D) electronic absorption spectra (----) of a cyclohexane extract of linolenic acid before reaction with Fe(II)/EDTA/H<sub>2</sub>O<sub>2</sub>.



Zero-order (—) and corresponding second-derivative (2D) electronic absorption spectra (----) of a cyclohexane extract of linolenic acid after treatment with Fe(II)/EDTA/H<sub>2</sub>O<sub>2</sub>.

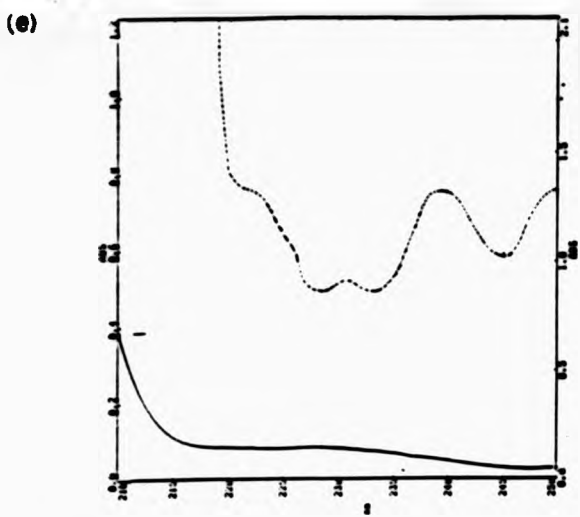
**Figure 4.7**



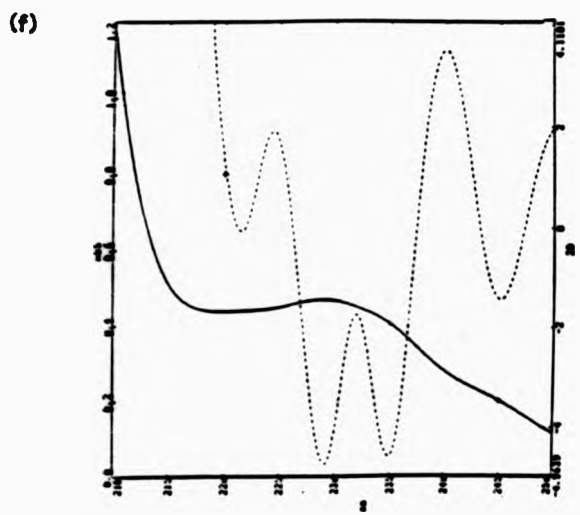
Zero-order absorption spectra of cyclohexane extracts of linoleic acid before (—) and after (---) exposure to a catalytic Fe(II)/EDTA/H<sub>2</sub>O<sub>2</sub> system.



Figure 4.7



Zero-order (—) and corresponding second-derivative (2D) electronic absorption spectra (---) of a cyclohexane extract of linoleic acid before treatment with Fe(II)/EDTA/H<sub>2</sub>O<sub>2</sub>.



Zero-order (—) and corresponding second-derivative (2D) electronic absorption spectra (---) of a cyclohexane extract of linoleic acid after reaction with Fe(II)/EDTA/H<sub>2</sub>O<sub>2</sub>.



#### 4.3.4 2D Spectrophotometric Analysis of Conjugated Diene Species in Corn Oil Subjected to Peroxidation

The 2D spectrophotometric technique was also extended to the determination of conjugated diene species arising in irradiated samples of corn oil. Since lipid peroxidation can also be initiated by factors other than irradiation<sup>106</sup>, studies were also conducted on samples of corn oil which had undergone artefactual peroxidation.

The corn oil was subjected to a variety of treatments including (i)  $\gamma$ -irradiation at a dose level of 5.0 kGy, (ii) heating at 60°C for a period of 24 hr. and (iii) exposure to air at ambient temperature for 24 hr. In each case a control sample was also analysed.

Figures 4.8(a), (b), (c) and (d) show the resulting zero-order and corresponding 2D electronic absorption spectra of cyclohexane extracts of corn oil subjected to the three different treatments. The 2D spectra of the irradiated sample (Figure 4.8(a)) exhibit minima located at 229, 234 and 242 nm respectively which correspond to conjugated diene absorption maxima in the zero-order spectra. The 2D minima located at 234 and 242 nm (marked by the arrows) are conceivably attributable to *trans,trans* (t,t)- and *cis,trans* (c,t)- conjugated diene species<sup>112</sup>. The 2D absorption spectra of corn oil subjected to oxidation by heating and exposure to air (Figures 4.8(b) and (c) respectively) were also obtained and compared with those of the irradiated sample.

Figures 4.8(b) and (c) also exhibit minima located at 229

and 242 nm. However, the 2D signal at 234 nm present in the irradiated sample of corn oil is absent. The 2D spectra for the control sample (Figure 4.8(d)) exhibits one minimum located at 229 nm and both 2D signals at 234 and 242 nm (attributable to isomeric conjugated diene species) are absent. Therefore, peroxidation is manifested by the presence of the 2D signal at 234 nm.

The conjugated dienes arising in all samples of corn oil were monitored over a period of time, and modifications in the intensities of the 234 and 242 nm 2D signals with increasing time were monitored. Figures 4.9(a) and (b) show plots of the intensity of the 2D signals at (a) 234 nm (corresponding to (t,t)-) and (b) 242 nm (corresponding to (c,t)- conjugated dienes) versus time for all four samples of corn oil.

Analysis of Figures 4.9(a) and (b) show <sup>5</sup> clear differences between the four samples of corn oil subjected to the various treatments. In general, for all four samples studied the 2D intensity of the signals at 234 nm and 242 nm increase initially followed by a decrease with time. This observation is readily attributable to the instability of the lipid hydroperoxydienes and hydroxydienes which after a period of time breakdown to give secondary peroxidation products.

For the sample of corn oil subjected to irradiation treatment, the intensity of the signal at 234 nm is at a maximum during the first 48 hrs. of analysis following irradiation (Figure 4.9(a)). For all other samples, the

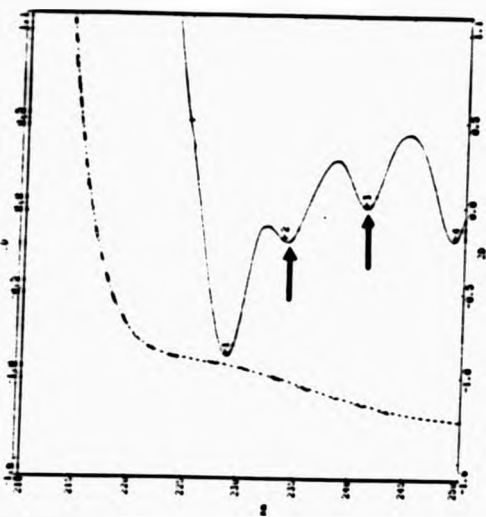
signal at 234 nm is absent initially although after a period of 72-96 hrs. of analysis it appears in the spectrum. The intensity of the 234 nm signal increases slowly during the 96-144 hr. post-irradiation time period. This observation may be attributable to artefactual peroxidation by exposure to atmospheric oxygen or light.

The 2D intensity of the signal at 242 nm (Figure 4.9 (b)) however, is present in all corn oil samples studied from day 1 of analysis, its intensity being the greatest in corn oil samples subjected to peroxidation by  $\gamma$ -irradiation, heating, and exposure to air. As expected, the intensity of this signal was lowest in the control sample.



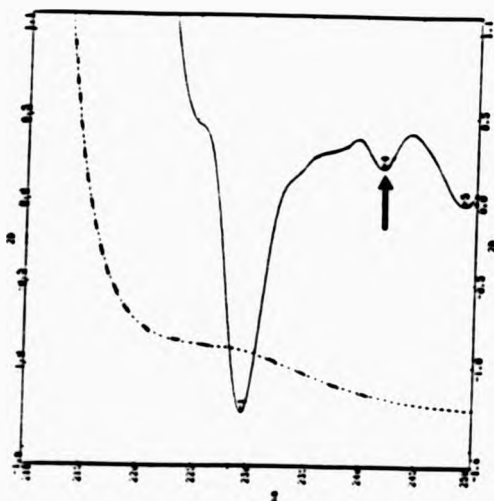
**Figure 4.8**

(a)



Zero-order (----) and corresponding 2D electronic absorption spectra (—) of a cyclohexane extract of corn oil irradiated at a dose of 5.0 kGy (spectra recorded on day 1).

(b)

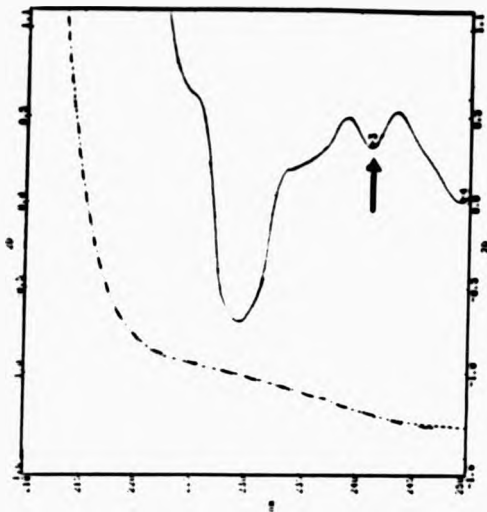


Zero-order (----) and corresponding 2D electronic absorption spectra (—) of a cyclohexane extract of corn oil heated at 80°C for 24 hr. (spectra recorded on day 1).



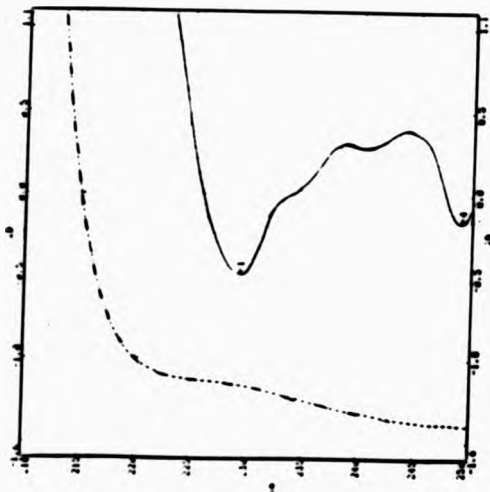
Figure 4.8

(c)



Zero-order (----) and corresponding 2D electronic absorption spectra (—) of a cyclohexane extract of corn oil subjected to oxidation in air for 24 hr. (spectra recorded on day 1).

(d)

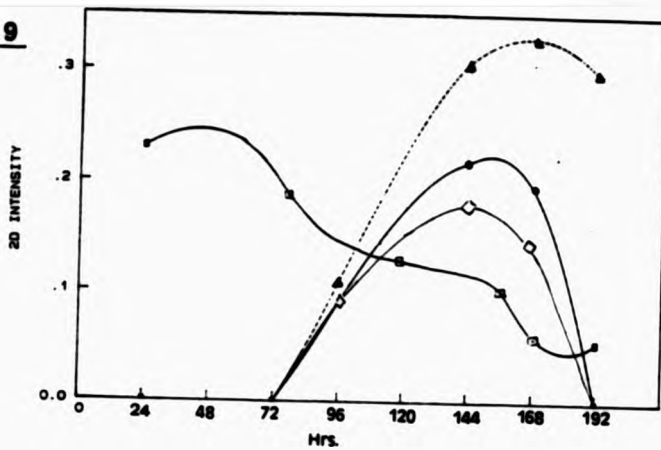


Zero-order (----) and corresponding 2D electronic absorption spectra (—) of a cyclohexane extract of corn oil control (spectra recorded on day 1).



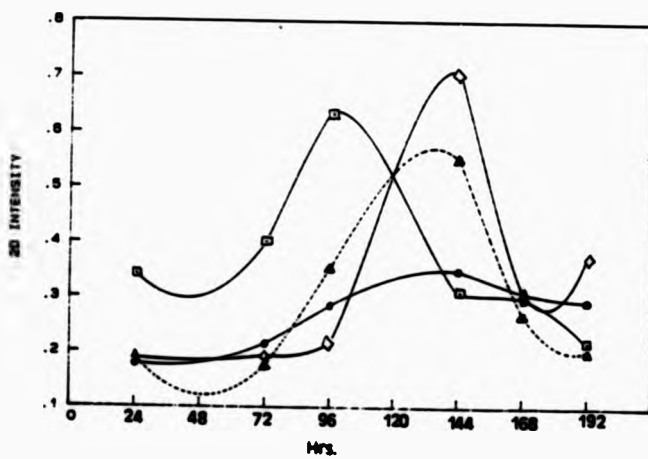
**Figure 4.9**

(a)



A typical plot of the intensity of the 2D signal at 234 nm for corn oil subjected to (i) irradiation (□ □ □), (ii) heating at 60°C (◇ ◇ ◇), (iii) oxidation in air (▲ ▲ ▲) and a control sample (• • •).

(b)



A typical plot of the intensity of the 2D signal at 241 nm for corn oil subjected to (i) irradiation (□ □ □), (ii) heating at 60°C (◇ ◇ ◇), (iii) oxidation in air (▲ ▲ ▲) and a control sample (• • •).

#### 4.4 SUMMARY AND CONCLUSION

##### 4.4.1 Conjugated Diene Method

The autocatalytic self-perpetuating nature of the lipid peroxidation process results in the formation of measurable concentrations of its end-products produced during autoxidation of corn oil and standard fatty acids. The determination of isomeric conjugated diene lipid hydroperoxydienes and hydroxydienes by 2D spectrophotometry is a method which shows some promise for the assessment of oxidative damage to lipids in fat-containing foods.

Samples of corn oil peroxidised by the various treatments ( $\gamma$ -radiation, heat and air autoxidation) resulted in the formation (from their 2D spectra) of minima located at 234 and 242 nm, attributable to *t,t*- and *c,t*- conjugated diene lipid hydroperoxydienes. Initially however, the signals at 232 and 242 nm (measured within 24 hrs. after irradiation treatment) were found to be present only in the sample subjected to peroxidation by  $\gamma$ -radiation treatment. Time-dependent studies resulted in the development and increase in intensities of both signals (in all samples) over a period of time.

The analytical system employed here is rapid, sensitive and clearly illustrates its ability to detect products generated in the peroxidation process, specifically *t,t*- and *c,t*- conjugated diene lipid hydroperoxydienes.

#### 4.4.2 Thiobarbituric Acid Method

The determination of MDA by the application of 2D spectrophotometry to the analysis of TBA-reactive material present in peroxidised corn oil and standard fatty acids is also a promising method for the assessment of free radical-mediated oxidative damage to lipids. The selectivity of the TBA test can be further increased by HPLC separation followed by spectrophotometric detection at 270 nm of the 2:1 TBA-MDA adduct<sup>118</sup>, or alternatively by exploiting the adduct's fluorescence properties<sup>119</sup>.

All peroxidised samples of corn oil (subjected to the various treatments) resulted in the formation of 2D absorption minima located at 452, 496 and 532 nm respectively. However, the increased absorbance of the Fe(II)/EDTA/H<sub>2</sub>O<sub>2</sub>-treated sample demonstrated the ability of this system to trigger and consequently enhance the lipid peroxidation process, since iron serves as a catalyst for the formation of the highly reactive 'OH radical.

Under the highly acidic conditions employed in the test and, in the presence of catalytic redox-active transition metal-ions (e.g. Fe(II)), linoleic and linolenic acids are also rapidly autoxidised to give TBA-reactive materials.

The potential application of these two methods (i.e. TBA and conjugated diene method) as test systems for discriminating between irradiated and non-irradiated foodstuffs containing PUFAs however shows little promise. The lipid peroxidation process is time-dependent and may also proceed artefactually. Therefore, fat-containing foods not



subjected to gamma-irradiation, after a period of time, might additionally give positive results indicative of the peroxidation process. However, both methodologies do serve as useful and sensitive indicators for monitoring 'OH radical initiated oxidative degradation of PUFAs in foodstuffs subsequent to irradiation treatment.

**CHAPTER 5**

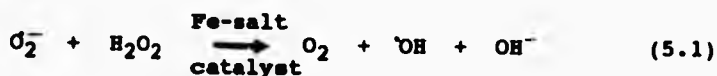
**RADIOLYTICALLY-MEDIATED**  
**OXIDATIVE DAMAGE TO CARBOHYDRATES**

## 5. RADIOLYTICALLY-MEDIATED OXIDATIVE DAMAGE TO CARBOHYDRATES

### 5.1 Introduction

The effects of ionising radiation on carbohydrates and carbohydrate-containing foodstuffs has been previously reviewed and studied in some detail<sup>96,119,120</sup>. The interaction of ionising radiation with carbohydrates results in oxidative degradation, which may lead to colour changes and to the development of "off-flavours".

Chemical modification by ionising radiation for carbohydrates occurring in the aqueous phase is predominantly an indirect effect of radiation. Consequently, any observed changes are mostly due to reactions with the primary products of water radiolysis. The major reactive species in the degradation process is the hydroxyl radical (OH). The OH radical is also known to be formed in biochemical systems by iron salt-oxygen interactions, the overall reaction summarised in equation 5.1 (the iron-catalysed Haber-Weiss reaction<sup>121,122</sup>).



#### 5.1.1 Hydroxyl Radical (OH) Attack on Glucose

Glucose (a monosaccharide and representative of simple sugars) is the most important basic unit of larger food carbohydrates such as starch and cellulose. Its oxidation and radiation chemistry have been studied in some detail<sup>123,124</sup>. Glucose reacts with the primary radicals with second-order rate constants of  $k_2 = 3 \times 10^5 \text{ mol}^{-1} \text{ dm}^3 \text{ s}^{-1}$  for the

hydrated electron ( $e_{aq}^-$ ),  $k_2 = 4 \times 10^7 \text{ mol}^{-1} \text{ dm}^3 \text{ s}^{-1}$  for the hydrogen atom (H) and  $k_2 = 1.9 \times 10^9 \text{ mol}^{-1} \text{ dm}^3 \text{ s}^{-1}$  for the hydroxyl radical<sup>3</sup> ( $\cdot\text{OH}$ ).

The mechanism of the reaction of H atoms and  $\cdot\text{OH}$  radicals with glucose is predominantly by hydrogen abstraction from carbon bound hydrogen atoms (C—H) to yield primary glucosyl radicals<sup>119,124</sup>. The  $\cdot\text{OH}$  radicals and H atoms are not very selective and abstraction occurs at all six positions (C<sub>1</sub>-C<sub>6</sub>) of the aldohexose. The radicals generated participate in a series of reactions resulting in the formation of a large number of primary and secondary products of carbohydrate degradation. The reactions responsible for the generation of these products have been studied in some detail by Dizdaroglu et al.<sup>124</sup> and consist of disproportionation reactions of the primary glucosyl radicals, elimination of water from  $\alpha$ - $\beta$ -dihydroxyalkyl radicals, rearrangement reactions and hydrogen abstraction from glucosyl radicals. One of the reaction schemes for  $\cdot\text{OH}$  radical attack on Carbon-2 of glucose is outlined in Figure 5.1<sup>119,124</sup>.

The products of  $\cdot\text{OH}$  radical attack on glucose have been previously identified by means of paper chromatography, radioactive tracers<sup>123</sup> and gas chromatography combined with mass spectrometry<sup>124</sup>. Some 26 radiolysis products of glucose have been identified. The products largely consist of D-gluconic acid, D-glucosone, D-glucuronic acid, 2-deoxy-gluconic acid, arabinose, deoxy-keto-glucose sugars and, in addition, 2C/3C fragments identified to be glyoxal, glycollic aldehyde, and D-glyceraldehyde. Furthermore, oxygen

influences the nature of the products arising. In its absence, water elimination and rearrangement processes are suppressed, no deoxy compounds are produced and the yields of sugar acids and keto acids are increased<sup>119</sup>.

One Of The Reactions Of  $\cdot\text{OH}$  Radical Attack On C-2 Of The Glucose Molecule<sup>119</sup>

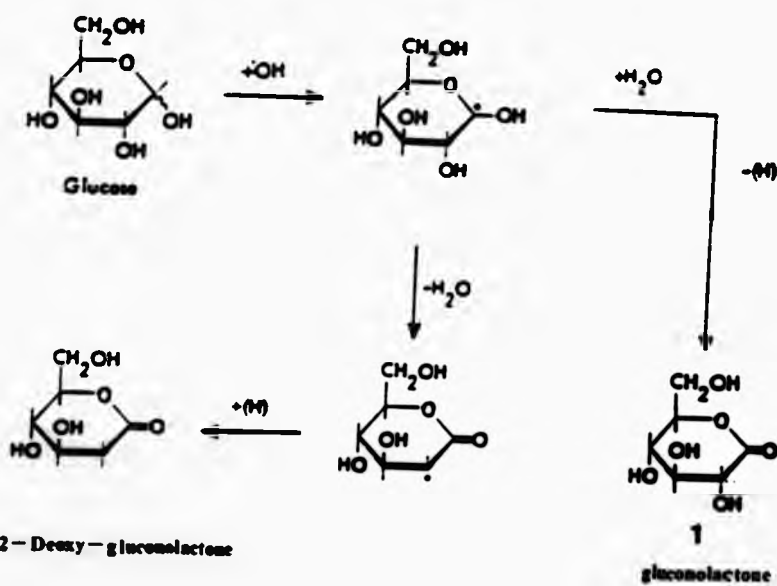


Figure 5.1

The primary and secondary products resulting from  $\cdot\text{OH}$  radical attack on a range of other aldohexoses have also been studied by Phillips et al.<sup>120,123</sup> with particular reference to the radiolysis of aqueous solutions of fructose and sucrose. Generally, the radiolytic products generated consist of aldonic and alduronic acids, osones and lower sugars. In addition, a common process is ring scission reactions which lead to the formation of two- and three- carbon atom aldehydic fragments. For higher saccharides (or polysaccharides), glycosidic scission also occurs.

#### 5.1.2 Formation of Malondialdehyde (MDA) from Carbohydrates Subjected to $\cdot\text{OH}$ Radical Attack

Another compound formed during oxidative degradation of deoxysugars is the dicarbonyl malondialdehyde (MDA) which is also a well known end-product of the lipid peroxidation process<sup>126</sup>. One of the most extensively studied deoxysugars is 2-deoxy-D-ribose<sup>94,126,127</sup>. This sugar is readily attacked by  $\cdot\text{OH}$  radical to form MDA which reacts on heating with thiobarbituric acid (TBA) under acidic conditions to yield a pink coloured chromogen. The degradation may be initiated by (i) a "site-specific" formation of  $\cdot\text{OH}$  radical derived from iron ions bound to the deoxyribose molecule<sup>128</sup>, (ii) by attack of  $\cdot\text{OH}$  radical generated free in solution<sup>127</sup> (iron ions bound to EDTA in the Fenton reaction) or (iii) by radiolysis of water<sup>94</sup>. Reducing agents such as ascorbate or the superoxide ion ( $\text{O}_2^-$ ) are capable of accelerating the reaction by converting  $\text{Fe}^{3+}$  ions to accessible  $\text{Fe}^{2+}$  ions required in

the Fenton reaction. Free MDA may be characterised by HPLC coupled with UV detection at 270 nm and the MDA-TBA adduct by its absorbance at 532 nm<sup>127,129</sup>.

Deoxyribose damage is inhibited by scavengers of  $\cdot\text{OH}$  radical such as mannitol, thiourea and catechol (i.e. these react with  $\cdot\text{OH}$  radical at higher rate constants than that of deoxyribose<sup>130</sup>), suggesting that  $\cdot\text{OH}$  radical is indeed responsible for its degradation. Consequently, the "deoxyribose assay" has been employed as a method for detecting  $\cdot\text{OH}$  radical production in biochemical systems.

Other researchers have also studied the iron-ion dependent degradation of various carbohydrates (deoxysugars), amino acids and a range of nucleosides to yield TBA-reactive intermediates which have been detected by fluorescence, UV absorption spectrophotometry or high performance liquid chromatography<sup>129,130</sup>. Further analysis reveals that, of all the compounds tested, only deoxyribose yielded a volatile TBA-reactive product after acid steam distillation of the reaction mixture<sup>93</sup>. This product exhibited properties characteristic to those of standard MDA. The precise identity of the TBA-reactive products generated by all other carbohydrates, amino acids and nucleosides may be attributable to alternative secondary oxidation products. Iron damage to carbohydrates and amino acids is thought to give rise to an increased range of toxic and potentially damaging free radical-derived intermediates formed from biomolecules *in vivo*.

The oxidative degradation of sugars in aqueous solution

(generated by a Fenton reaction or ionising radiation) results in the formation of a range of carbonyl compounds which are also TBA reactive. These include gluconic acid, glycollaldehyde, glyceraldehyde and acetaldehyde. The nature of these TBA-reactive products have been determined by second-derivative (2D) electronic absorption spectrophotometry. The 2D technique for TBA-reactive intermediates has not been previously applied in the study of radiolytic damage to carbohydrates.



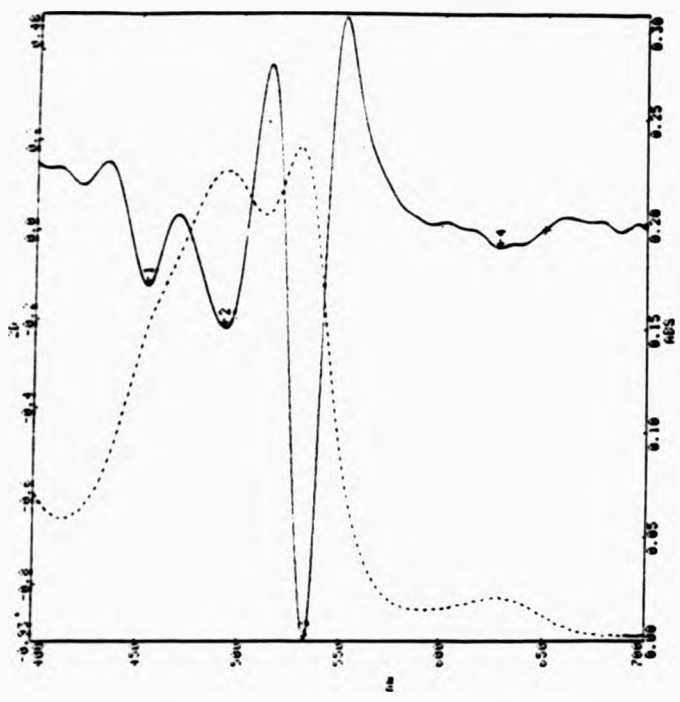
## 5.2 RESULTS

### 5.2.1 2D Spectrophotometric Analysis of TBA-Reactive Material in a Range of Carbohydrates Subjected to an OH Radical Flux Generated by the Fenton System

#### (a) 2-Deoxyribose

The 2D spectrophotometric technique was employed to resolve overlapping absorption maxima present in visible spectra obtained from the reaction of carbohydrates (subjected to oxidative degradation by the Fenton system) with TBA. Following treatment with an Fe(II) ( $1.0 \times 10^{-4}$  mol.  $\text{dm}^{-3}$ )/EDTA ( $1.0 \times 10^{-4}$  mol.  $\text{dm}^{-3}$ )/ $\text{H}_2\text{O}_2$  ( $3.3 \times 10^{-4}$  mol.  $\text{dm}^{-3}$ ) - system, all sugar solutions yielded a pink-coloured chromogen upon heating with TBA at acid pH, suggesting free-radical-mediated oxidative damage to the carbohydrates. ?

Figure 5.2 shows the zero-order and corresponding 2D electronic absorption spectra obtained from the reaction of an Fe(II)/EDTA/ $\text{H}_2\text{O}_2$ - treated sample of 2-deoxyribose with TBA. The 2D spectrum exhibits relatively intense absorption minima centred at 452, 494 and 532 nm. The minimum located at 532 nm (attributable solely to the 2:1 TBA:MDA adduct) is of stronger intensity than the minima at 452 and 494 nm, indicating that the major degradation product derived from 2-deoxyribose is MDA. The iron-catalysed degradation of 2-deoxyribose has been previously studied in great detail by Gutteridge and co-workers<sup>127,129,130</sup>, but in these investigations only zero-order spectrophotometry was employed.



**Figure 5.2**

Zero-order (----) and corresponding 2D electronic absorption spectra (—) obtained from the reaction of TBA with products derived from the interaction of 2-deoxyribose ( $1.0 \times 10^{-4} \text{ mol. dm}^{-3}$ ) with an  $\cdot\text{OH}$  radical-generating  $\text{Fe(II)/EDTA/H}_2\text{O}_2$  system.

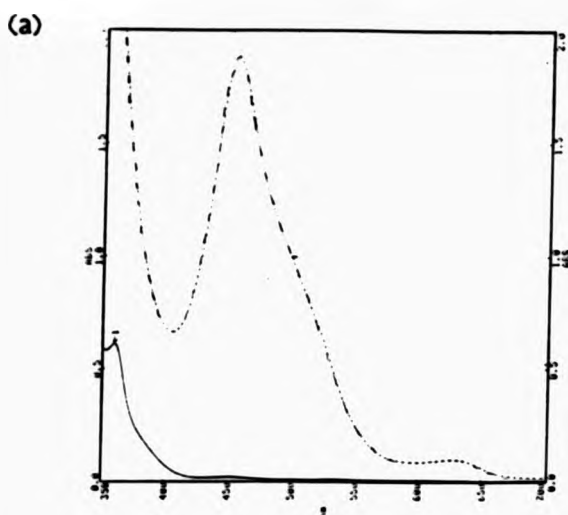
(b) Glucose, Fructose, Sucrose, Lactose and Maltose

Figure 5.3(a) exhibits the zero-order absorption spectra obtained after allowing both control and Fe(II)/EDTA/H<sub>2</sub>O<sub>2</sub>-treated samples of glucose to react with TBA. For the glucose sample, the oxidative degradation by the Fenton system is manifested by the formation of large overlapping absorption bands in the 400-650 nm region of the zero-order spectra, which can be readily resolved by the recording and subsequent examination of corresponding 2D spectra. Figures 5.3(b), (c), (d), (e) and (f) exhibit the zero-order and corresponding 2D electronic absorption spectra obtained for the sugars glucose, fructose, sucrose, lactose and maltose following their treatment with Fe(II)/EDTA/H<sub>2</sub>O<sub>2</sub> and reaction with TBA. All control samples for each sugar solution showed no absorbance in the 400-650 nm region, giving similar results to those shown in Figure 5.3(a).

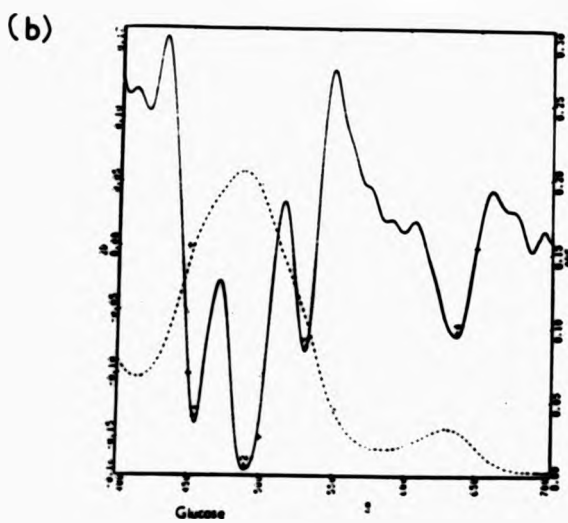
The zero-order absorption spectra for the five sugars contain intense overlapping bands for each sugar investigated, but analysis of the 2D spectra show distinct similarities for glucose with fructose and sucrose, and for lactose with maltose. The 2D spectra for glucose, fructose and sucrose exhibit minima located at 454, 490, 530 nm (attributable to the 2:1 TBA:MDA adduct), and for maltose and lactose minima are located at 452, 495, 503, 525 and 554 nm respectively.



**Figure 5.3**



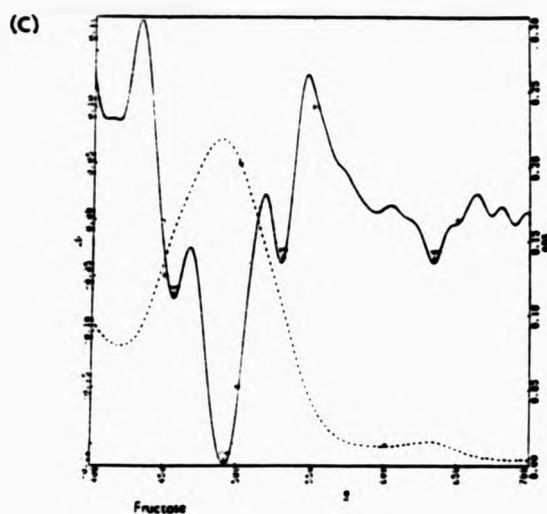
Zero-order absorption spectra obtained from the reaction of TBA with a control sample of glucose (—) and with products derived from the interaction of glucose ( $1.0 \times 10^{-4} \text{ mol.dm}^{-3}$ ) with an  $\text{OH}^{\bullet}$  radical-generating  $\text{Fe(II)/EDTA/H}_2\text{O}_2$  system (-----).



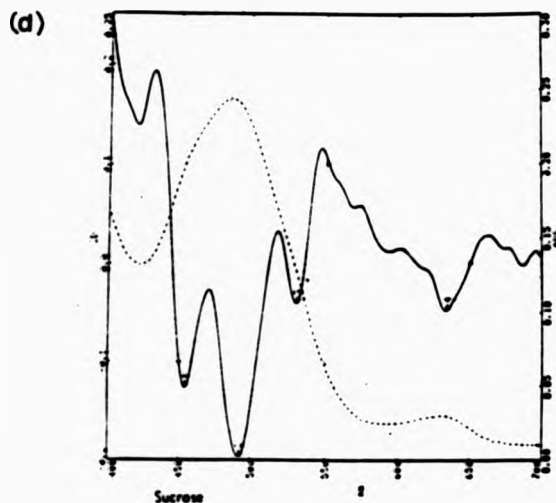
Zero-order (-----) and corresponding 2D electronic absorption spectra (—) obtained from the reaction of TBA with products derived from the interaction of glucose ( $1.0 \times 10^{-4} \text{ mol.dm}^{-3}$ ) with an  $\text{OH}^{\bullet}$  radical-generating  $\text{Fe(II)/EDTA/H}_2\text{O}_2$  system.



**Figure 5.3**



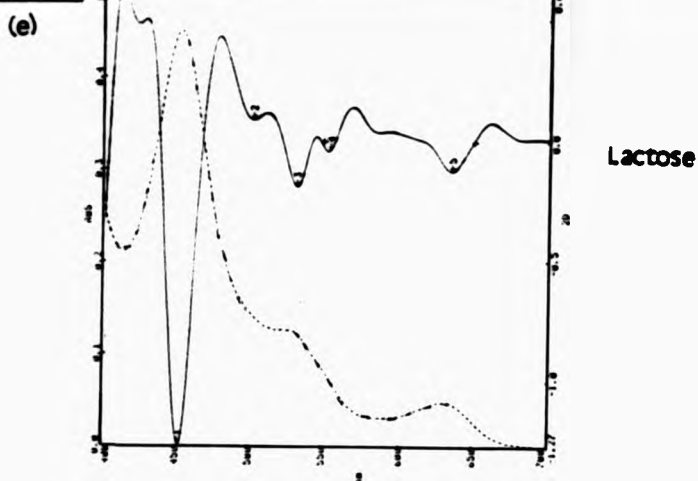
Zero-order (----) and corresponding 2D electronic absorption spectra (—) obtained from the reaction of TBA with products derived from the interaction of fructose ( $1.0 \times 10^{-4} \text{ mol.dm}^{-3}$ ) with an 'OH radical-generating Fe(II)/EDTA/H<sub>2</sub>O<sub>2</sub> system.



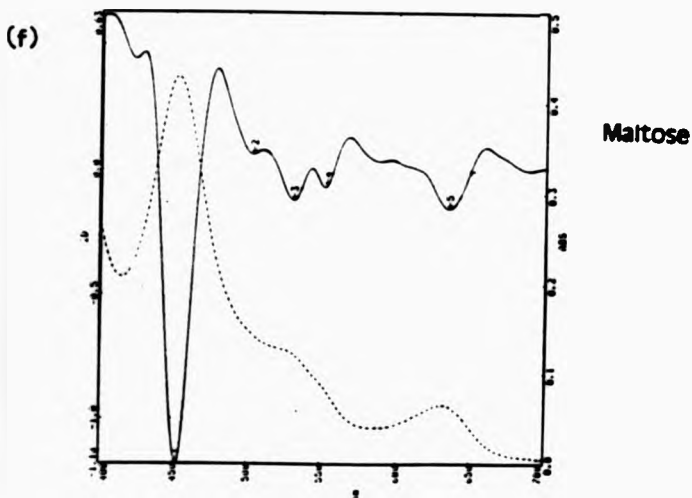
Zero-order (----) and corresponding 2D electronic absorption spectra (—) obtained from the reaction of TBA with products derived from the interaction of sucrose ( $1.0 \times 10^{-4} \text{ mol.dm}^{-3}$ ) with an 'OH radical-generating Fe(II)/EDTA/H<sub>2</sub>O<sub>2</sub> system.



Figure 5.3



Zero-order (----) and corresponding 2D electronic absorption spectra (—) obtained from the reaction of TBA with products derived from the interaction of lactose ( $1.0 \times 10^{-4} \text{ mol.dm}^{-3}$ ) with an  $\text{OH}$  radical-generating  $\text{Fe(II)/EDTA/H}_2\text{O}_2$  system.



Zero-order (----) and corresponding 2D electronic absorption spectra (—) obtained from the reaction of TBA with products derived from the interaction of maltose ( $1.0 \times 10^{-4} \text{ mol.dm}^{-3}$ ) with an  $\text{OH}$  radical-generating  $\text{Fe(II)/EDTA/H}_2\text{O}_2$  system.



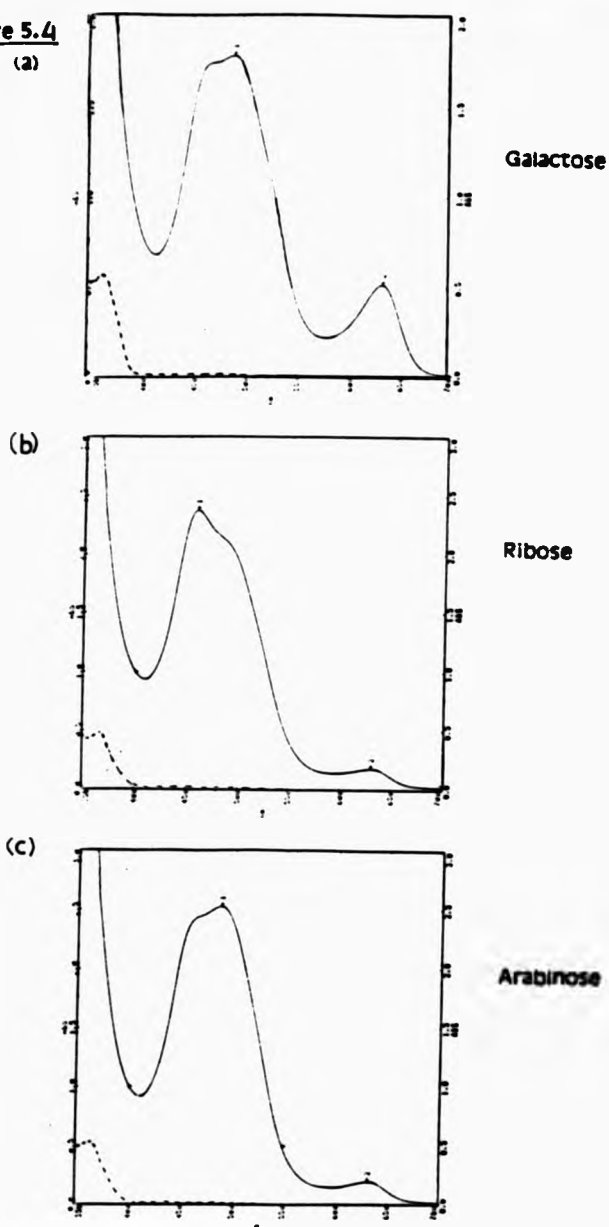
(c) Galactose, Ribose and Arabinose

Figures 5.4(a), (b) and (c) show zero-order absorption spectra obtained after allowing control and Fe(II)/EDTA/H<sub>2</sub>O<sub>2</sub>-treated samples of galactose, ribose and arabinose to react with TBA. The large overlapping bands bear much similarity to each other. However, they are distinctly different to the zero-order absorption spectra obtained for Fe(II)/EDTA/H<sub>2</sub>O<sub>2</sub>-treated samples of glucose, sucrose, fructose, lactose and maltose.

Figures 5.4(d), (e) and (f) show the corresponding 2D electronic absorption spectra obtained for the treated samples of galactose, ribose and arabinose. The 2D spectra for all three samples exhibit minima located at 452 (2D spectra for this minimum is not shown on scale for this signal), 495, 525 and 637 nm respectively.



**Figure 5.4**



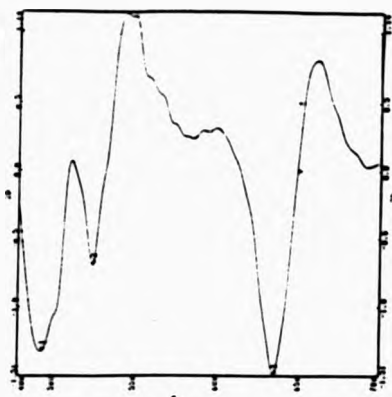
Zero-order absorption spectra obtained from the reaction of TBA with (i) control samples ( $1.0 \times 10^{-2}$  mol.dm<sup>-3</sup>) of galactose, ribose and arabinose (-----) and (ii) with products derived from the interaction of the sugars with an <sup>OH</sup> radical-generating Fe(II)/EDTA/H<sub>2</sub>O<sub>2</sub> system (—).





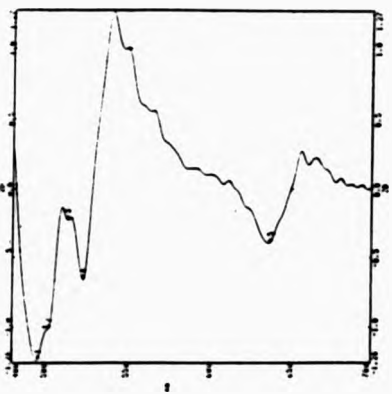
Figure 5.4

(d)



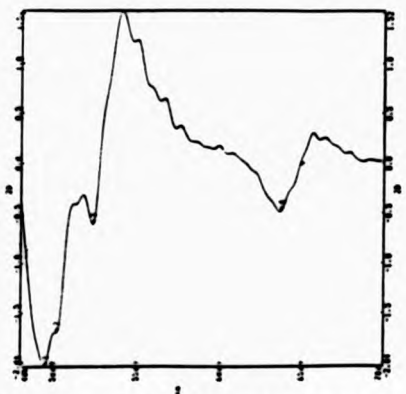
Galactose

(e)



Ribose

(f)



Arabinose

2D electronic absorption spectra obtained from the reaction of TBA with products derived from the interaction of (a) galactose, (b) ribose and (c) arabinose ( $1.0 \times 10^{-4}$  mol.dm<sup>-3</sup>) with an 'OH radical-generating Fe(II)/EDTA/H<sub>2</sub>O<sub>2</sub> system.

### 5.2.2 2D Spectrophotometric Identification of the TBA-Reactive Products

Although the identity of the peak at 532 nm (in 2-deoxyribose samples only) can be assigned to the 2:1 TBA-MDA adduct, the origin of the bands at the various other wavelengths in the 2D spectra arise from the reaction of alternative secondary oxidation products (from carbohydrate degradation) with TBA. Carbohydrate degradation products in addition to MDA include gluconic acid, glyceraldehyde, glyoxal and glycollaldehyde, amongst others<sup>120,123</sup>.

Figures 5.5(a), (b), (c) and (d) show the zero-order and corresponding 2D electronic absorption spectra obtained from the reaction of gluconic acid, glyceraldehyde, glyoxal and glycollaldehyde with TBA. The 2D spectrum obtained from the reaction of gluconic acid with TBA exhibits absorption minima centred at 456, 492 (most intense), 530 and 634 nm, identical to the 2D bands found for oxidatively damaged glucose, fructose and sucrose, indicating its possible formation from  $\cdot\text{OH}$  radical-mediated attack on these sugars.

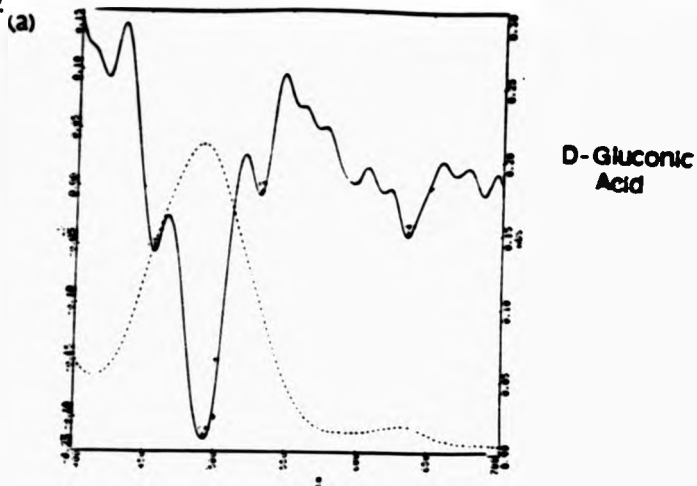
The 2D spectrum of TBA-reacted glyceraldehyde exhibits a fairly intense absorption minimum located at 455 nm and a relatively smaller minimum of lower intensity centred at 554 nm. Both the 2D bands at 455 and 554 nm are found in  $\text{Fe(II)/EDTA/H}_2\text{O}_2$ -treated samples of lactose and maltose. Glyoxal and glycollaldehyde also exhibit characteristic absorption minima located at 454 nm (present in both), 490 nm (very intense 2D band present only in the spectrum of products derived from the reaction of TBA with

glycollaldehyde), 525 nm (present in both) and 552 nm (very intense 2D band present only in the spectrum obtained from the reaction of TBA with glyoxal).

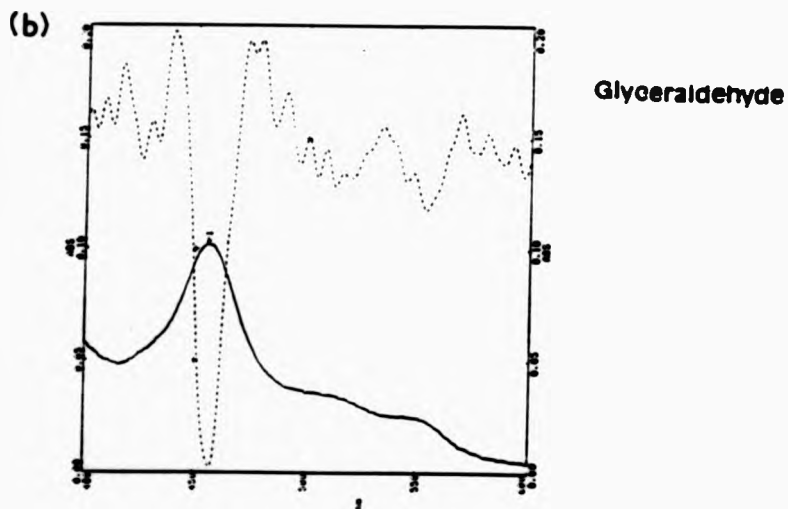
Consequently, it is likely that the 2D minima located at 525 nm arising in spectra of Fe(II)/EDTA/H<sub>2</sub>O<sub>2</sub>- treated samples of galactose, ribose and arabinose may be attributable to glyoxal and glycollaldehyde. In addition, the 2D band centred at 552 nm arising in treated samples of maltose and lactose could be attributable to glyoxal which gives an intense band located at this wavelength. Therefore, the 2D bands located at 454, 490 and 552 nm in the various carbohydrates subjected to <sup>•</sup>OH radical-mediated degradation may be attributable to glyceraldehyde, glycollaldehyde and glyoxal. Table 5.1 depicts the structures of all sugars and the secondary products of degradation investigated.



**Figure 5.5**



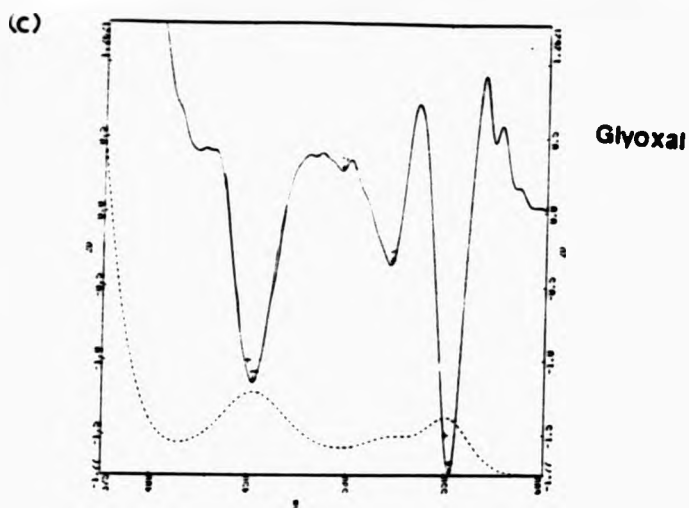
Zero-order (----) and corresponding 2D electronic absorption spectra (——) of D-gluconic ( $1.0 \times 10^{-4} \text{ mol.dm}^{-3}$ ) acid obtained after reaction with TBA.



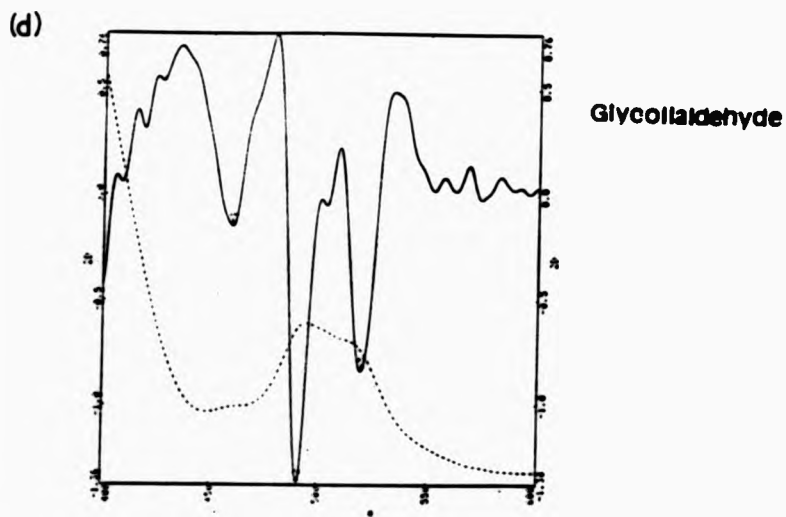
Zero-order (——) and corresponding 2D electronic absorption spectra (----) of glyceraldehyde ( $1.0 \times 10^{-4} \text{ mol.dm}^{-3}$ ) obtained after reaction with TBA.



**Figure 5.5**



Zero-order (----) and corresponding 2D electronic absorption spectra (——) of glyoxal ( $1.0 \times 10^{-4} \text{ mol.dm}^{-3}$ ) obtained after reaction with TBA.



Zero-order (----) and corresponding 2D electronic absorption spectra (——) of glycolaldehyde ( $1.0 \times 10^{-4} \text{ mol.dm}^{-3}$ ) obtained after reaction with TBA.

**TABLE 5.1**

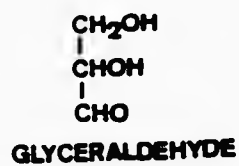
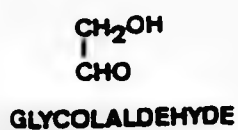
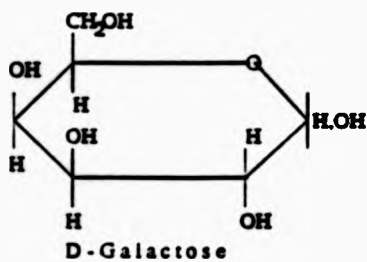
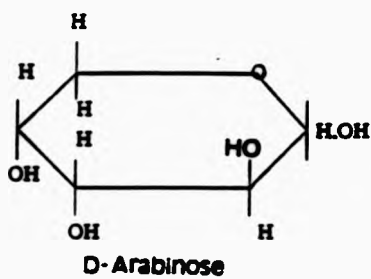
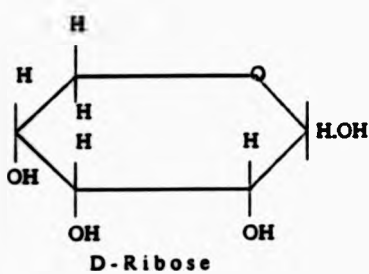
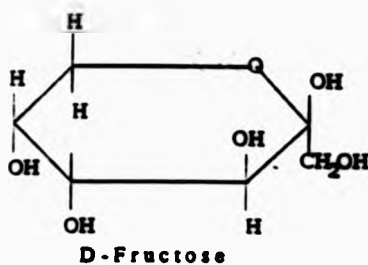
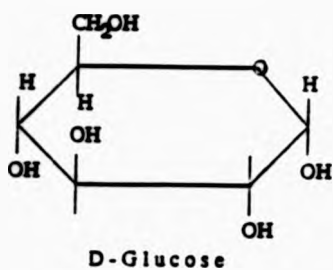
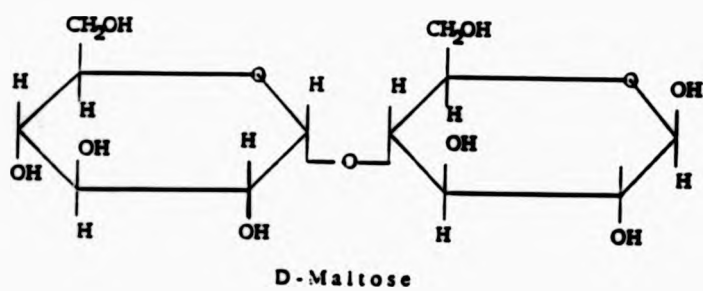
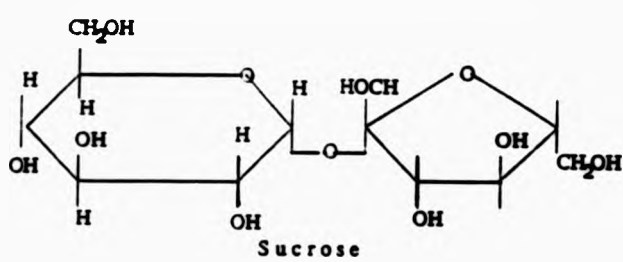
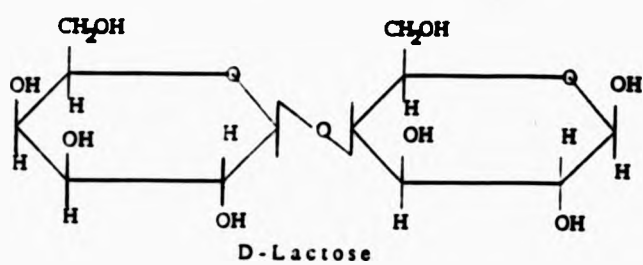


TABLE 53 (contd.)



#### 5.4 DISCUSSION AND CONCLUSION

During the stringent acid/heating stages of the TBA assay, it should be noted that gluconic acid (a primary degradation product of glucose) is further degraded to give a combination of secondary products in the mixture which also react with TBA. The secondary products of  $\cdot\text{OH}$  radical attack on glucose and fructose include glyoxal, glyceraldehyde, glycollaldehyde, glucosone and glucosan<sup>120,123</sup>. Sucrose, however, is a disaccharide consisting of a unit of glucose and fructose joined together by a disaccharide linkage.  $\cdot\text{OH}$  radical-mediated attack on aqueous solutions of sucrose results in hydrolysis of the sucrose molecule, yielding glucose and fructose as the primary products. Further  $\cdot\text{OH}$  radical attack produces the secondary products arising from glucose and fructose. Consequently, the 2D spectra obtained for the three sugars show similar 2D bands.

The absorption spectra obtained from the reaction of TBA with products derived from  $\cdot\text{OH}$  radical-mediated oxidative damage to ribose and arabinose are analogous to that obtained for galactose after treatment with  $\text{Fe(II)/EDTA/H}_2\text{O}_2$  and reaction with TBA. However, as expected, further analysis by 2D spectrophotometry has shown that the 2D spectra for the aldopentoses, ribose and arabinose are almost identical in comparison to the aldohexose, galactose. In general,  $\cdot\text{OH}$  radical attack on aldohexoses or aldopentoses in aqueous solution results in end-group oxidation followed by chain scission to yield the lower fragments<sup>131</sup>. For the sugars



studied, a possible initial product formed includes the corresponding hexonic/pentonic acids (formed from the primary radicals generated by abstraction of carbon-bound hydrogen atoms of the sugar ); for example, gluconic acid from the glucosyl radical or ribonic acid from the ribosyl radical<sup>132</sup>. The lower 2C/3C aldehydic fragments from all sugars investigated include glyoxal, glycollaldehyde and glyceraldehyde.

The determination of TBA-reactive material in aqueous sugar solutions subjected to 'OH radical attack by the application of 2D spectrophotometry appears to be a promising method for the assessment of oxidative damage to carbohydrates. In all cases, no TBA-reactive material was generated by control (untreated) sugar solutions. However, its possible application as a method for detecting the irradiation status of foodstuffs is questionable. The results presented here are confined solely to chemical model systems, but in foodstuffs carbohydrates are found to occur in combination with various other food components. The presence of these additional components, e.g. proteins and fats, may very likely suppress the formation of radiolytic products from carbohydrates. Furthermore, oxidative damage to proteins and fats generate TBA-reactive material which may be indistinguishable from that of carbohydrates. However, the 2D technique does appear to be relatively promising for foodstuffs comprised primarily of carbohydrates. Indeed, the method may be employed as a supplement to alternative methods

for assessing radiolytically-mediated oxidative damage to carbohydrates.

**CHAPTER 6**

**NMR ANALYSIS**  
**OF**  
**PRAWN SUPERNATANTS**

## 6. NMR SPECTROSCOPY OF FRAGRANCE SUPPLEMENTANTS

### 6.1 Introduction

A variety of spectroscopic techniques, including thermoluminescence<sup>23</sup> (TL) and electron spin resonance (ESR) spectroscopy<sup>10</sup> have previously been applied in the detection of irradiated foodstuffs. With respect to TL, the technique has been utilised for the assessment of light emitted by trapped free radicals arising predominantly in irradiated spices<sup>17</sup>.

ESR spectroscopy, which exploits the spin properties of the unpaired electron in free radicals (trapped in hard parts of foodstuffs) when exposed to an external magnetic field, has been more widely employed as a detection technique to a larger variety of foodstuffs. These include chicken bone, spices, seeds and pips (in a variety of fruits and vegetables<sup>16,18</sup>) and seafoods<sup>15</sup> (cf. Section 1.2.1).

More recently, the development of high-field NMR spectroscopy in the study of the chemical composition of biological systems has become fairly widespread<sup>70,133</sup>. NMR spectroscopy is a non-destructive, non-invasive and highly sensitive technique. In biological systems, majority of the compounds of interest contain hydrogen. This abundance of hydrogen-containing compounds together with the greater inherent sensitivity of <sup>1</sup>H NMR spectroscopy has led to its widespread use.

#### 6.1.1 Application of High-Field $^1\text{H}$ NMR Spectroscopy to the Analysis of Irradiated Foodstuffs

High-field proton NMR spectroscopy has recently been used to investigate the assessment of radiolytic damage to naturally-occurring carbohydrates, with particular reference to sucrose and glycosaminoglycan hyaluronate<sup>70</sup>. The  $^1\text{H}$  NMR spectrum of sucrose revealed the formation of formaldehyde and formate (the final products of gamma-radiolysis of aqueous sucrose<sup>123</sup>). Gamma-radiolysis of aqueous solutions of the glycosaminoglycan hyaluronate gave rise to the formation of the NMR-detectable N-acetylglucosamine-containing oligosaccharide species<sup>87</sup>.

$^1\text{H}$  NMR spectroscopy may also be utilised to assess radiolytically-induced modifications occurring in the chemical composition of foodstuffs, such as seafoods (e.g. prawns, shrimps). The exoskeletal matrix of prawns is composed of the polysaccharide chitin [ $\alpha, \beta$  (1 $\rightarrow$ 4)-linked polymer of N-acetyl-D-glucosamine<sup>129</sup>]. Indeed, Desrosiers<sup>15</sup> analysed shrimp exoskeleton by electron spin resonance (ESR) spectroscopy. The ESR signals obtained from irradiated shrimp shell and irradiated N-acetyl-D-glucosamine showed spectral similarities.

In this study  $^1\text{H}$  NMR spectroscopy has been utilised to determine radiolytically-induced chemical modifications occurring in fresh and frozen prawns, with reference to OH radical attack on the amino acid constituent methionine. Proton Hahn spin-echo methods in NMR spectroscopy have been employed, resulting in spectral simplification by suppressing

and resolving broad overlapping resonances arising from macromolecules present in the samples investigated. In the analysis, the Hahn spin-echo sequence D[90°x- $\tau$  - 180°y- $\tau$  - collect] was repeated 128 times with  $\tau = 68$  ms.

## 6.2 RESULTS

### 6.2.1 Analysis of Radiolytically-Mediated Modifications in the Chemical Composition of Prawn Samples by $^1\text{H}$ NMR Spectroscopy

Figures 6.1(a) and (b) exhibit the 500 MHz  $^1\text{H}$  Hahn Spin-echo NMR spectra of control and gamma-irradiated ( 5.0 kGy) portions of the supernatant (n=5 for each) obtained from commercially available fresh prawns with shells intact. The control sample (Figure 6.1(a)) contains a number of resonances attributable to a variety of endogenous prawn metabolites, including leucine (Leu), isoleucine (Ile), valine (Val), threonine (Thr), arginine (Arg), methionine (Met), succinate (Suc), dimethylamine (DMA) and trimethylamine (TMA) respectively.

The identity of the components in the prawn supernatant was confirmed on the basis of their characteristic chemical shift values and coupling patterns observed from the reference spectra obtained under identical experimental conditions.

A comparison of the  $^1\text{H}$  NMR spectra for the control and gamma-irradiated prawn sample supernatants reveals a number of differences. The intensities of the methionine-S- $\text{CH}_3$  group singlet and  $\gamma$ - $\text{CH}_2$ - group triplet resonances at 2.13 and 2.635 ppm decrease substantially as a consequence of gamma-irradiation treatment. In addition, the  $^1\text{H}$  NMR spectra of the irradiated prawn sample supernatant exhibits a resonance at 2.752 ppm, located slightly downfield to the intense dimethylamine signal. This resonance is attributable to

methionine sulphoxide-SO-CH<sub>3</sub> group which was previously undetectable in the control prawn sample supernatant. Formation of radiolytic methionine sulphoxide was also observed in gamma-irradiated supernatants of frozen deshelled prawn samples (data not shown).

Another notable difference between the control and gamma-irradiated prawn sample supernatants (obtained from intact shells) is an increase in the intensity of the acetate-CH<sub>3</sub> group resonance (component A in Figures 6.1(a) and (b)) in the irradiated treated sample.

The increase in intensity of the acetate resonance as a consequence of irradiation is most probably attributable to radiolytically-generated <sup>•</sup>OH radical attack on N-acetylglucosamine present in polysaccharides (e.g. polymeric glycosaminoglycan (hyaluronate) or the polysaccharide chitin (a prominent feature of the exoskeleton of prawns<sup>70</sup>)). Indeed, the prawn sample supernatants studied were derived from prawns irradiated with their shells intact. Furthermore, the <sup>1</sup>H NMR spectrum of a gamma-irradiated (5.0kGy) aqueous solution of lactate (data not shown), which is present in large quantities in prawn sample supernatants, also contained signals attributable to the -CH<sub>3</sub>-group protons of acetate and acetone. Consequently, the radiolytically-mediated elevations in acetate levels of prawn supernatants may additionally arise from <sup>•</sup>OH radical attack on lactate<sup>136</sup>.



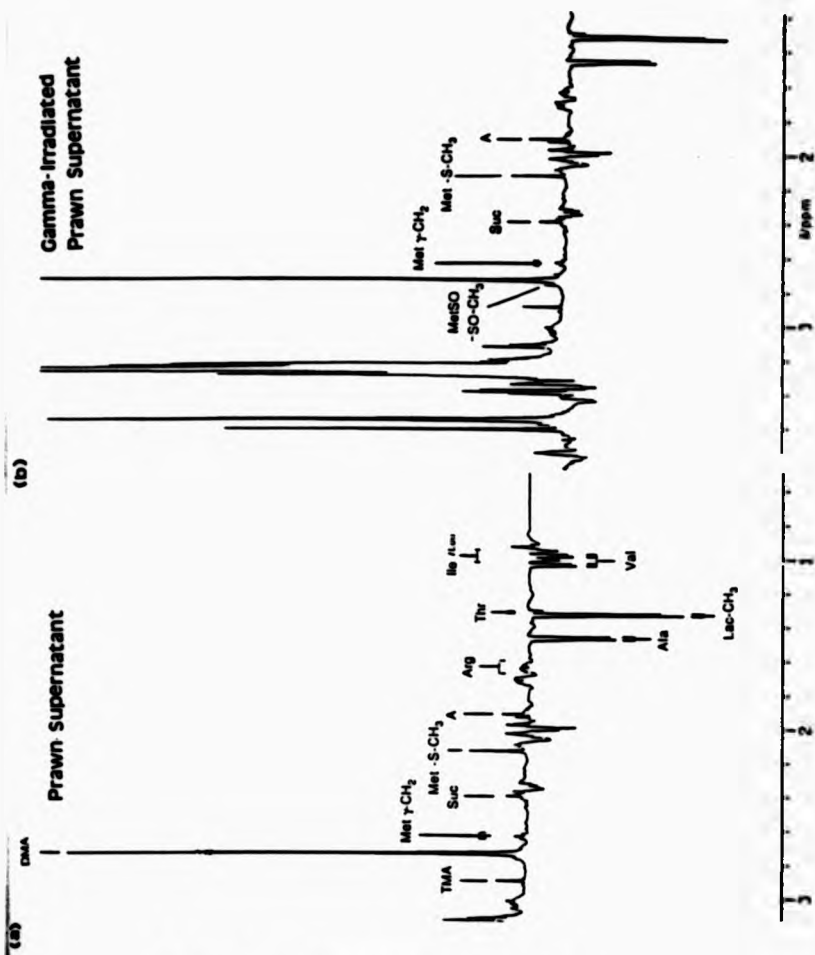
### 6.2.2 Radiolytic Damage to the Amino Acid Methionine

A standard aqueous solution of L-methionine (concentration,  $0.10 \text{ mol dm}^{-3}$ ) prior and subsequent to gamma-irradiation treatment at a dose of 5.0 kGy was analysed by  $^1\text{H}$  NMR spectroscopy. Figures 6.2(a) and (b) exhibit 400 MHz single pulse  $^1\text{H}$  NMR spectra obtained before and after gamma-radiolysis of aqueous solutions of L-methionine.

Subsequent to gamma-radiolysis, the methionine proton resonances decrease in intensity. Furthermore, the singlet resonance located at 2.752 ppm, attributable to methionine-SO-CH<sub>3</sub>-group and at 3.021 ppm, attributable to methionine-SO-CH<sub>2</sub>- multiplet are also visible in the spectrum (Figure 6.2(b)).

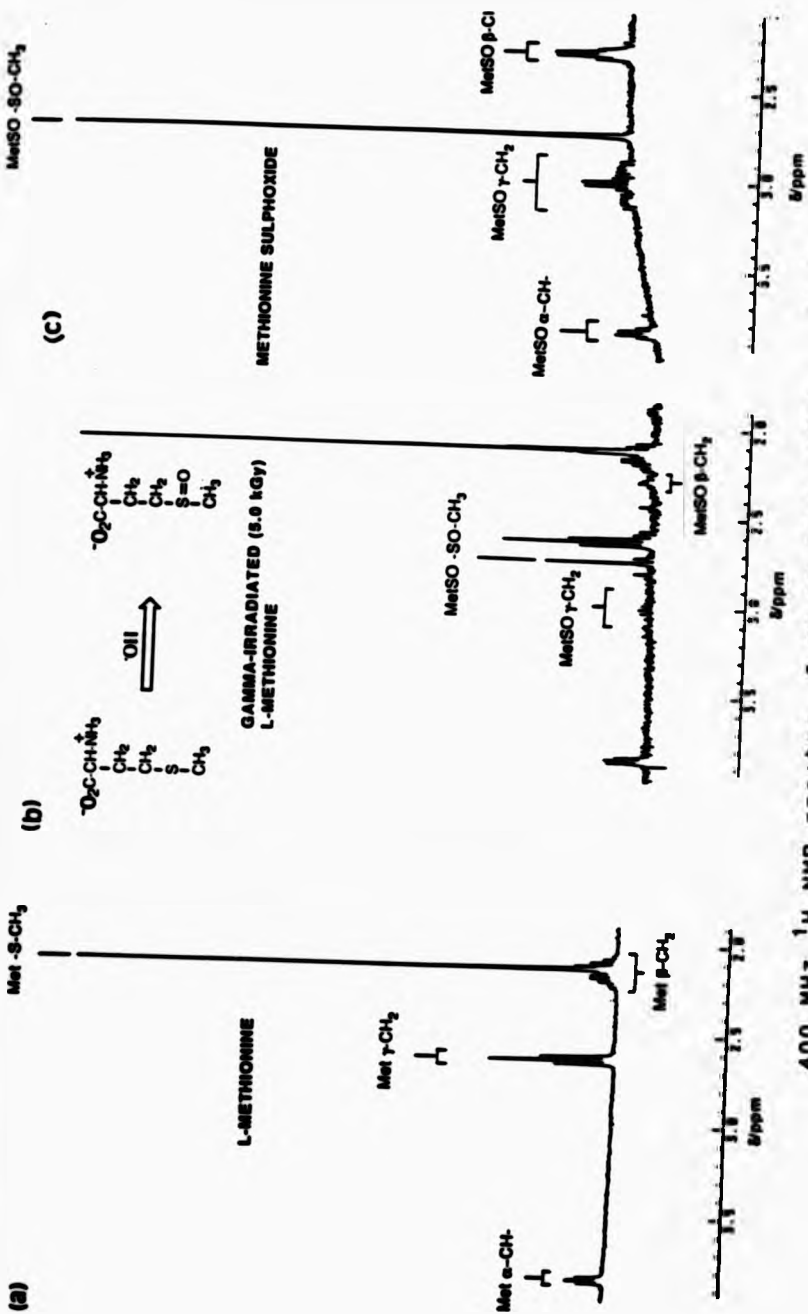
This observation therefore demonstrates the conversion of methionine to methionine sulphoxide by radiolytically-generated  $^{\bullet}\text{OH}$  radical. In addition, Figure 6.2(c) shows the corresponding  $^1\text{H}$  NMR spectrum of a standard aqueous solution of DL-methionine sulphoxide. These results are consistent with those obtained for the radiolytically-mediated modifications to methionine present in gamma-irradiated prawn sample supernatants (Figures 6.3(a) and (b)), thereby further demonstrating that methionine sulphoxide is indeed a radiolytic product derived from  $^{\bullet}\text{OH}$  radical attack on methionine.

Figure 6.1



500 MHz  $^1\text{H}$  spin-echo NMR spectra of a prawn sample supernatant obtained (a) before and (b) after irradiation at a dose level of 5.0 kGy. Abbreviations: Leu, leucine-CH<sub>3</sub>; Ile, isoleucine-CH<sub>3</sub>; Val, valine-CH<sub>3</sub>; Ala, alanine-CH<sub>3</sub>; Arg, arginine-CH<sub>3</sub>; A, acetate-CH<sub>3</sub>; Met-S-CH<sub>3</sub>, methionine-S-CH<sub>3</sub> singlet; Suc, succinate-CH<sub>2</sub>; Met- $\gamma$ -CH<sub>2</sub> triplet; DMA, dimethylamine; TMA, trimethylamine; MetSO-SO-CH<sub>3</sub>, methionine sulphoxide-CH<sub>3</sub> singlet. The intense water signal and broad protein resonances were suppressed by continuous secondary radiation at the water frequency and the Hahn spin-echo sequence.

Figure 6.2



400 MHz  $^1\text{H}$  NMR spectra of an aqueous solution of L-methionine obtained (a) before and (b) after irradiation at a dose of 5.0 kGy, showing the Met-SO-CH<sub>3</sub> group singlet (2.725 ppm) and the -CH<sub>2</sub>- multiplet (3.021 ppm) resonances of methionine sulphoxide. Figure (c) shows the corresponding spectrum of an aqueous solution containing an authentic sample of DL-methionine sulphoxide.

### 6.3 SUMMARY AND CONCLUSION

Proton Hahn Spin-echo NMR spectroscopy has been successfully employed in the determination of radiolytically-mediated oxidative damage to endogenous components present in fresh and frozen prawns.

One particular aspect which may aid in discriminating between irradiated prawns from non-irradiated control samples is the formation of the NMR-detectable methionine sulphoxide (-SO-CH<sub>3</sub> group singlet resonance), presumably produced from the attack of radiolytically-generated <sup>•</sup>OH radical on methionine. However, a wide range of biological systems (e.g. rat and liver tissues, human lung and spinach leaves) contain the enzyme methionine sulphoxide reductase, and as a result the presence of very low concentrations of sulphoxide in non-irradiated (control) prawns cannot be ruled out. However, under the experimental conditions employed in this study, methionine sulphoxide was not detectable in non-irradiated control samples, and therefore it was possible to distinguish between irradiated and non-irradiated prawns.

Methionine reacts with <sup>•</sup>OH radical with a very high second-order rate constant,  $k_2 = 5.1 \times 10^9 \text{ mol}^{-1} \text{ dm}^3 \text{ s}^{-1}$  (at pH 7.135) and is therefore a suitable "target" molecule for scavenging <sup>•</sup>OH radical.

Furthermore, <sup>1</sup>H NMR spectroscopy also demonstrated that gamma-irradiation of prawn supernatants (with shells intact) resulted in significant increases in concentration of the component attributable to acetate, produced as a consequence of <sup>•</sup>OH radical attack on N-acetyl groups of glucosamine.

Acetate may also be generated by  $\cdot\text{OH}$  radical attack on lactate (second order rate constant,  $k_2 = 4.8 \times 10^9 \text{ mol}^{-1} \text{ dm}^3 \text{ s}^{-1}$ , at pH 9) which is present in prawns in relatively large amounts.

The potential application of  $^1\text{H}$  NMR spectroscopy as a detection method for irradiated foodstuffs (primarily shellfish) appears to be relatively promising, particularly in the detection of methionine sulphoxide, which is not normally detectable in non-irradiated samples.

**CHAPTER 7**

**DISCUSSION**  
**AND**  
**CONCLUSION**

## 7. DISCUSSION AND CONCLUSIONS

Chemical changes produced in foods as a consequence of the irradiation process are predominantly attributable to the highly reactive  $\cdot\text{OH}$  radical, which interacts with a large number of biomolecules present in foodstuffs. These interactions result in the production of vast numbers of chemical species which may be identified and/or quantified by application of appropriate analytical techniques.

Aromatic compounds such as phenols and phenolic acids (present in a variety of fruits and vegetables) react extremely rapidly with  $\cdot\text{OH}$  radical to form a mixture of hydroxylated products<sup>76,83</sup>. Detection of these products is achieved by a combination of HPLC with EC detection<sup>45,46</sup>, a methodology which unites the ability to separate complex mixtures of phenolic components with high sensitivity (i.e. concentrations of parts per billion or less). It provides substantial evidence of gamma-irradiation treatment (at doses of 1.0-5.0 kGy) of strawberry and celery homogenates in the presence of a non-irradiated control sample. One of the most striking modifications was the marked depletion of gentisic acid and formation of catechol in irradiated celery homogenates. Furthermore, the concentrations of further individual phenolic acids increase or decrease as a consequence of irradiation treatment. The concentration of gentisic acid in strawberry homogenates was found to decrease gradually as the radiation dose increased from 1.0 kGy to 5.0 kGy. The presence of large quantities of vitamin C (a potent radical scavenger) in strawberries may offer some protection

to phenolic components against radiolytic damage. The HPLC/ECD approach can indeed be employed to assess radiolytically-generated modifications in fruits and vegetables, but the technique does necessitate the presence of a non-irradiated control sample.

The self-propagating peroxidation of polyunsaturated fatty acids has been studied for many years<sup>105</sup>. The conjugated dienes and diene hydroperoxides in extracts of irradiated foodstuffs (specifically *trans,trans*- and *cis,trans*- isomers) can be conveniently determined by 2D spectrophotometric analysis. However, parameters such as temperature, exposure to light and the availability of oxygen and traces of catalytic metal ions can all promote their production.

From the studies conducted, it appears that peroxidation is manifested by the formation of the 2D signal at 234 nm (attributable to *t,t*- conjugated diene lipid hydroperoxide) which was found initially only in a sample of corn oil subjected to peroxidation by irradiation. In all samples of corn oil artefactually peroxidised, the 2D signal at 234 nm appeared 6-7 days after initiation of the peroxidation process. Measurement of intermediates in and end-products (TBA-reactive products) of the lipid peroxidation process by 2D spectrophotometry is a useful methodology and relatively sensitive indicator for monitoring oxidative degradation to PUFAs by  $\cdot\text{OH}$  radical.

TBA-reactive products generated by  $\cdot\text{OH}$  radical attack on aqueous solutions of carbohydrates have also been studied by



2D spectrophotometry. The results demonstrated that in addition to MDA, a large number of alternative secondary oxidation products are formed, which are also TBA-reactive. The identity of the products has been successfully determined by their 2D spectra. These species consist of glyoxal, glyceraldehyde, glycolaldehyde and gluconic acid. Indeed, the methodology provides a convenient approach for monitoring  $\cdot\text{OH}$  radical activity in model systems containing carbohydrates. No TBA-reactive products were produced in control carbohydrate solutions.

Radiolytically-induced modifications to biomolecules in prawn supernatants have been determined by application of proton Hahn spin-echo NMR spectroscopy. A suitable endogenous "target" molecule in prawns for radiolytically-generated  $\cdot\text{OH}$  radical is the naturally occurring amino acid methionine. Hydroxyl radical attack on methionine results in the production of NMR-detectable methionine sulphoxide<sup>135</sup> which was detectable only in irradiated prawn supernatants. Indeed, it was possible to distinguish between control and gamma-irradiated prawn sample supernatants by the absence or presence, respectively, of the methionine sulphoxide-SO-CH<sub>3</sub> group resonance in <sup>1</sup>H Hahn spin-echo spectra.


Although the NMR technique does appear to be specific for the detection of methionine sulphoxide in irradiated prawn supernatants, the presence of this radiolytic product in non-irradiated (control) samples cannot be ruled out. This is due to the known presence of the enzyme methionine sulphoxide reductase (in very low concentrations) in a variety of animal

and plant tissues. However, methionine sulphoxide was not detectable by NMR spectroscopy (the sensitivity of which is approximately  $1.0 \times 10^{-5} \text{ mol.dm}^{-3}$  at an operating frequency of 500 MHz) in non-irradiated, control prawn samples. The NMR technique is highly sensitive and provides an alternative procedure for the detection of radiolytically-generated  $\text{'OH}$  radical.

A variety of analytical techniques have been employed in this study with the objective of monitoring radiolytically-generated  $\text{'OH}$  radical attack on biomolecules in a variety of foodstuffs. The nature of the analytical technique employed is highly dependent on the nature of the foodstuff to be analysed.

From this work it can be concluded that there appears to be no one specific test for distinguishing between irradiated and non-irradiated foods. However, for individual foodstuffs, several methods are possible depending upon the chemical composition of the foods.

Indeed, interaction of ionising radiation results in the formation of reactive free radicals (e.g.  $\text{'OH}$  radical) leading to a large number of possible reactions with "target" molecules in foodstuffs. Chemical identification of irradiated foods therefore relies on the relative concentrations of several chemical species present in the system under study. While individual chemical model systems (i.e. sugars, proteins, fats, aromatic compounds) are easily destroyed when irradiated in aqueous solutions, they are less



susceptible to radiolytic damage when irradiated in a complex food matrix. The presence and influence of additional food components in combination will result in lower yields of radiolytic products than expected from studies of chemical model systems. In addition, the extent of radiolytic damage is also dependent upon the second-order rate constant ( $k_2$ ) for the reactions of  $\cdot\text{OH}$  radical with biomolecules, some reacting faster than others.

Furthermore, the influence of independent variables such as temperature, irradiation dose, water content and oxygen concentration may play an important role in the nature and extent of radiation-induced damage.

In these studies, aromatic compounds in a number of fruits and vegetables have been investigated. It would be interesting to test a wider variety of class of foodstuffs and observe how these correlate with previous results. From the research conducted in this work, it appears that a high concentration of vitamin C offers protection against radiolytic damage to phenolic components. The concentration of the phenolic component gentisic acid in irradiated strawberries was found to be 950 ppb at 5.0 kGy, whilst its concentration in celery irradiated at the same dose was 50 ppb. The gentisic acid concentration in irradiated strawberries was therefore found to be markedly higher than that in irradiated celery, perhaps due to the high vitamin C content of strawberries. This phenomena could be investigated and extended to other fruits and vegetables.

Additionally, non-irradiated control strawberry samples

were found to contain large quantities of an unknown component, the concentration of which was found to decrease with an increase in radiation dose (from 1.0 to 5.0 kGy). The identity or nature of this component needs to be determined, preferably by some on-line analytical technique such as HPLC-MS. This unknown component may be employed as a "marker" of irradiation status.

The research conducted on carbohydrates has been restricted to chemical model systems only. The methodology employed could be applied to foodstuffs high in carbohydrate content (e.g. dry skimmed milk and fruits).

From the research conducted, a number of differences are found to occur between irradiated and non-irradiated foodstuffs. However, these chemical modifications have been observed only above a radiation dose of 0.5 kGy. Further work should involve quantifying chemical changes at a lower and wider range of radiation dosages.

#### REFERENCES

- (1) Draganic, I.G. and Draganic, Z.D. *"The Radiation Chemistry of Water"*. Academic Press, New York, (1971).
- (2) Josephson, E.S. and Peterson, M.S. *"Preservation of Food by Ionising Radiation"*, Volume 1, CRC Press (1973).
- (3) Spinks, J.W.T. and Woods, R.J. *"An Introduction to Radiation Chemistry"*, 3rd. Edn., John Wiley and Sons. INC. (1990).
- (4) Ebert, M., Keene, J.P., Swallow, A.J. and Baxendale, J.H. (Eds). *"Pulse Radiolysis"*, Academic Press, London and New York (1985).
- (5) Josephson, E.S. and Peterson, M.S. *"Preservation of Food by Ionising Radiation"*. CRC: Vol. 2. (1983).
- (6) *"Improvement of Food Quality by Irradiation"*. Proceedings of a Panel, Vienna, June (1973), Joint FAO/AEA Division of Food and Agriculture.
- (7) Buxton, G.V. and Greenstock, C.L. *J. Phys. Chem. Ref. Data.*, 1988, 17(2), 513.
- (8) Diehl, J.F. *"Safety of Irradiated Foods"*. Marcel Dekker, INC, New York (1990).
- (9) Wertz, J.E. and Bolton, J.R. *"Electron Spin Resonance, Elementary Theory and Practical Applications"*. Chapman and Hall, New York and London (1986).
- (10) Dodd, N.J.F., Swallow, A.J. and Ley, F.J. *Radiat. Phys. Chem.* 1985, 26, 451.
- (11) Dodd, N.J.F., Lea, J.S. and Swallow, A.J. *Nature, Lond.* 1988, 334, 387.
- (12) Symons, M.C.R. *Free Rad. Res. Comms.*, 1988, 5, No. 3.

131.

(13) Stevenson, M.H. and Gray, R. *J. Sci. Food. Agric.* 1989, 48, 261.

(14) Stevenson, M.H. and Gray, R. *J. Sci. Food. Agric.* 1989, 48, 269.

(15) Desrosiers, M.F. *J. Agric. Fd. Chem.* 1989, 37, 96.

(16) Desrosiers, M.F.J. and Simic, M.G. *J. Agric. Fd. Chem.* 1988, 36, 601.

(17) Delincee, H., Ehlermann, D.A.E. and Bogl, K.W. (1988). "Health Impact, Identification and Dosimetry of Irradiated Foods", Report of a WHO Working Group, Bericht des Instituts für Strahlenhygiene des Bundesgesundheitsamtes, Neuherberg, F.R.G., ISH-125.

(18) Raffi, J.J., Agnel, J.P.L., Buscarlet, L.A. and Martin, C.C. *J. Chem. Soc., Faraday Trans 1*, 1988, (84), 3359.

(19) Heide, L. and Bogl, K.W. *Int. J. Fd. Sci. Technol.* 1987, 22, 93.

(20) Kricka, L.J. and Thorpe, G.H.G. *Analyst*, 1988, 108, No. 1287-1293, 1275.

(21) Oberhofer, M. and Scharmann, A. "Applied Thermoluminescence Dosimetry". Bristol: Adam Higler Ltd. (1981).

(22) McKeever, S.W.S. "Thermoluminescence of Solids". Cambridge University Press. (1985).

(23) Bogl, W. and Heide, L. *Radiat. Phys. Chem.*, 1985, 25, Nos. 1-3, 173.

(24) Sanderson, D.C.W., Slater, C. and Cairns, K.J. *Radiat.*

- Phys. Chem.*, 1989, 34(6), 915.
- (25) Nawar, W.W. and Balboni, J.J. *J. Ass. Offic. Anal. Chem.*, 1970, 53, 726.
- (26) Vajdi, M. and Nawar, W.W. *J. Amer. Oil. Chem. Soc.*, 1979, 56, 611.
- (27) Seo, C.W. and Joel, D.L., *J. Fd. Sci.*, 1980, 45, 36.
- (28) Nawar, W.W. (1988). Analysis of Volatiles as a Method for the Identification of Irradiated Foods. In: "Health Impact, Identification and Dosimetry of Irradiated Foods", pg. 287. Report of a WHO Working Group, Bericht des Instituts für Strahlenhygiene des Bundesgesundheitsamtes, ISH-125, Neuherberg, F.R.G.
- (29) Floyd, R.A., Watson, J.J., Harris, J., West, M. and Wong, P.K. *Biochem. Biophys. Res. Commun.*, 1986, 137, 841.
- (30) Aruoma, O.I., Halliwell, B., Gajewski, E. and Dizdaroglu, M. *J. Biol. Chem.*, 1989, 264(34), 20509.
- (31) Aruoma, O.I., Halliwell, B., Gajewski, E. and Dizdaroglu, M. *Biochem. J.*, 1991, 273, 601.
- (32) Gajewski, E., Aruoma, O.I., Dizdaroglu, M. and Halliwell, B. *Biochemistry*, 1991, 30, 2944.
- (33) Jabir, A.W., Deeble, D.J., Wheatley, P.A., Smith, C.J., Parsons, B.J., Beaumont, P.C. and Swallow, A.J. *Radiat. Phys. Chem.*, 1989, 34, No. 6, 935.
- (34) Beland, F.A., Dooley, K.L. and Casciano, D.A. *J. Chromatog.*, 1979, 174, 177.
- (35) Mello Filho, A.C. and Meneghini, R. *Biochem. Biophys. Acta.*, 1984, 781, 56.
- (36) Jansson, G. *Arch. Biochem. Biophys.*, 1981, 206, 414.

- (37) Meier, W., Burgin, R. and Frohlich, D. *Radiat. Phys. Chem.*, 1990, 35(1-3), 332.
- (38) Diehl, J.F., Adam, S., Delincee, H. and Jakubick, V. *J. Agric. Fd. Chem.*, 1978, 26(1), 15.
- (39) Nawar, W.W. *J. Agric. Fd. Chem.*, 1978, 26(1), 21.
- (40) Beyers, M., Thomas, A.C. and Van Tander, A.J. *J. Agric. Fd. Chem.*, 1979, 27, 37.
- (41) Christian, G.D and O'Reilly, J.E. "Instrumental Analysis", 2nd Edn. Alley and Bacon, Inc. (1986).
- (42) Snyder, L.R. and Kirkland, J.J. "Introduction to Modern Liquid Chromatography". 2nd Edn. Wiley Interscience, New York (1979).
- (43) Horvath, C. "High Performance Liquid Chromatography: Advances and Perspectives". Vol. 3, Academic Press, New York (1983).
- (44) Simpson, C.F. "Techniques in Liquid Chromatography". Wiley-Haden, New York (1982).
- (45) Roston, D.A and Kissinger, P.T. *Anal. Chem.*, 1981, 53, 1695.
- (46) Lunte, C.E., Wheeler, J.F. and Heineman, W.R. *Analyst.*, 1988, 113, 95.
- (47) Fleet, B. and Little, C.J. *J. Chromatog. Sci.*, 1974, 12, 747.
- (48) Nagels, L.J. and Creten, W.L. *Anal. Chem.* 1985, 57, 2706
- (49) Samuel, A.J. and Webber, T.J.N., "Some Applications of Electrochemical Oxidation as a Detection Technique in High Performance Liquid Chromatography", pp. 43-59. In:



- "Electrochemical Detectors: Fundamental Aspects and Analytical Applications"*. ED. Ryan, T.H. Plenum Press, London and New York (1984).
- (50) Kissinger, P.T., *"Liquid Chromatography and Electrochemistry"*. pp. 55-65. In: *"Detectors and Chromatography"*. Ed. Nicholson, A.J.C. Proceedings of an International Conference, Melbourne, Australia (1983).
- (51) Kissinger, P.T. *"Introduction to Detectors for Liquid Chromatography"*, BAS Press, W. Lafayette (1981).
- (52) Adams, R.N. *"Electrochemistry at Solid Electrodes"*, Dekker pp. 372, (1969).
- (53) Jacobson, W.A. and Kissinger, P.T. *J. Liq. Chromatog.*, 1982, 5(5), 881.
- (54) Skoog, D.A. *"Principles of Instrumental Analysis"*, 3rd. Edn. Saunders College Publishing, (1984).
- (55) Kemp, W. *"Organic Chemistry"*, 2nd. Edn. Macmillan Publishers Ltd. (1987).
- (56) Knowles, A. and Burgess, C. *"Techniques in Visible and Ultra-Violet Spectrometry: Practical Absorption Spectrometry"*. Vol. 3 Chapman and Hall, London and New York (1984).
- (57) O'Haver, T.C. *Anal Chem.*, 1979, 1, 343.
- (58) Harris, R.K. *"Nuclear Magnetic Resonance Spectroscopy: A Physicochemical View"*. Longman Scientific and Technical Publications, 2nd. Edn. (1986).
- (59) Morrison, R.T. and Boyd, R.N. *"The Nuclear Magnetic Resonance Spectrum"*, Chapter 16, p. 569. In: *"Organic Chemistry"*. 5th Edn. Allyn and Bacon INC. (1987).

- (60) Streitwieser, A. and Heathcock, C.H. "Nuclear Magnetic Resonance Spectroscopy", Chapter 13, p. 302. In: "Introduction to Organic Chemistry". 3rd Edn. Macmillan Publishers INC. (1989).
- (61) Brown, F.F., Campbell, I.D. and Kuchel, P.W. *FEBS. Lett.*, 1977, 82(1), 12.
- (62) Rabenstein, D.L. *Anal. Chem.*, 1978, 50(13), 1265A.
- (63) Rabenstein, D.L. and Nakashima, T.T. *Anal. Chem.*, 1979, 51(14), 1465A.
- (64) Halliwell, B. *FEBS. Lett.*, 1978, 92(2), 321.
- (65) Graf, E., Mahoney, J.R., Bryant, R.G. and Eaton, J.W. *J. Biol. Chem.*, 1983, 102, 3620.
- (66) Raghavan, N.V. and Steeken, S. *J. Am. Chem. Soc.*, 1980, 102, 3495.
- (67) Walling, C. and Johnson, R.A. *J. Am. Chem. Soc.*, 1975, 97, 363.
- (68) Grootveld, M. and Jain, R. *Free. Rad. Res. Commun.*, 1989, 6, 271.
- (69) Grootveld, M. and Jain, R. *Radiat. Phys. Chem.*, 1989, 34(6), 925.
- (70) Grootveld, M. and Jain, R. *Trends in Fd. Sci. Technol.*, 1990, 1(1), 7.
- (71) Milhailo, L.J., Cekovic, M. and Cekovic, Z. "Oxidation and Reduction of Phenols", In: "The Chemistry of the Hydroxyl Group", (Eds). Patai, S., Chapter 10. John Wiley and Sons, 1971.
- (72) McMurray, J. "Chemistry of Benzene: Electrophilic

*Aromatic Substitution*", In: "Organic Chemistry", Chapter 15, p. 478. Wadsworth, Inc., Belmont California (1984).

(73) McCord, J.M. and Day, E.D. *FEBS. Lett.*, 1978, 86, 139.

(74) Beauchamp, C. and Fridovich, I. *J. Biol. Chem.*, 1970, 245, 4641.

(75) Halliwell, B. and Gutteridge, J.M.C. *FEBS. Lett.*, 1981, 128, 347.

(76) Richmond, R., Halliwell, B., Chauhan, J. and Darbre, A. *Anal. Chem.*, 1981, 118, 328.

(77) Grootveld, G. and Halliwell, B. *Free. Rad. Res. Comms.*, 1985, 1(4), 243.

(78) Floyd, R.A., Watson, J.J. and Wong, P.K. *J. Biol. Chem.*, 1984, 10, 221.

(79) Grootveld, M. and Halliwell, B. *Free Radical Res. Commun.*, 1986, 1, 242.

(80) Moorhouse, C.P., Halliwell, B., Grootveld, M. and Gutteridge, J.M.C. *Biochem. Biophys. Acta.*, 1985, 843, 261.

(81) Grootveld, M. and Halliwell, B. *Biochem. J.*, 1986, 237, 499.

(82) Ribereau-Gayon, P. "Plant Phenolics", Oliver and Boyd Publishers (1972).

(83) Nagels, L.J. *Anal. Chem.*, 1985, 57, 2706.

(84) Roston, D.A. and Kissinger, P.T. *Anal. Chem.*, 1981, 53, 1695.

(85) Halliwell, B. and Grootveld, M. *FEBS. Lett.*, 1981, 213(1), 9.

(86) Kaur, H., Fagerheim, I., Grootveld, M., Puppo, A. and Halliwell, B. *Anal. Biochem.*, 1988, 172, 360.

- (87) Karam, L.R. and Simic, M.G. *Anal. Chem.*, 1988, 60(19), 1117A.
- (88) Karam, L.R. and Simic, M.G. "Methods for the Identification of Irradiated Chicken Meat". Presented at the WHO Working Group on Health, Impact and Control of Irradiated Foods: Neuherberg, FRG, Nov (1986).
- (89) Hart, R.J., White, J.A. and Reid, W.J. *Int. J. Fd. Sci. Technol.*, 1988, 23, 643.
- (90) Ishimitsu, S., Fujimoto, S. and Ohara, A. *Chem. Pharm. Bull.*, 1986, 34(2), 768.
- (91) Karam, L.R., Dizdaroglu, M. and Simic, M.G. *Int. J. Radiat. Biol.*, 1984, 46, 715.
- (92) Mee, L.K., "Radiation Chemistry of Biopolymers", in "Radiation Chemistry- Principles and Applications", (Eds) Farahataziz and Rodgers, M.A.J., Chapter 10, pp. 477 (1990).
- (93) Gutteridge, J.M.C. *FEBS. Lett.*, 1979, 105(2), 278.
- (94) Cheeseman, K.M., Beavis, A. and Esterbauer, H. *Biochem. J.*, 1988, 252, 649.
- (95) Murray, D.R. "Biology of Food Irradiation", Research Studies Press Ltd. John Wiley and Sons INC. (1990).
- (96) Seib, P.A. and Tolbert, B.M. "Ascorbic Acid: Chemistry, Metabolism and Uses", Advances in Chemistry, series 200, American Chemical Society, Washington DC, USA (1982).
- (97) Nagay, N.Y. and Moly, J.H. *J. Fd. Sci.*, 1985, 50, 215.
- (98) Elias, P.S. and Cohen, A.J. "Radiation Chemistry of Major Food Components", Elsevier Biomedical Press (1983).
- (99) Villeneuve, F. and Abbavanel, G. *J. Chromatog.*, 1982,

- 234, 131.
- (100) Miller, J.M. and Miller, J.N. (Eds). "Statistics for Analytical Chemistry", 2nd. Edn. John Wiley and Sons Publishers, New York, 1988.
- (101) Paul, A.A., Southgate, D.A.J. and Russel, J. First Supplement to McLance and Widdowsons, "The Composition of Foods". HMSO. London. (1987).
- (102) Christie, W.W. (Ed.) "Lipid Analysis", 2nd. Edn. Pergamon Press Publications (1982).
- (103) Halliwell, B. and Gutteridge, J.M.C. *Biochem. J.*, 1988, 219, 1.
- (104) Halliwell, B. and Gutteridge, J.M.C. "Free Radicals in Biology and Medicine", Clarendon Press, Oxford, England 2nd. Edn. (1989).
- (105) Allen, J.C. and Hamilton, R.J. (Eds). "Rancidity in Foods". Applied Science, Barking (1983).
- (106) Frankel, E.N. "Recent Advances in the Chemistry of Rancidity of Fats". Specialist Publications No. 47. Royal Society of Chemistry, London (1984).
- (107) Gutteridge, J.M.C. and Halliwell, B. *Trends Biochem. Sci.*, 1990, 15, 129.
- (108) Khayat, A. and Schwall, D. *Food Technol.*, 1983, 132.
- (109) Burton, G.W. and Ingold, K.U. *Acc. Chem. Res.*, 1986, 19, 194.
- (110) Marshall, P.J., Warso, M.A. and Lands, W.E.M. *Anal. Biochem.*, 1985, 145, 192.
- (111) Robards, K., Kerr, A.F. and Pastalides, E. *Review. Analyst.*, 1988, 113, 213.

- (112) Corongui, F.P., Poli, G., Dianzani, M.U., Cheeseman, K.H. and Slater, T.F. *Chem-Biol. Interactions.*, 1986, 59, 147.
- (113) Nair, V. and Turner, G.A. *Lipids.*, 1984, 19, 804.
- (114) Kosugi, H., Kato, T. and Kikugawa, K. *Anal. Biochem.*, 1987, 165, 456.
- (115) Shamberger, R.J., Shamberger, B.A. and Willis, C.E. *J. Nutr.*, 1977, 107, 1404.
- (116) Demann, J.M. "Principles of Food Chemistry", Westport T., pp. 60 (1978).
- (117) Largillere, C. and Melancon, S.B. *Anal. Biochem.*, 1988, 170, 123.
- (118) Fletcher, B.L., Dillard, C.J. and Tappel, A.L. *Anal. Biochem.*, 1973, 52, 1.
- (119) Diehl, J.F., Adam, S., Delincee, H. and Jakubick, V. *J. Agric. Fd. Chem.*, 1978, 26, 15.
- (120) Phillips, G.O. *Radiat. Res. Rev.*, 1972, 3, 335.
- (121) Rowley, D.A. and Halliwell, B. *FEBS. Lett.*, 1982, 142(1), 39.
- (122) Gutteridge, J.M.C. and Halliwell, B. *Biochem. J.*, 1988, 253, 931.
- (123) Phillips, G.O. and Moody, G.J. *J. Chem. Soc.*, 1960, 154, 754.
- (124) Dizdaroglu, M., Henneberg, D., Schomburg, G. and von Sonntag, C. *Z. Naturforsch.*, 1975, 30B, 416.
- (125) Gardner, H.W. *J. Agric. Fd. Chem.*, 1979, 27, 221.
- (126) Gutteridge, J.M.C. and Halliwell, B. *Biochem. J.*, 1988,

253, 931.

(127) Halliwell, B. and Gutteridge, J.M.C. *FEBS. Lett.*, 1981, 128(2), 347.

(128) Aruoma, O.I., Grootveld, M. and Halliwell, B. *J. Inorg. Biochem.*, 1987, 29, 289.

(129) Gutteridge, J.M.C. *FEBS. Lett.*, 1981, 128(2), 343.

(130) Gutteridge, J.M.C. *Biochem. J.*, 1984, 224, 761.

(131) Phillips, G.O. "The Effects of Radiation on Carbohydrates", Chapter 26, p. 1217-1297. In: "The Carbohydrates, Chemistry and Biochemistry", (Eds). Pigman, W. and Horton, D. 2nd. Edn. Volume IB. Academic Press, (1980).

(132) von Sonntag, C. and Dizdaroglu, M. *Carbohydr. Res.*, 1977, 58, 21.

(133) Bell, J.D., Brown, J.C.C., Nicholson, J.K. and Sadler, P.J. *FEBS. Lett.*, 1987, 215(2), 511.

(134) Muzzarelli, R.A.A. "Chitin". Chapter 6, p. 418. In: "The Polysaccharides", (Ed). Aspinall, G.O. Academic Press. INC. (1985).

(135) Gajewski, E., Dizdaroglu, M., Krutzsch, H.C. and Simic, M.G. *Int. J. Radiat. Biol.*, 1984, 46, 47.

(136) Grootveld, M., Henderson, E.B., Claxson, A.W.D., Haycock, P., Naughton, D., Herz, M.S., Jain, R. and Blake, D. Paper in press.

**PUBLISHED  
PAPERS  
NOT  
FILMED  
FOR  
COPYRIGHT  
REASONS**

10 END





THE BRITISH LIBRARY DOCUMENT SUPPLY CENTRE

**TITLE** **AN INVESTIGATION OF RADIOLYTIC DAMAGE TO BIOMOLECULES IN FOODSTUFFS**

**AUTHOR** **REETU JAIN**

**INSTITUTION and DATE** **(Polytechnic of North London) CNA**  
**1991.**

Attention is drawn to the fact that the copyright of this thesis rests with its author.

This copy of the thesis has been supplied on condition that anyone who consults it is understood to recognise that its copyright rests with its author and that no information derived from it may be published without the author's prior written consent.



THE BRITISH LIBRARY  
DOCUMENT SUPPLY CENTRE  
Boston Spa, Wetherby  
West Yorkshire  
United Kingdom

20

REDUCTION X

CAMERA 5



**DX**



**170578**

